VERHANDELINGEN DER KONINKLIJKE NEDERLANDSE
AKADEMIE VAN WETENSCHAPPEN, AFD. NATUURKUNDE
EERSTE REEKS - DEEL XXV, No. 2

GEOPHYSICAL INVESTIGATIONS OF THE NETHERLANDS LEEWARD ANTILLES

R. A. LAGAAY

N.V. NORTH-HOLLAND PUBLISHING COMPANY
AMSTERDAM - 1969

LIBRARY OF CONGRESS
CATALOGUE CARD NUMBER: 69–16401

AANGEBODEN: MAART 1968
AANVAARD: SEPTEMBER 1968
GEPUBLICEERD: MAART 1969

CONTENTS

		Page
1.	INTRODUCTION	5
	Previous work	5
2.	MEASUREMENTS AND REDUCTIONS	8
	Gravity	8
	Geomagnetism	23
3.	GEOLOGY	34
	The western Leeward Antilles	34
	Bathymetry	38
	Regional structural elements	39
4.	GEOMETRICAL INTERPRETATION	41
	Gravity anomalies	41
	Total magnetic-intensity anomalies	51
	Comparison with a section at 68° W	56
	Discussion of results	59
5.	MECHANISM OF DEFORMATION	61
	Discussion of hypotheses	61
	Deformation of the Netherlands Leeward Antilles area	67
6.	THE REGIONAL STRUCTURAL PATTERN	71
	Seismicity in the Caribbean	71
	Structural pattern of northern South America	71
	Comparison with the southern Caribbean	74
7.	ISLAND ARCS, ISOSTATIC EQUILIBRIUM AND GEOSYNCLINES	77
	REFERENCES	82

1. INTRODUCTION

Island arcs belong to the tectonically most active features at the earth's surface. From a geological viewpoint these modern tectonic belts serve as a key to the interpretation of the past i.e. the development of ancient tectonic belts. Vening Meinesz' discovery of strips of large negative anomalies associated with island arc systems in Indonesia and the Caribbean led to the hypothesis that the crust had buckled into a great downward root, which, if free to come to isostatic equilibrium, would become a high mountain range. The island arcs would thus represent embryonic mountain chains. Later, seismological work by Worzel and Ewing demonstrated that part of the deficiency of gravity in the Greater Antilles is due to the existence of considerable accumulations of light sediments, casting serious doubt on the validity of some of the assumptions of the buckling hypothesis for that area.

The Netherlands Leeward [1]) Antilles – Aruba, Curaçao and Bonaire – form part of the Caribbean system of island arcs. These Antilles are studied in the light of the foregoing outline. Gravimetric and geomagnetic observations were made on the islands during the summer of 1962 and in the surrounding sea round the turning of the year 1964/1965. In the interpretation of these observations many of the principal lines set by earlier workers will be met.

Previous work

In previous years a fairly large number of geophysical measurements has been made in the southern part of the Caribbean Sea. Of these are many gravity observations, starting with the work of Vening Meinesz. Geomagnetic and seismic data also cover the area. The credit of a great part of the geophysical work in the Caribbean goes to the Lamont Geological Observatory.

The earlier gravity measurements were made with the pendulum apparatus during cruises of Netherlands and American submarines. The first gravity observations in the Caribbean area were carried out by Vening Meinesz (1934) during a cruise of H.Neth.M.S. *K XIII* in 1926. In the southern Caribbean 5 stations were occupied, of which station 73 is

---

[1]) In the present study, the Caribbean islands are divided into three groups, which cover practically all islands of the region. The isles lying on the southern side of the Caribbean Sea are described by Leeward Antilles, according to the original sense of the term. The islands between Saba and Grenada are denoted by volcanic Lesser Antilles, which are located on the eastern side of the Caribbean Sea. The Greater Antilles, lying on the northern side of the Caribbean Sea comprise the islands of Cuba, Jamaica, Hispaniola and Puerto Rico (cf. Weyl, 1966).

locating in what is now known to be a zone of negative anomalies off the north coast of the South American continent. Station 71 is situated in the harbour of Willemstad, Curaçao and gives evidence of the large positive anomaly in that area, which is part of the positive zone coinciding with the Netherlands Leeward Antilles. A second gravity expedition was undertaken by VENING MEINESZ (1948) on board H.Neth.M.S. *O XII*, which in 1937 occupied 8 gravity stations (816–823) in the southern Caribbean. During a cruise of U.S.S. *Barracuda* from Coco Solo to Port of Spain 12 observations were made (EWING, 1937 and HESS, 1937) of which 3 in the vicinity of the Netherlands Leeward Antilles. Nearly 50 observations, locating on profiles that are approximately normal to the northern coast of South America, were carried out on board U.S.S. *Conger* in 1947 (EWING, WORZEL and SHURBET, 1957). Two of these profiles, approximately along the meridians of 68°W and of 71°W, lie in the vicinity of the Netherlands Antilles. The isostatic reductions of the gravity measurements during the cruises of U.S.S. *Conger* and U.S.S. *Barracuda* were carried out by KÄRKI and PAANANEN (1961). The last pendulum stations in the area were made during cruises of H.Neth.M.S. *O 24* (1949), H.Neth.M.S. *Tijgerhaai* (1951) and H.Neth.M.S. *Walrus* (1957). Stations 845–849, 907–918 and 1017–1032 of these cruises are located in the southern Caribbean (BRUINS, DORRESTEIN, VESSEUR, BAKKER and OTTO, 1960).

The fairly large number of gravity observations enables one to construct an anomaly chart as has been done by DE BRUYN (1951). De Bruyn did not yet have the disposal of the data of the *Conger* cruise and the Netherlands cruises of 1949–1957, so that large parts of his chart were left blank. DE BRUYN (1951), HESS (1938) and VENING MEINESZ (1964) interpreted the pattern of gravity anomalies in the Caribbean area. The region of the Netherlands Leeward Antilles is referred to briefly in these studies; it is generally thought that plastic buckling of the crust brought about the zone of negative anomalies in the southern Caribbean. Hambleton interpreted the profile at 68°W (see WORZEL, 1965a, 1965b); his section will be compared with our results.

EWING, ANTOINE and EWING (1960) published a chart of the Caribbean Sea showing magnetometer traverses and total field intensities. Most of the area was covered with an airborne instrument; the remainder was measured with a sea magnetometer. Several tracks cross the region of deeps and island chains off the north coast of South America. The object in the presentation of the map was to show the areas of smooth and rough magnetic field.

Magnetic observations on Curaçao and Bonaire were carried out by the geomagnetic section of the Venezuelan National Cartographic Service (ROMERO, 1961). On each of the islands one station was occupied in 1952. At these stations the declination, inclination and the horizontal component were measured. The measurements served the construction of isodynamic magnetic charts of Venezuela.

A great number of seismic refraction measurements were made in the Caribbean area (e.g. OFFICER, EWING, HENNION, HARKRIDER and MILLER, 1959) of which, however, only few are located in the southern Caribbean. Important are the seismic refraction lines at 68°W. Results from these experiments combined with gravity data form the basis of Hambleton's interpretation, mentioned above. Depths and velocities as determined by seismic refraction measurements are presented in his section. As regards continuous seismic reflection, a number of profiles were made in the area (EDGAR, EWING and HENNION, 1967; EWING, TALWANI, EWING and EDGAR, 1967).

Data on the seismicity in the southern Caribbean were presented in regional studies of the whole Caribbean area (RUTTEN and VAN RAADS-hoven, 1940; SYKES and EWING, 1965). MENDIGUREN (1966) studied focal mechanisms in Central and South America. These results are of interest for the structural relations in the Caribbean.

In the following investigation use is made of many of the mentioned studies and data; for instance in the construction of an isostatic anomaly map of the area surrounding the Netherlands Leeward Antilles from earlier pendulum observations and our own data.

2. MEASUREMENTS AND REDUCTIONS

Gravity

Gravity observations

Gravity observations on the islands

The instrument used for the gravity observations on the islands was the North American Gravimeter 105. In the period from May to August 1962 over 250 stations were occupied on Aruba, Bonaire and Curaçao. The observations were made on or close to bench-marks of the Cadastral Survey Department of the Netherlands Antilles. The grid co-ordinates and the height of these bench-marks were supplied by the Cadastral Survey and K.L.M. Aerocarto, Delft. The grid of the islands (1963 map issue) is based on the Universal Transverse Mercator Projection on the international spheroid. The geographic co-ordinates (φ, λ) of the observation points have been obtained from the grid co-ordinates (y, x) by the following relations:

$$30.73\,(\varphi_c-\varphi)=y_c-y$$

$$30.19\,(\lambda_c-\lambda)=x-x_c$$

where (φ_c, λ_c) and (y_c, x_c) are respectively the geographical and grid co-ordinates of the reference point of the map grid, expressed in seconds and meters respectively. The new co-ordinates of the islands appeared to be shifted with respect to those given on the old topographic maps of 1911. As a result the geographic co-ordinates for the pendulum harbour station Curaçao III, as determined from the new topographic maps, viz. 12°07′11″N–68°55′46″W, differ from the co-ordinates given earlier.

The distance between the gravity stations as a rule is about 1 km. The selection of the site of the stations was limited by the accessibility of the terrain and by the presence of bench-marks. The observations were made with the assistance of a surveyor of the Cadastral Survey Department.

Before and after the survey the scale factor was determined in the tower of the Meteorological Institute at De Bilt, giving a value of 0.09000 mgal/division, no change occurring in the interval. The drift of the N.A.G. 105 generally was small. The drift of the instrument was about 0.001 scale units per hour, as determined from periods of 96 hours. Rough transport. conditions sometimes produced jumps; if such a jump occurred, the stations were reoccupied.

All values refer to the pendulum station Curaçao III (Bruins, Dorrestein, Vesseur, Bakker and Otto, 1960; our station no. 7). This station is situated in the Diesel-engine room of the naval base Parera in Willemstad, Curaçao. Pendulum observations have been carried out at the site during two cruises, giving the following values:

station	serial number	year	gravity in mgal
Curaçao III	845 914	1949 1951	978441 978442

The value used for the observations in the Antilles is 978441 mgal.

Gravity observations at sea

At the request of the author H.Neth.M.S. *Snellius* made two approximately N–S running traverses; one through the Aruba–Curaçao passage, one through the Curaçao–Bonaire passage. The gravity measurements were made in the Navado III project (1964–1965). The instrument used was the Askania Seagravimeter Gss 2–no. 19 of the Geodetic Institute at Delft.

The observations were corrected for instrumental drift and for the Eötvös effect, this effect being computed assuming constant speed and course between successive navigational fix points. Since the navigation on the traverse running through the Curaçao–Bonaire passage suffered from gyro-compass troubles, the possible error in the correction for the Eötvös effect for this line is more than the 4 mgal under more favourable conditions. On account of the accuracy of the dead reckoning on this traverse, as estimated by the navigation officer, the error in the Eötvös correction is less than 10 mgal. The accuracy for the other traverse was normal i.e. 4 mgal. The cross-coupling effect has not been measured. Sea state was calm during the measurements.

Gravity reductions

General

For the computation of the free air anomalies, Bouguer anomalies and isostatic anomalies the normal procedure (cf. HEISKANEN and VENING MEINESZ, 1958) was used with the exception of the reduction for the land stations. These latter reductions were computed, using an electronic computor as will be explained in the following pages. The isostatic anomalies are based on the Airy-Heiskanen system, with a crustal thickness of 30 km and local compensation.

The reduction of the gravity observations on land

The reduction of our gravity measurements on the islands was carried out by the means of an electronic computor. The major advantage of the use of an electronic computor lies in the time saved, since topographic heights need to be read only once and not, as in conventional zone chart methods, for each station separately. The method is only advantageous for areal surveys, and not for the reduction of widely-spread measurements. The program utilized for the computations is an extension of the one described by BOTT (1959) for the terrain corrections.

1. *Free air and Bouguer plate corrections*

The free air and simplified Bouguer anomalies were computed according to the following formulas (HEISKANEN and VENING MEINESZ, 1958)

$$g_{FA} = g_0 - 978.0490(1 + 0.0052884 \sin^2 \varphi - 0.0000059 \sin^2 2\varphi) + 0.3086\ h_s$$

and

$$g_{BS} = g_{FA} - 0.04184\varrho\ h_s$$

where g_0 is the observed gravity, φ is the station latitude, h_s is the station height and ϱ is the assumed rock density (2.67 g/cm³).

2. *Corrections for topography and isostatic compensation*

a. Zones A to 0_2 (166,7 km)

(i) General

The correction for the effects of the topographic masses deviating from a horizontal slab and the isostatic compensation to a radius of 166.7 km was calculated with digital computing methods, with the exception of the topographic correction for the area closer than 1 km around the station, as is discussed further on. In its outline the method of computation consists of the following steps. The topography is divided in a grid of equal squares, the average height of which must be estimated from the topographic maps. The correction is then obtained by computing the incremental contribution of all squares.

The contribution of the squares to the topographic and the isostatic correction was computed with the formula for the vertical component of the attraction of a segment $d\varphi$ of a hollow vertical cylinder, with inner and outer radius r_1 and r_2 and height h, at a point lying at the end of its axis

$$\Delta g = -\varrho k\ d\varphi \int_{r_1}^{r_2} \int_0^h \frac{rh\ dr\ dh}{(r^2+h^2)^{3/2}} \tag{1}$$

with k = gravitational constant, and
ϱ = density, or

$$\Delta g = \varrho k\{\sqrt{r_2^2+h^2} - \sqrt{r_1^2+h^2} + r_1 - r_2\}d\varphi \tag{1a}$$

For convenience we write $r_2 = R + p$ and $r_1 = R - p$, p being the half width of a square and R being the distance between the point for which the attraction is calculated and the centre of the square. The horizontal cross-section of the segment is taken to be equal to the surface of one square, or

$$d\varphi \int_{R-p}^{R+p} r\ dr = 4p^2, \text{ which gives } d\varphi = \frac{2p}{R}.$$

Formula (1a) then becomes

$$\Delta g = \frac{2p\,\varrho k}{R}\{\sqrt{(R+p)^2+h^2}-\sqrt{(R-p)^2+h^2}-2p\} \qquad (2)$$

This formula cannot be used when the centre of a square coincides with the calculation point. From formula (1a) it follows that the attraction of a cylinder at a point at the end of its axis, since in that case $d\varphi = 2\pi$ and $r_1 = 0$, and writing $r_2 = r$, becomes

$$\Delta g = 2\pi\,\varrho k\{\sqrt{r^2+h^2}-r-h\} \qquad (3)$$

With $r = (2p/\sqrt{\pi})$, the cross-section of the cylinder again is equal to the surface of the square.

For the computation of the topographic correction, formula (2) was approximated by taking the first term of the development into a power series

$$\Delta g = 2\varrho k\, p^2 \frac{h^2}{R(R^2-p^2)} \qquad (4)$$

This approximation considerably saves computing time (BOTT, 1959).

The actual computation was carried out in two steps: first the correction for topographic irregularities up to a distance of 20 km was computed for each gravity station using formula (4) and a grid of 1×1 km². Next, the correction for the topography beyond 20 km and out to 166.7 km, and the reduction for isostatic compensation up to a distance of 166.7 km, was computed for a number of selected points using formulas (2) and (3) for the compensation, and formula (4) for the topography.

(ii) The influence of nearby topography

A size of 1×1 km² of the grid squares is convenient for the computation of the topographic correction to a distance of 20 km. For each square the contribution to the correction is computed and added to the total correction.

The contribution of a topographic mass in a continental area, where the average height of the square, $\bar{h}$, is positive or zero, was computed taking $h = \bar{h} - h_s$, h_s being the station height, and using a density of 2.67 g/cm³. If the square is situated in an oceanic area, $\bar{h} < 0$, the contribution of this square was computed by putting

$h = h_s$ with density 1.03 g/cm³ and

$h = \bar{h} - h_s$ with density $2.67 - 1.03 = 1.64$ g/cm³

These contributions are all positive.

The presence of topographic irregularities on land, and of a water layer at sea is then accounted for, out to a distance of 20 km. However, as the error involved in the approximated formula (4) is largest for squares in the vicinity of the station, the contribution of squares, the centres of which are less than 1 km from the station, must be computed by another method. For this purpose LEJAY's tables (1947) are convenient. Since the digital computations are based on a square grid and Lejay's tables on Hayford's circular zones, the computation involves contributions of incomplete zones. This was done by simple estimation. Zones A to F_1 covered the area to be computed by table readings.

(iii) The topographic correction beyond 20 km to 166.7 km and the correction for isostatic compensation to 166.7 km.

The computations of the remaining topographic correction and of the correction for isostatic compensation both extending to the outside of zone 0_2 or 166.7 km, are based on the incremental contributions of squares of 8×8 km^2. One 8×8 km^2 square is formed by 64 squares of the 1×1 km^2 grid. The corrections were computed for the centres of all squares on the islands and in the immediate neighbourhood. Next, a chart with iso-correction lines was constructed. The corrections for the gravity stations were read from this chart by interpolation.

A correction for the earth's curvature was taken into account, the formulas used being valid for a plane earth only. The correction height, h_c, which is the distance between sea level and the tangent plane at the station is approximated by $(r^2/2R)$, where r is the distance of the centre of the square to the station and R is the earth's radius.

The topographic correction was calculated with formula (4). The contribution of a square was computed in two steps, i.e. for

$$h = h_c \qquad \text{(a)}$$

$$\text{and for } h = \bar{h} - h_c \qquad \text{(b)}$$

(a) and (b) to be taken with opposite sign.

If $\bar{h} \geqslant 0$ a density of 2.67 g/cm^3 was used. If $\bar{h} < 0$ a density of 1.64 g/cm^3 was used. The station height, being very small compared with the horizontal distance of the squares, was neglected.

The correction for the isostatic compensation was calculated with formula (2), except for the central square, in which case formula (3) must be applied. The corrections were computed for a mantle-crust contrast of $3.27 - 2.67 = 0.6$. If the average height of a square $\bar{h} \geqslant 0$, the contribution of this square to the correction was computed

$$\text{for } h = 4.45\,\bar{h} + h_c + T \qquad \text{(a)}$$

$$\text{and for } h = h_c + T \qquad \text{(b)}$$

where T is the crustal thickness, taken to be 30 km, and where 4.45 $\bar{h}$ is the thickness of the compensation under a continental area. If the average height of a square $\bar{h} < 0$, the contribution of this square to the correction was computed

$$\text{for } h = 2.73\,\bar{h} + h_c + T \qquad \text{(a)}$$

$$\text{and for } h = h_c + T \qquad \text{(b)}$$

where 2.73 $\bar{h}$ is the thickness of the compensation under an oceanic area. (a) and (b) should again be taken with opposite sign.

b. Zones 18–1

The corrections for topography and its compensation for the zones 18–1, i.e. farther than 166.7 km and out to 180°, were read from the world reduction maps of Kärki, Kivioja and Heiskanen (1961) for the Airy-Heiskanen system T = 30, R = 0.

3. Recapitulation of the computations

Recapitulating, the output of the digital program gives:

1. the free air anomaly, g_{FA}
2. the simplified Bouguer anomaly, g_{BS}
3. the correction for topographic irregularities to the outside of zone O_2, with the exception of squares the centres of which are nearer than 1 km to the station
4. the correction for isostatic compensation for the zones A–O_2.

Computed by conventional methods were:

5. the correction for topographic irregularities near to the station
6. the correction for topography and compensation for the zones 18–1

Corrections 3 and 5 give, added to the simplified Bouguer anomaly, the Bouguer anomaly. Corrections 3 to 6 give, added to the simplified Bouguer anomaly, the isostatic anomaly.

The corrections for the nearby topography were computed by the El–X4 computor of the Electronic Computing Centre at Utrecht. The corrections for isostatic compensation and the topography farther away, were computed by the El–X1 computor of the Technological University at Delft.

On the error involved in the digitally computed corrections the following is remarked. Errors arise from the assumption of uniform height of the squares and from the approximations made in obtaining the formulas for the program. The first approximation was that the gravitational effect of a square can be represented by a segment of a hollow cylinder; the second was made in converting formula (2) into formula (4). Bott (1959) discussed the errors due to these assumptions and concluded that the overall error is seldom likely to exceed 5 %, which is an acceptable figure. For illustration the corrections for the pendulum station no. 914 (Curaçao III), as given by Vening Meinesz, are compared with the correction obtained with the method described above (Curaçao station 7). It appears that the differences in the topographic and in the isostatic corrections are less than 5 %.

Corrections for Curaçao in 0.1 milligal, zones A–O_2

Topog.	Comp. (R=0, T=30)	Corrections obtained by:
+63	—579	zone chart readings
+64	—598	digital computing

Tables 1, 2 and 3 give for each island the station numbers, geographic position, station heights, the free air anomalies, the Bouguer anomalies and the isostatic anomalies.

The reduction of the gravity observations at sea

The normal value of gravity and the Eötvös effect were computed at the navigational fixes by linear interpolation of these values. The free air anomaly curve was obtained by graphical interpolation.

As mentioned the digital method was not applied for the corrections of the gravity profiles at sea, since the method is only of advantage for areal surveys. The topographic corrections and the correction for the compensation were computed with the aid of the tables of LEJAY (1947, topographic correction for the zones A to O_2), of VENING MEINESZ (1941, correction for the compensation for the zones A to O_2) and the isocorrection charts of KÄRKI, KIVIOJA and HEISKANEN (1961, topography and compensation for the zones 18–1). The complete correction curve along the ship's track was obtained by graphical interpolation; the corrections for the nearer zones were computed for a larger number of points along the track than for the zones farther away. The corrections for zones A–H were computed every 7 miles, for zones I–L every 14 miles, for zones M–O_2 every 20 miles and for zones 18–1 every 30 miles.

The Bouguer corrections include the corrections for topographic irregularities for the zones A to O_2. The free air anomaly curve, the Bouguer anomaly curve and the isostatic anomaly curve are presented in figures 15 and 16; for a number of points on the profiles the corrections are given in table 4.

The free air anomalies for the traverse through the Curaçao–Aruba passage have been computed by Ir G. Strang van Hees of the Geodetic Institute at Delft.

Charts and profiles

Based on our measurements isostatic anomaly charts (T=30, R=0) were constructed for the islands Aruba, Curaçao and Bonaire (respectively fig. 1, 2 and 3). The interval of the contour lines is 10 mgal. From these charts it may be seen that the islands lie in a region of positive gravity

TABLE 1
Gravity observations on Aruba

Station number	Latitude N	Longitude W	Station Height, m	Free Air Anomaly, mgal	Bouguer Anomaly, mgal	Isostatic Anomaly, R=0, T=30 mgal
1	12°30′02.9″	69°57′00.4″	67.2	+ 97.8	+ 93.7	+ 38.9
2	12 29 53.8	69 56 30.2	77.0	+101.9	+ 98.0	+ 42.9
3	12 29 48.8	69 54 53.8	41.6	+ 98.9	+ 98.0	+ 41.2
4	12 28 30.3	69 53 29.8	28.9	+ 95.7	+ 96.2	+ 39.6
5	12 29 56.1	69 56 08.5	65.7	+102.0	+ 98.7	+ 43.1
6	12 27 19.9	69 54 07.2	59.9	+ 84.2	+ 80.8	+ 26.7
7	12 28 41.1	69 58 46.7	11.7	+ 53.4	+ 54.5	+ 3.6
8	12 31 21.7	70 02 24.1	2.2	+ 45.0	+ 47.2	— 3.8
9	12 31 16.4	70 01 01.7	17.1	+ 65.2	+ 65.7	+ 13.6
10	12 30 53.5	69 59 30.3	24.0	+ 80.8	+ 80.8	+ 27.7
11	12 30 29.4	69 58 11.9	50.3	+ 88.8	+ 86.1	+ 32.8
12	12 31 07.1	70 00 32.0	20.8	+ 74.1	+ 74.3	+ 21.8
13	12 30 17.6	70 01 22.1	3.4	+ 41.2	+ 43.2	— 7.3
14	12 29 43.7	70 00 41.8	4.5	+ 42.0	+ 44.0	— 6.4
15	12 29 19.1	69 58 32.4	44.1	+ 78.8	+ 76.5	+ 24.5
16	12 28 54.8	69 58 02.1	1.1	+ 74.9	+ 77.4	+ 25.4
17	12 29 52.0	69 58 38.9	30.2	+ 82.8	+ 82.1	+ 29.5
18	12 31 05.2	69 58 43.7	33.0	+ 86.2	+ 85.4	+ 31.1
19	12 31 57.1	69 58 41.1	47.8	+ 94.1	+ 92.0	+ 36.4
20	12 32 58.6	69 58 39.2	20.8	+ 92.5	+ 93.7	+ 36.6
21	12 32 25.8	69 58 37.7	31.4	+ 93.1	+ 92.9	+ 36.5
22	12 31 47.3	70 01 47.2	11.2	+ 65.0	+ 66.2	+ 14.1
23	12 32 08.8	70 01 26.2	18.2	+ 78.9	+ 79.5	+ 26.7
24	12 32 31.1	70 01 04.2	26.4	+ 85.1	+ 84.8	+ 31.1
25	12 33 27.6	70 00 27.3	31.3	+ 92.9	+ 92.5	+ 36.7
26	12 34 07.8	69 59 42.2	6.8	+ 90.8	+ 93.8	+ 36.1
27	12 33 41.6	70 00 11.5	52.0	+ 95.4	+ 92.9	+ 36.5
28	12 32 56.3	70 00 42.1	26.2	+ 90.8	+ 90.7	+ 36.0
29	12 32 20.0	70 02 11.4	12.4	+ 68.8	+ 69.9	+ 17.3
30	12 33 12.2	70 02 36.0	5.8	+ 68.2	+ 70.1	+ 16.9
31	12 33 59.1	70 02 09.0	3.7	+ 77.2	+ 79.5	+ 24.8
32	12 34 16.9	70 02 40.7	2.2	+ 67.7	+ 70.2	+ 15.5
33	12 33 43.2	70 03 16.0	1.6	+ 60.7	+ 63.1	+ 9.8
34	12 31 54.3	70 01 40.3	13.5	+ 70.0	+ 71.0	+ 18.6
35	12 29 16.5	70 00 00.4	5.3	+ 46.0	+ 47.8	— 2.6
36	12 27 55.0	69 57 52.3	2.9	+ 48.1	+ 50.3	0.0
37	12 27 09.6	69 57 00.1	2.5	+ 46.2	+ 48.5	— 1.8
38	12 27 32.6	69 56 34.9	40.8	+ 68.8	+ 67.1	+ 15.9
39	12 26 54.9	69 55 33.5	15.1	+ 55.4	+ 56.4	+ 4.9
40	12 27 12.6	69 54 45.8	55.3	+ 77.6	+ 74.3	+ 21.0
41	12 26 26.2	69 53 54.5	29.4	+ 67.5	+ 67.1	+ 13.8
42	12 26 12.2	69 54 32.4	9.4	+ 50.3	+ 52.0	+ 0.3
43	12 28 08.4	69 54 49.0	76.6	+ 90.9	+ 85.6	+ 31.1
44	12 28 31.4	69 54 53.9	72.0	+ 93.4	+ 88.6	+ 33.7
45	12 28 49.4	69 54 46.8	70.5	+ 95.8	+ 91.3	+ 35.8

TABLE 1 (*continued*)

Station number	Latitude N	Longitude W	Station Height, m	Free Air Anomaly, mgal	Bouguer Anomaly, mgal	Isostatic Anomaly, R=0, T=30 mgal
46	12°27′37.9″	69°54′43.7″	52.2	+ 84.0	+ 81.2	+ 27.3
47	12 27 32.0	69 53 47.1	53.5	+ 86.1	+ 83.4	+ 28.7
48	12 27 55.3	69 53 32.0	43.0	+ 91.7	+ 90.4	+ 34.7
49	12 29 07.1	69 53 51.3	9.1	+ 93.9	+ 96.7	+ 39.6
50	12 29 46.9	69 54 16.6	8.0	+ 94.2	+ 97.4	+ 39.9
51	12 29 28.7	69 54 18.9	27.8	+ 96.9	+ 97.7	+ 40.6
52	12 29 13.4	69 54 28.5	41.6	+ 97.8	+ 96.8	+ 40.2
53	12 26 55.4	69 54 55.7	24.0	+ 62.2	+ 62.3	+ 10.1
54	12 25 59.1	69 55 17.8	1.3	+ 35.9	+ 38.5	— 12.1
55	12 26 28.5	69 55 38.3	0.2	+ 42.4	+ 45.0	— 5.9
56	12 26 45.8	69 55 36.1	10.4	+ 48.6	+ 50.1	— 1.2
57	12 25 58.7	69 54 20.8	10.5	+ 49.3	+ 50.9	— 0.7
58	12 26 05.4	69 52 36.3	18.2	+ 77.7	+ 78.8	+ 24.7
59	12 24 59.0	69 52 08.0	3.2	+ 76.1	+ 79.2	+ 26.9
60	12 25 24.5	69 53 12.4	17.0	+ 63.9	+ 64.9	+ 12.7
61	12 25 35.8	69 52 38.1	21.4	+ 74.1	+ 74.8	+ 21.2
62	12 29 55.9	69 59 49.7	7.2	+ 63.0	+ 64.6	+ 13.1
63	12 30 30.3	69 59 05.1	24.1	+ 82.1	+ 82.1	+ 29.1
64	12 31 36.0	69 59 41.5	37.2	+ 85.5	+ 84.1	+ 30.2
65	12 32 08.5	70 00 22.7	36.7	+ 86.6	+ 85.3	+ 31.3
66	12 32 35.2	69 59 40.4	45.0	+ 93.8	+ 91.8	+ 36.4
67	12 33 01.0	69 58 52.9	14.1	+ 92.0	+ 94.5	+ 37.6
68	12 32 46.5	69 57 44.5	8.0	+ 91.4	+ 94.5	+ 36.5
69	12 31 24.0	70 02 42.3	2.0	+ 41.5	+ 43.6	— 7.1
70	12 32 45.1	70 03 36.2	2.3	+ 49.6	+ 51.8	0.0
71	12 35 04.8	70 02 41.3	1.0	+ 75.0	+ 77.8	+ 21.4
72	12 36 14.2	70 03 03.5	3.9	+ 86.4	+ 89.1	+ 31.5
73	12 37 25.2	70 03 17.5	3.7	+ 87.9	+ 91.2	+ 31.4
74	12 36 01.8	70 02 24.7	2.0	+ 88.7	+ 91.6	+ 33.7
75	12 35 01.7	70 02 08.9	6.7	+ 88.5	+ 90.8	+ 34.0
76	12 34 16.9	70 02 14.0	3.5	+ 77.6	+ 80.0	+ 24.3
77	12 33 16.4	70 01 49.6	14.5	+ 82.9	+ 84.1	+ 29.9
78	12 31 24.8	70 02 05.4	4.1	+ 50.6	+ 52.5	+ 1.2
79	12 32 28.0	70 02 53.0	4.4	+ 56.7	+ 58.6	+ 6.6
80	12 36 53.5	70 02 36.6	4.8	+ 87.5	+ 90.4	+ 30.9
81	12 35 16.8	70 01 22.2	20.9	+ 91.6	+ 92.8	+ 35.0
82	12 34 32.0	70 01 21.2	29.0	+ 93.1	+ 93.0	+ 36.1
83	12 27 25.8	69 52 56.8	11.8	+ 85.1	+ 87.3	+ 31.5
84	12 26 34.2	69 52 39.7	11.6	+ 79.2	+ 81.1	+ 26.3
85	12 32 03.8	70 03 10.5	2.5	+ 45.7	+ 47.8	— 3.4
86	12 30 19.7	70 00 39.5	18.7	+ 54.2	+ 54.6	+ 3.3
87	12 28 49.3	69 58 42.9	21.8	+ 63.4	+ 63.4	+ 12.3
88	12 26 41.6	69 54 50.2	18.7	+ 57.8	+ 58.5	+ 6.5
89	12 26 08.2	69 53 57.4	15.3	+ 58.8	+ 59.9	+ 7.5

TABLE 2

Gravity observations on Curaçao.

Station number	Latitude N	Longitude W	Station Height, m	Free Air Anomaly, mgal	Bouguer Anomaly, mgal	Isostatic Anomaly, R=0, T=30 mgal
1	12°07′45.3″	68°58′07.0″	3.0	+144.4	+152.6	+ 76.8
2	12 08 41.4	68 50 23.1	33.8	+164.8	+167.6	+ 85.1
3	12 16 43.7	69 03 49.3	20.0	+132.9	+137.3	+ 51.9
4	12 22 11.9	69 09 23.2	10.6	+115.8	+132.8	+ 41.8
5	12 07 03.3	68 57 20.6	2.4	+140.8	+150.8	+ 75.3
6	12 06 57.5	68 55 35.5	37.8	+161.0	+163.7	+ 87.3
7 [1]	12 07 11.0	68 55 46.0	2.0	+165.9	+172.3	+ 95.4
8	12 06 39.0	68 53 12.5	15.1	+173.0	+177.1	+ 99.5
9	12 06 33.0	68 51 20.7	22.9	+175.5	+178.7	+ 99.8
10	12 04 16.0	68 51 02.4	1.4	+158.5	+167.1	+ 90.7
11	12 05 44.7	68 50 05.7	7.1	+173.7	+178.8	+100.0
12	12 07 09.8	68 50 51.3	22.8	+173.5	+176.8	+ 96.6
13	12 08 09.0	68 53 03.1	30.8	+171.6	+173.8	+ 94.3
14	12 07 40.0	68 54 02.2	3.5	+165.7	+170.8	+ 92.6
15	12 05 39.0	68 53 57.5	0.6	+154.2	+162.7	+ 86.8
16	12 08 37.0	68 54 21.0	7.5	+164.1	+168.8	+ 89.6
17	12 09 34.3	68 56 10.0	36.8	+160.3	+162.0	+ 82.7
18	12 11 41.6	68 56 03.3	7.6	+126.7	+133.6	+ 50.2
19	12 09 32.2	68 54 49.4	36.1	+160.3	+162.0	+ 81.5
20	12 09 15.5	68 53 22.2	29.3	+162.8	+165.4	+ 84.1
21	12 10 53.1	68 51 13.4	9.2	+128.4	+136.3	+ 50.1
22	12 08 11.4	68 48 20.8	4.5	+151.7	+159.2	+ 75.7
23	12 10 33.6	68 58 07.4	35.5	+155.9	+158.0	+ 77.7
24	12 10 44.2	68 57 40.2	53.1	+155.0	+155.2	+ 74.4
25	12 08 18.0	68 57 05.8	10.1	+162.0	+166.9	+ 89.8
26	12 06 20.8	68 47 17.8	5.7	+162.7	+170.3	+ 88.6
27	12 05 40.2	68 46 44.1	6.4	+162.8	+171.2	+ 89.9
28	12 03 04.4	68 44 52.4	1.4	+147.5	+157.0	+ 77.0
29	12 03 59.3	68 45 14.2	3.7	+157.3	+166.0	+ 85.7
30	12 07 13.6	68 47 53.0	6.7	+162.3	+169.3	+ 86.9
31	12 02 46.8	68 47 11.6	3.0	+155.4	+164.5	+ 86.9
32	12 03 03.3	68 46 39.6	2.4	+154.6	+163.6	+ 85.4
33	12 04 17.0	68 50 25.0	21.2	+171.1	+177.9	+101.1
34	12 05 40.3	68 49 06.2	50.7	+176.1	+177.9	+ 98.4
35	12 04 14.3	68 48 25.1	29.9	+172.1	+175.4	+ 97.1
36	12 03 02.5	68 49 01.3	1.7	+153.7	+163.9	+ 87.4
37	12 10 29.0	68 55 44.5	25.6	+151.4	+154.6	+ 73.6
38	12 11 00.2	68 55 56.0	57.8	+144.2	+144.5	+ 62.0
39	12 11 20.2	68 59 31.5	43.0	+145.5	+147.1	+ 66.6
40	12 12 39.8	69 00 55.2	67.5	+137.3	+136.7	+ 55.4

[1]) Station no. 7 has the location of the pendulum station Curaçao III.

TABLE 2 (*continued*)

Station number	Latitude N	Longitude W	Station Height, m	Free Air Anomaly, mgal	Bouguer Anomaly, mgal	Isostatic Anomaly, R=0, T=30 mgal
41	12°13′03.1″	69°02′43.5″	21.5	+130.1	+134.5	+ 53.9
42	12 13 28.3	69 05 08.6	1.0	+119.2	+129.7	+ 49.7
43	12 15 35.5	68 04 21.8	48.2	+131.7	+133.0	+ 49.8
44	12 14 55.3	68 02 48.6	83.9	+131.7	+129.3	+ 46.0
45	12 16 50.2	69 02 58.0	8.5	+126.2	+132.8	+ 46.6
46	12 15 07.9	69 01 50.5	8.7	+119.7	+126.2	+ 41.9
47	12 14 20.5	69 01 02.5	5.6	+118.5	+125.4	+ 41.8
48	12 13 02.8	68 59 31.2	5.5	+120.3	+127.0	+ 44.1
49	12 08 42.4	68 59 44.6	4.4	+136.2	+147.4	+ 70.8
50	12 14 20.3	69 02 14.8	72.8	+131.1	+129.9	+ 47.1
51	12 19 52.8	69 03 21.5	9.5	+145.3	+153.3	+ 61.4
52	12 19 48.1	69 05 16.8	50.3	+141.9	+143.8	+ 53.7
53	12 17 54.2	69 05 04.7	35.9	+136.7	+139.5	+ 53.0
54	12 18 25.1	69 06 15.9	41.3	+133.9	+136.4	+ 49.9
55	12 16 29.1	69 07 41.8	1.0	+101.0	+112.7	+ 29.9
56	12 16 13.9	69 05 35.6	25.4	+125.1	+129.4	+ 46.0
57	12 09 19.0	68 58 41.3	17.0	+157.3	+161.8	+ 84.0
58	12 10 41.6	69 00 42.7	32.4	+137.3	+142.4	+ 63.6
59	12 09 54.3	68 59 25.2	2.1	+151.6	+157.9	+ 79.3
60	12 20 10.1	69 08 54.5	12.0	+115.1	+125.6	+ 37.7
61	12 21 05.8	69 08 38.5	40.6	+127.4	+133.9	+ 44.2
62	12 22 40.2	69 09 03.3	7.5	+130.6	+142.8	+ 50.1
63	12 22 14.7	69 06 59.1	15.3	+143.6	+151.7	+ 58.1
64	12 20 50.8	69 06 10.2	18.7	+138.9	+144.9	+ 53.5
65	12 21 25.5	69 04 19.1	7.6	+146.7	+155.1	+ 61.2
66	12 23 29.7	69 09 32.8	9.5	+128.7	+145.6	+ 51.1
67	12 15 09.3	69 06 19.3	1.5	+110.4	+122.7	+ 41.1
68	12 20 00.7	69 06 37.8	64.5	+140.9	+141.5	+ 52.0
69	12 19 52.2	69 07 03.0	64.5	+139.8	+140.7	+ 51.6
70	12 09 51.0	68 54 55.3	21.6	+155.7	+159.1	+ 78.1
71	12 17 13.7	69 06 56.7	12.9	+119.5	+125.9	+ 41.6
72	12 18 46.4	69 08 25.5	9.0	+118.1	+126.5	+ 40.7
73	12 17 57.2	69 05 36.5	58.6	+137.0	+137.6	+ 51.5
74	12 18 12.8	69 03 13.0	8.3	+130.3	+137.8	+ 49.4
75	12 07 40.4	68 56 53.3	5.5	+159.8	+165.7	+ 89.3

TABLE 3

Gravity observations on Bonaire

Station number	Latitude N	Longitude W	Station Height, m	Free Air Anomaly, mgal	Bouguer Anomaly, mgal	Isostatic Anomaly, R=0, T=30 mgal
1	12°07′01.0″	68°17′33.9″	2.9	+162.7	+171.1	+ 76.7
2	12 05 10.8	68 16 47.1	1.7	+164.5	+172.2	+ 79.9
3	12 30 48.8	68 16 47.8	4.5	+160.5	+169.1	+ 78.2
4	12 01 44.1	68 14 56.1	2.0	+162.3	+171.0	+ 81.0
5	12 07 54.1	68 14 33.4	3.2	+170.6	+177.3	+ 80.5
6	12 06 19.3	68 14 21.1	1.4	+170.6	+177.2	+ 82.4
7	12 05 52.4	68 14 04.4	0.8	+170.6	+177.4	+ 83.0
8	12 08 07.3	68 15 54.5	6.1	+166.8	+173.1	+ 76.9
9	12 06 20.0	68 13 11.2	1.0	+168.4	+175.8	+ 80.2
10	12 09 51.8	68 12 41.0	17.4	+174.0	+180.4	+ 79.4
11	12 09 55.4	68 15 33.2	16.9	+177.2	+182.8	+ 83.6
12	12 10 21.1	68 14 14.7	20.2	+179.1	+184.7	+ 83.9
13	12 11 05.8	68 12 51.5	0.3	+161.3	+170.0	+ 66.9
14	12 11 36.4	68 15 44.3	26.5	+168.6	+174.0	+ 71.9
15	12 14 45.7	68 17 23.0	10.8	+144.1	+155.2	+ 46.8
16	12 14 38.7	68 19 20.5	10.0	+151.6	+161.4	+ 54.0
17	12 13 35.3	68 16 41.1	43.0	+147.1	+152.4	+ 46.2
18	12 09 38.4	68 16 12.6	4.0	+164.4	+171.8	+ 72.9
19	12 10 11.3	68 16 06.6	15.8	+173.2	+179.0	+ 79.6
20	12 10 56.6	68 16 05.6	10.2	+176.1	+182.9	+ 82.2
21	12 12 42.7	68 16 10.6	48.4	+154.5	+158.3	+ 54.2
22	12 14 32.8	68 17 04.6	8.8	+142.8	+153.5	+ 45.5
23	12 14 55.4	68 18 40.4	9.8	+146.1	+156.8	+ 48.5
24	12 14 28.9	68 20 32.4	38.5	+159.4	+166.3	+ 59.5
25	12 14 30.5	68 21 15.5	23.7	+162.6	+173.1	+ 66.4
26	12 14 24.3	68 22 01.9	1.0	+167.7	+179.4	+ 73.0
27	12 14 24.3	68 20 15.8	61.1	+159.7	+164.2	+ 57.5
28	12 12 07.3	68 15 47.0	49.6	+163.1	+166.8	+ 63.2
29	12 11 17.8	68 15 52.4	17.5	+174.1	+180.3	+ 78.8
30	12 10 25.7	68 17 10.9	3.7	+156.9	+164.7	+ 65.3
31	12 11 29.1	68 17 37.8	4.7	+156.0	+164.4	+ 63.4
32	12 12 08.5	68 18 22.0	3.7	+152.8	+162.8	+ 60.8
33	12 13 17.2	68 20 43.6	13.4	+153.3	+165.6	+ 62.0
34	12 12 36.2	68 18 56.8	5.0	+151.7	+162.1	+ 59.3
35	12 14 32.8	68 21 40.8	13.5	+166.4	+176.3	+ 69.5
36	12 14 43.9	68 21 55.6	8.9	+167.1	+177.8	+ 70.6
37	12 15 06.2	68 22 34.3	7.6	+167.7	+179.2	+ 71.3
38	12 15 14.3	68 23 25.0	17.0	+170.3	+182.0	+ 73.7
39	12 15 31.2	68 24 27.4	9.3	+166.1	+182.0	+ 73.0
40	12 16 00.6	68 24 42.9	0.4	+156.8	+175.6	+ 65.4
41	12 12 30.7	68 15 33.4	40.0	+156.0	+160.6	+ 56.7
42	12 06 45.8	68 17 08.1	0.7	+163.6	+171.0	+ 76.8
43	12 12 19.3	68 14 49.5	35.0	+156.8	+161.9	+ 57.8
44	12 11 49.7	68 13 25.9	23.8	+156.4	+162.8	+ 58.7
45	12 12 53.9	68 11 43.8	4.7	+135.4	+146.9	+ 39.0

TABLE 3 (*continued*)

Station number	Latitude N	Longitude W	Station Height, m	Free Air Anomaly, mgal	Bouguer Anomaly, mgal	Isostatic Anomaly, R=0, T=30 mgal
46	12°12′02.6″	68°12′20.2″	4.7	+141.6	+151.1	+ 45.6
47	12 11 25.0	68 13 01.2	22.4	+157.7	+164.2	+ 60.2
48	12 11 31.2	68 12 32.7	4.7	+151.0	+159.8	+ 55.6
49	12 08 37.3	68 15 30.3	8.1	+169.9	+176.0	+ 78.8
50	12 04 51.6	68 13 48.2	3.4	+176.7	+183.5	+ 90.3
51	12 04 04.7	68 13 31.9	3.1	+182.6	+189.6	+ 97.0
52	12 02 51.2	68 13 29.0	1.7	+178.1	+185.7	+ 94.0
53	12 01 52.8	68 14 07.3	10.5	+170.2	+178.3	+ 87.7
54	12 02 26.1	68 15 40.7	1.5	+162.0	+170.0	+ 80.0
55	12 14 45.8	68 20 03.4	22.1	+154.4	+163.1	+ 55.6
56	12 15 28.2	68 20 19.1	9.5	+151.2	+162.3	+ 53.2
57	12 16 05.1	68 20 19.6	5.0	+145.4	+158.2	+ 47.7
58	12 16 39.1	68 21 18.2	4.4	+145.7	+159.8	+ 48.0
59	12 18 10.4	68 22 17.7	9.8	+131.7	+150.0	+ 33.7
60	12 18 22.1	68 23 49.1	5.0	+128.1	+149.8	+ 33.2
61	12 17 16.3	68 21 45.6	10.7	+141.6	+156.3	+ 42.6
62	12 17 26.9	68 22 06.8	27.7	+142.6	+156.1	+ 41.8
63	12 17 17.1	68 22 36.4	41.1	+148.2	+160.0	+ 46.4
64	12 17 11.5	68 23 19.0	49.0	+149.6	+161.1	+ 47.6
65	12 17 07.9	68 23 48.6	28.0	+151.7	+165.8	+ 52.4
66	12 17 11.3	68 24 06.2	11.5	+147.7	+164.4	+ 50.9
67	12 17 05.1	68 24 42.0	7.5	+144.9	+165.2	+ 51.9
68	12 14 15.4	68 20 04.7	34.0	+156.9	+163.9	+ 57.5
69	12 13 59.4	68 20 31.0	106.0	+163.2	+163.1	+ 57.4
70	12 10 13.0	68 18 07.1	1.5	+150.9	+159.4	+ 60.9
71	12 09 56.8	68 17 40.8	1.4	+153.6	+161.5	+ 63.2
72	12 09 33.2	68 17 28.5	1.4	+154.6	+162.8	+ 65.1
73	12 09 42.3	68 18 05.7	3.0	+152.4	+160.2	+ 62.5
74	12 09 59.2	68 17 04.2	0.6	+157.2	+165.0	+ 66.4
75	12 08 51.1	68 15 50.4	2.3	+165.4	+172.3	+ 74.9
76	12 09 17.7	68 15 02.9	13.7	+177.2	+183.0	+ 84.4
77	12 09 22.4	68 14 31.6	17.0	+183.7	+189.3	+ 90.3
78	12 09 14.3	68 13 57.4	19.0	+184.5	+189.9	+ 90.7
79	12 09 13.6	68 12 40.6	10.0	+178.1	+184.9	+ 84.8
80	12 09 43.5	68 13 20.6	16.9	+179.0	+185.2	+ 84.8
81	12 09 18.7	68 15 34.3	8.5	+172.2	+178.6	+ 80.3
82	12 09 22.5	68 16 15.2	2.2	+161.7	+168.9	+ 70.8
83	12 09 19.4	68 11 55.1	3.8	+164.7	+173.1	+ 72.3
84	12 08 28.2	68 13 14.3	14.0	+184.3	+190.2	+ 91.7
85	12 07 38.4	68 13 33.6	0.8	+175.4	+182.5	+ 85.4
86	12 06 58.6	68 13 00.6	0.9	+178.1	+185.3	+ 88.7
87	12 01 44.3	68 14 36.3	0.6	+165.4	+173.9	+ 83.7
88	12 09 10.1	68 16 29.0	2.0	+160.5	+168.0	+ 70.4

TABLE 4

Gravity observations at sea.

Profile	Latitude N	Longitude W	Depth m	Anomalies in milligal			Corrections in 0.1 milligal		
				Free-air	Bouguer	Isostatic T=30, R=0	Topog.	R=0 comp. A—O2	R=0 t+c 18—1
A	15°03.7′	68°49.0′	4322	+ 10	+307	+ 12	+2969	—2666	—283
	14 10.0	69 07.8	4836	— 35	+289	— 8	+3239	—2702	—262
	13 29.7	69 22.9	3943	—112	+156	— 85	+2679	—2175	—235
	13 16.2	69 26.7	2900	— 91	+114	— 83	+2049	—1740	—228
	12 49.4	69 36.1	1577	— 46	+ 53	— 53	+ 990	— 856	—205
	12 29.2	69 43.2	940	— 65	— 4	— 79	+ 608	— 570	—175
	12 22.5	69 45.5	510	+ 15	+ 50	— 9	+ 350	— 417	—175
C	12 11.6	69 50.4	48	+ 27	+ 28	— 6	+ 11	— 178	—160
	12 11.6	69 41.0	350	— 2	+ 22	— 28	+ 246	— 343	—160
	12 15.4	69 14.4	1244	— 60	+ 19	— 56	+ 781	— 566	—180
D	12 03.0	68 57.0	713	+ 55	+104	+ 34	+ 489	— 537	—170
	11 46.5	69 02.0	1348	— 23	+ 66	+ 8	+ 887	— 420	—155
	11 31.9	69 05.5	53	— 9	— 5	— 31	+ 40	— 126	—130
B	11 58.8	68 48.8	896	+ 30	+ 78	+ 9	+ 483	— 524	—170
	12 02.2	68 41.8	604	+101	+139	+ 58	+ 380	— 636	—170
	12 20.5	68 29.2	2041	— 47	+ 87	— 36	+1340	—1049	—180
	12 34.4	68 21.2	3435	—167	+ 51	—118	+2182	—1484	—205
	12 48.2	68 13.1	1802	— 64	+ 93	—104	+1567	—1748	—220
	13 15.9	67 56.7	4726	— 90	+209	— 58	+2993	—2435	—235
	13 43.6	67 40.3	5063	— 24	+315	— 1	+3392	—2916	—250
	14 11.3	67 23.9	5070	— 15	+329	+ 7	+3440	—2951	—270
	14 39.0	67 07.5	5066	— 18	+327	— 3	+3455	—3021	—284

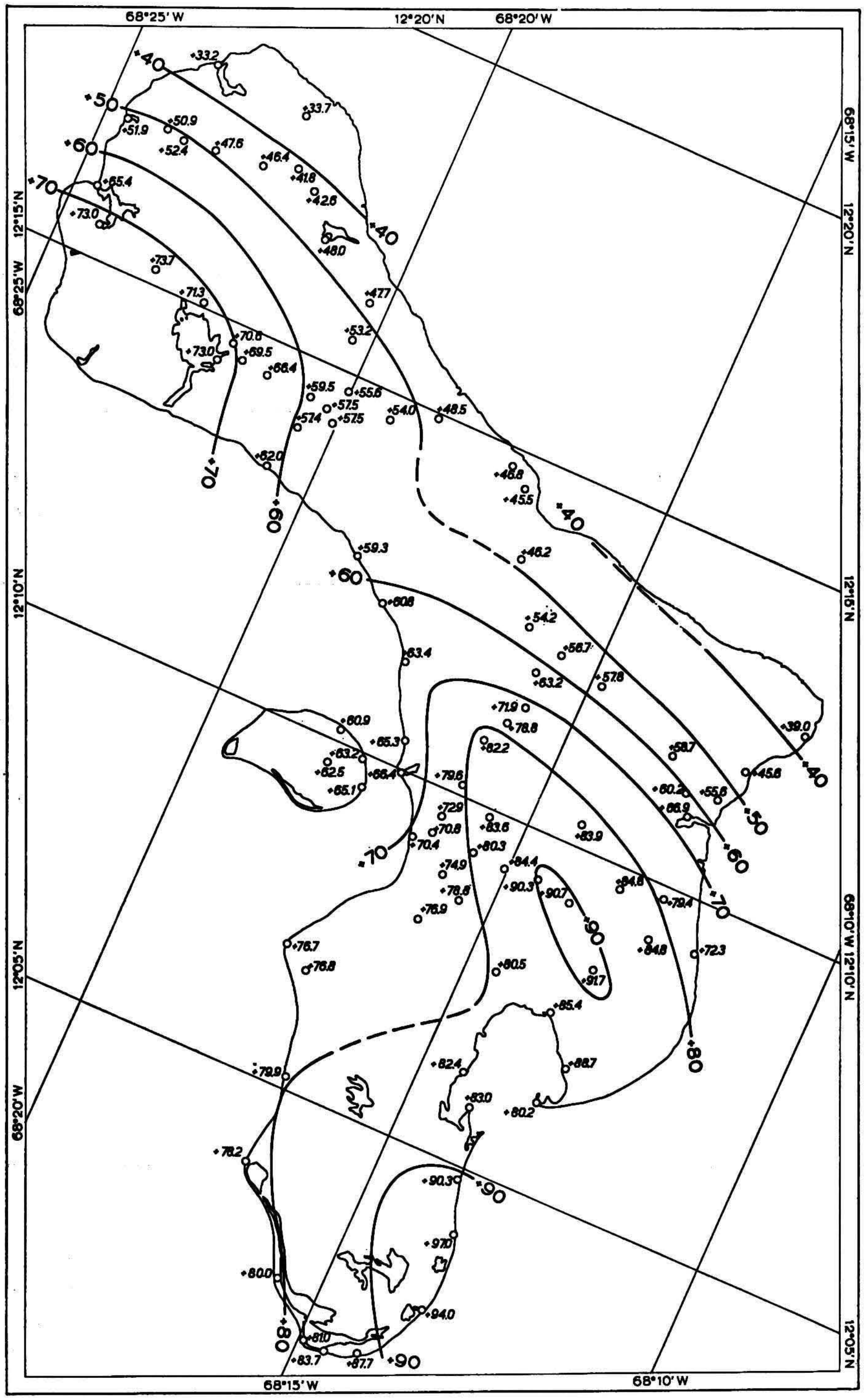

Fig. 3. Isostatic anomaly map of Bonaire (T=30, R=0).

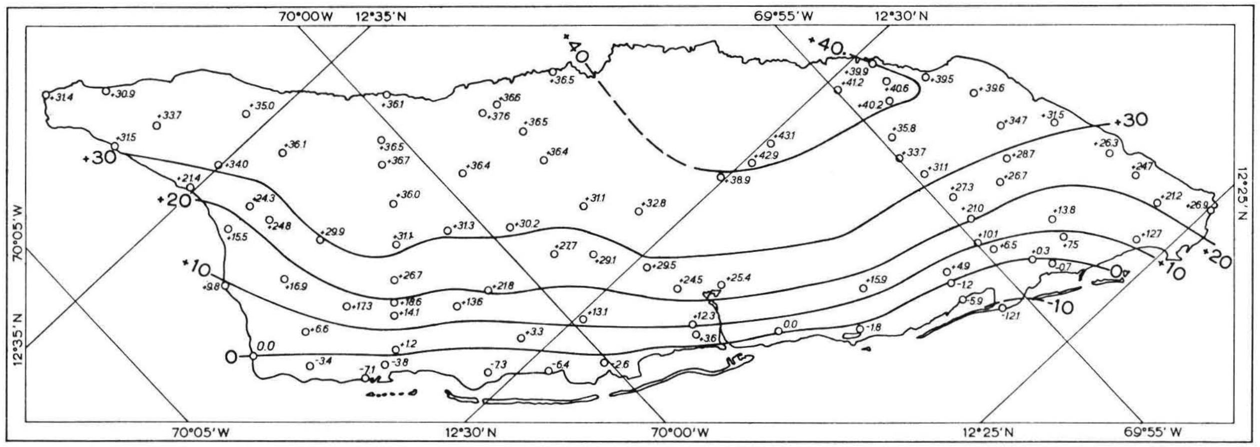

Fig. 1. Isostatic anomaly map of Aruba (T=30, R=0).

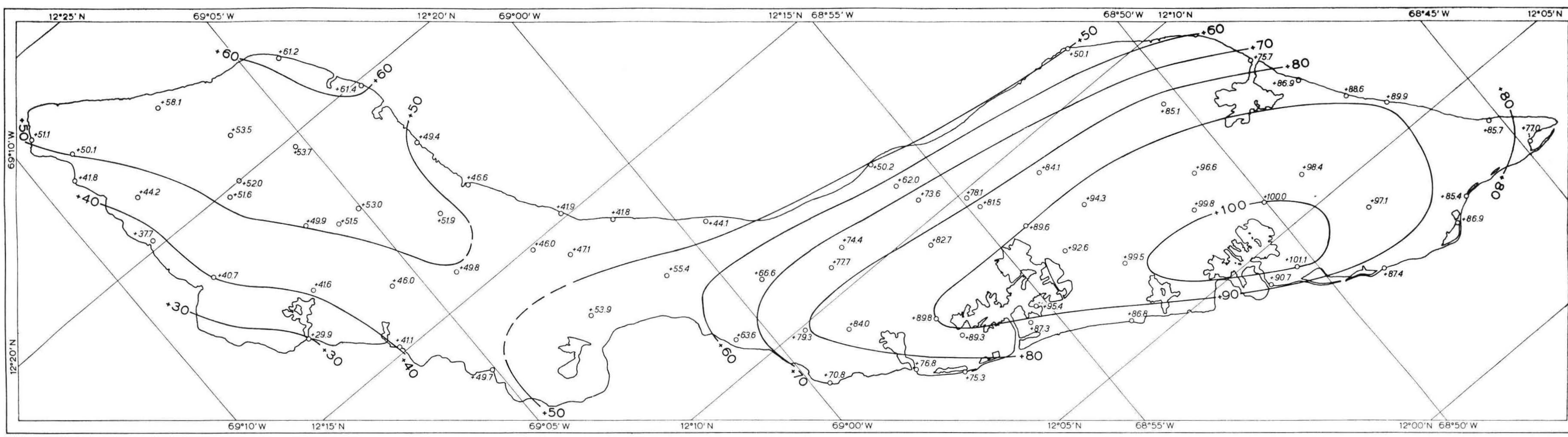

Fig. 2. Isostatic anomaly map of Curaçao (T=30, R=0).

anomalies. The anomalies generally follow the trend of the islands. The largest positive anomaly occurs on the eastern part of Curaçao, where values of more than 100 mgal are found. In the western part of Curaçao a positive anomaly of more than 60 mgal occurs. On Bonaire the largest anomaly has a value of more than +90 mgal; it is situated in the central part of the island. Towards the western edge of the island anomaly values of more than +70 mgal are met with. The largest anomaly on Aruba occurs in the northeastern part of the island; it attains a value of more than +40 mgal. All these anomalies are observed above outcrops of volcanic formations (see Geology and the geologic maps of fig. 11). Tentatively we may infer therefore that the large positive anomalies of the islands are related to the occurrence of high density volcanics near the surface. This inference will be elaborated in the chapter on the interpretation of the gravity data. The profile to be discussed in that chapter runs across the large anomaly in the eastern part of Curaçao.

The data of the anomaly charts of the islands have been incorporated in the chart of isostatic anomalies of the area surrounding the Netherlands Antilles. This area is bounded by the meridians of 66°30′ and 71°00′W and the latitudes of 10°45′ and 14°30′N. It comprises the islands of Los Monjes, Aruba, Curaçao, Bonaire, Las Aves and Los Roques. The contour lines at sea have been drawn on the basis of the gravity observations during cruises of Netherlands and American submarines (see 'Previous work') and of the continuous measurements on board H.Neth.M.S. *Snellius*. The contour interval is 25 mgal. The map will be discussed in the chapter on the interpretation of the gravity data.

A regional structural map of the southern Caribbean area has been drawn in which the axes of zones of gravity anomalies are represented by minus and plus signs for negative and positive zones respectively (fig. 23). The position of these axes at sea was determined from the pendulum stations, mentioned under the heading Previous work (local isostatic anomalies). On land the axes were taken from De Bruyn's map (1951) (Hayford–Bowie isostatic anomalies).

The gravity anomaly profiles based on the observations on board H.Neth.M.S. *Snellius* are presented in figures 15 and 16. The curves of free air anomalies, Bouguer anomalies (topographic correction out to zone O_2) and local isostatic anomalies are given together with the curve of anomalies of total magnetic intensity and with the bathymetry. With regard to the bathymetric profile it is noted that the depths have been corrected for the speed of sound in water by means of Matthew's tables (1939).

Geomagnetism

Geomagnetic observations

The geomagnetic measurements on the islands of Aruba, Curaçao and Bonaire were carried out in the summer of 1962. The components measured were: the horizontal force, the vertical force and the declination if possible. The observation sites all are near bench-marks of the Cadastral Service of the Netherlands Antilles, giving us the correct geographical position of the stations. The observation sites were selected at distances of about 5 km, avoiding objects which might produce artificial disturbances such as buildings, roadways and iron masses. The measurements for the vertical component in general were carried out two or three times within a distance of about 25 meters. If the outcome of these measurements indicated that, notwithstanding our precautions, artificial disturbances were present, the measurements were repeated in the vicinity, rejecting the first series.

The instruments used were placed at our disposal by the Royal Netherlands Meteorological Institute at De Bilt, with the exception of a Wild-theodolite for the declination measurements lent by the Cadastral Survey Department of the Netherlands Antilles. The instruments and methods of measurement have been described extensively by VELDKAMP (1951). Only a few additional remarks will be made here in this respect.

At sea the total force F, was measured along two lines running approximately N–S.

The declination

The declination D, the angle between the astronomical north and the magnetic north, was determined in the following way. The magnetic azimuth of lines connecting triangulated points was measured with a Wild-theodolite. The geographic azimuth was calculated from triangulation data by the Cadastral Survey Department. The difference gives the declination. On each site several azimuths were determined. The accuracy of the determinations appeared to be 0.3′.

The horizontal component

The horizontal component H, was determined with a QHM (quartz horizontal magnetometer). QHM 512 and QHM 344 were used. The quartz-wire of QHM 344 broke during transport in the field so that for the greater part of the survey only QHM 512 was available.

The horizontal component of the earth's field H was calculated from

$$\log H = C - \alpha t - \log \sin \varphi + \text{calibration term}$$

t = temperature

φ = measured mean deviation of the magnet of the instrument

The constant C is dependent on the torsion coefficient of the quartz-wire and on the magnetic moment of the magnets. This constant and the temperature coefficient α were provided by the Royal Netherlands Meteorological Institute at De Bilt. For QHM 512 these values are $C = 9.1917$ and $\alpha = 0.00200$, for QHM 344 these are $C = 9.39674$ and $\alpha = 0.000185$. An instrumental correction for the QHM's was obtained by calibrating them with the absolute H-instrument in the magnetic observatory Witteveen. The calibration term for QHM 512 was -5γ, for QHM 344 the calibration term was -11γ. The instrumental accuracy is estimated at 1γ.

The vertical component

A BMZ (magnetometric zero balance) was used. The vertical component of the earth's field, Z, was determined from the formula

$$Z = Z_c + Z_s + Z_p - \alpha t$$

Z_c depends on the magnetic moment of the main magnet of the instrument and on the distance between the main magnet and the balance magnet. Z_s is the field-strength of an auxiliary magnet. Z_p is the field strength of the turning magnet, the values of which are tabulated for different angles. The temperature coefficient α is proportional to Z_c and $Z_s + Z_p$; it may be supposed to be constant if Z_p does not vary too much, as in our measurements. The instrument used was the BMZ 26A. The value of Z_s and of Z_p at different angles and the value of α were provided by the Royal Netherlands Meteorological Institute. The influence of the auxiliary magnet 26–1 amounted to 981γ (Z_s). Z_p may vary between 0 and 1155γ.

Z_c was determined from a comparison of BMZ measurements and computed values of the vertical component as derived from measurements of the horizontal component and the inclination. The determination of Z_c was carried out twice: at the beginning of the survey and at its end. The first determination took place near Antriol on Bonaire, the second near St. Jacob on Curaçao. Before and after the measurements of the inclination, I, two QHM and BMZ measurements were made. The values of H and Z thus obtained, were averaged for the determination of Z_c. The values of Z from the BMZ measurements were obtained using a provisional value for Z_c. Correcting this value for the difference between Z determined from the BMZ measurements and Z determined from the relation $Z = H \tan I$, gives Z_c:

	Antriol (Bonaire)	St. Jacob (Curaçao)
Position	12°09′55″N – 68°15′33″W	12°10′21″N – 68°55′08″W
H	29022	28729
I	43°55′.1	44°11′.8
Z from H and I . . .	27947	27934
Z_c	28603	60284

It therefore was assumed that Z_c remained the same throughout the survey.

The formula for Z used for BMZ 26A without auxiliary magnet is:

$$Z = 28604 + Z_p - 8.3\ t$$

The instrumental accuracy was estimated at 1γ under favourable conditions.

The inclination

The inclination I was measured with the earth inductor. The measurements were carried out in the open field. It is estimated that the accuracy of the determinations is no more than about 0.3′, resulting in an inaccuracy of about 4γ in the vertical force derived from I and H.

The total force

At sea the total force was measured with a proton-precession-magnetometer. The instrument was built at the Royal Netherlands Meteorological Institute. The total force was measured and recorded every 30 seconds. No correction is needed for this instrument with respect to the basic value of the station Witteveen. The error resulting from the ship's magnetic influence was less than 5γ if the magnetometer-fish was towed at a distance of more than 115 m astern. The report NAVADO III (1967) gives details of the instrument and its accuracy.

The reduction of the magnetic intensities H, Z and F

Since there exists no magnetic observatory on the Netherlands Antilles no direct information is available of the variations of the magnetic field on the islands with time. Nevertheless, an attempt was made to reduce the magnetic intensities measured in 1962, for the daily and secular variation.

The nearest observatory is the San Juan Magnetic Observatory on Puerto Rico, which lies at a distance of about 6° to the north from the Netherlands Antilles. Since according to CHAPMAN and BARTELS (1940, p. 140) the records of a magnetic observatory in a moderate or low latitude fairly well represent the changes with time within about 500 km distance, it was assumed that the San Juan magnetograms were sufficiently adequate. It is true that San Juan lies further away from the Netherlands Antilles than 500 km, but the fact that the variations in D on August 1st and 6th, 1952 at Bonaire and Curaçao respectively (measured by ROMERO, 1961) are of the same magnitude as those at San Juan with respect to local time, justifies our assumption.

A correction for the daily variation of H and Z was applied, based on the variations at San Juan with respect to the mean values of the pertinent measuring periods. The magnetograms were kindly provided by the U.S. Coast and Geodetic Survey. The correction for the daily variation was between +40 and −50 γ for H and Z.

It was further decided to reduce all H and Z determinations to the year 1965, since this facilitated the construction of the magnetic anomaly charts. The charts of the magnetic elements for 1965 of the U.S. Hydrographic Office (H.O. 1701–1703) also represent the isolines of the secular variation. The values of the secular variation relative to the three islands were determined from this map and added to the H and Z values corrected for the daily variation to obtain H and Z for the year 1965. The correction for the secular variation of Z was about $-230\ \gamma$; for H it was about $-60\ \gamma$.

As regards the continuous measurements of the total magnetic intensity at sea the daily variations were neglected. Since the apparent wave lengths resulting from the daily variation are about 150 to 200 km for the ships speed, the variations in question are not likely to be confused with the magnetic disturbances from sources within the earth's crust. The measurements of F were made in December 1964 and January 1965, so no correction for the secular variation was made.

The magnetic anomalies

A regional field has to be subtracted from the observed field in order to obtain the magnetic disturbances of local character. This regional field must be chosen such that it corresponds to the undisturbed part of the field in the surveyed area. Since the magnetic field in the Netherlands Antilles is highly disturbed, it is not well possible to obtain this regional field from the land measurements. The formulas for the components of the regional field have therefore been obtained from the world charts of the magnetic elements for the year 1965 of the U.S. Hydrographic Office and from the profiles of total intensity at sea.

Assuming that in a small area as the one under consideration the components of the normal fields are sufficiently described by a linear function of the latitude, φ, and the longitude, λ, the function for the regional value of the total intensity, F_n, was obtained by drawing average base lines through the measured intensities on both of the ship tracks, the slope and the intersection of which gives the function:

$$F_n = 40000 + 11.56(\varphi - \varphi_0) + 1.18(\lambda - \lambda_0)$$

$$\text{where } \varphi_0 = 12°34'.5$$

$$\lambda_0 = 69°00'.0$$

The differences are expressed in minutes.

This function agrees reasonably well with the one that may be obtained from the H.O. chart of total intensities for the year 1965. The functions for the components H and Z, were in first instance taken from the H.O. charts in question. However, considering that $H_n^2 + Z_n^2 = F_n^2$ some alterations of the functions for H_n and Z_n were necessary to adapt them to the function of F_n, this gave

$$H_n = 28930 - 2.00(\varphi - \varphi_0) + 1.44(\lambda - \lambda_0)$$

$$Z_n = 27623 + 18.83(\varphi - \varphi_0) + 0.20(\lambda - \lambda_0)$$

TABLE 5

Geomagnetic observations on the Netherlands Leeward Antilles.

Station no. [1]	Latitude N	Longitude W	Measured magnetic components [2]			Magnetic components reduced to 1965		Magnetic anomalies	
			D	H	Z	H	Z	ΔH	ΔZ
1	12°07′01″	68°17′34″		28860 γ	27869 γ	28782 γ	27615 γ	—141 γ	+517 γ
2	12 05 11	68 16 47	2°56.0′	28998	27837	28932	27578	+ 6	+515
3	12 01 44	68 14 56		29090	27582	29018	27330	+ 87	+333
4	12 07 54	68 14 33		29112	27695	29060	27443	+142	+330
5	12 05 52	68 14 04	5 34.7	28839	27698	28789	27442	—132	+367
6	12 06 20	68 13 11		28876	27707	28802	27453	—117	+369
7	12 09 52	68 12 41		28965	27718	28895	27479	— 16	+329
8	12 09 55	68 15 33		29022	27947	28963	27691	+ 48	+540
9	12 11 06	68 12 52		28798	27584	28746	27345	—163	+172
10	12 11 36	68 15 44		28655	27665	28565	27426	—347	+243
11	12 14 46	68 17 23		28623	28475	28531	28236	—377	+993
12	12 14 39	68 19 21		28504	27718	28615	27479	—296	+238
13	12 14 24	68 22 02	5 39.0	28631	27952	28533	27706	—383	+469
14	12 13 14	68 20 11		28806	27749	28741	27495	—174	+281
15	12 12 36	68 18 57		28893	27667	28828	27413	— 86	+210
16	12 16 01	68 24 43		28976	27579	28862	27340	— 54	+ 72
17	12 13 19	68 12 49		28818	27541	28753	27297	—151	+ 82
18	12 04 05	68 13 32		28915	27841	28876	27582	— 47	+541
19	12 16 06	68 20 20		28802	28074	28741	27824	—168	+555
20	12 18 23	68 23 49		28928	27906	28880	27662	— 30	+350
21	12 09 14	68 16 26		28838	27651	28786	27397	—132	+259
22	12 17 08	68 23 49		28811	27806	28728	27551	—184	+262
23	12 09 42	68 18 06		28738	27709	28688	27465	—251	+317
24	12 09 57	68 17 41	6 21.2						
25	12 11 43	68 15 59	0 03.2						
26	12 07 45	68 58 07		29023	27499	28964	27268	— 17	+149
27	12 08 41	68 50 23	4 54.0	28951	27564	28915	27369	— 53	+234
28	12 06 19	68 53 55		29047	27510	29006	27248	+ 9	+157
29	12 16 44	69 03 49		29093	27706	29034	27452	+ 62	+163
30	12 05 23	68 48 17		29124	27626	29074	27362	+103	+290
31	12 22 12	69 09 23	4 36.3	29110	28024	29041	27785	+ 72	+392
32	12 10 21	68 55 08		28729	27934	28679	27739	—292	+572
33	12 16 55	69 06 48		29065	27719	29006	27460	+ 31	+167
34	12 08 09	68 53 03		28980	27654	28917	27444	— 56	+318
35	12 10 53	68 51 13		29120	28332	29048	28142	+ 84	+966
36	12 10 44	68 57 40		28380	28176	28344	27966	—631	+791
37	12 03 04	68 44 52		29094	27437	29040	27234	+ 69	+206
38	12 02 47	68 47 12		29022	27437	28983	27222	+ 8	+199
39	12 04 17	68 50 25		29032	27462	29001	27260	+ 25	+208
40	12 05 40	68 49 06		28520	27499	28492	27289	—481	+211

41	12 12 40	69 00 55		29090	27606	29058	27418	+ 83	+206
42	12 13 28	69 05 09		29000	27610	28959	27420	— 20	+192
43	12 15 08	69 01 51		29152	27869	29114	27679	+142	+424
44	12 08 42	68 59 45		29168	27523	29097	27333	+115	+196
45	12 19 48	69 05 17		29081	28087	29048	27888	+ 81	+541
46	12 16 51	69 06 25		29388	27814	29321	27615	+346	+330
47	12 19 07	69 08 29		29038	27741	28972	27541	— 1	+206
48	12 22 15	69 06 59		28700	28109	28659	27902	—306	+509
49	12 06 06	68 47 07	5 0.3						
50	12 :1 52	68 51 51	6 32.7						
51	12 09 17	68 55 58	5 13.7						
52	12 12 12	69 00 38	4 44.9						
53	12 16 33	69 03 40	1 32.3						
54	12 22 20	69 06 55	4 49.3						
55	12 16 46	69 06 01	4 53.1						
56	12 16 15	69 03 27	4 21.3						
57	12 29 54	69 56 30		28996	27780	28946	27570	+ 88	+ 26
58	12 31 04	69 58 55		29280	28314	29228	28095	+376	+525
59	12 28 55	69 58 02		29270	28080	29238	27855	+380	+329
60	12 32 47	70 01 05		28526	28172	28478	27962	—368	+362
61	12 34 08	69 59 42		28527	28417	28470	28214	—378	+586
62	12 34 21	70 02 06		28678	29014	28624	28789	—216	+1157
63	12 27 33	69 56 35		28890	28171	28818	27961	— 34	+458
64	12 27 26	69 53 44		28727	27776	28643	27571	—224	+ 70
65	12 29 29	69 54 19		29132	27974	29039	27749	+177	+210
66	12 25 41	69 52 20		28797	28132	28738	27907	—135	+242
67	12 29 56	69 59 50		29265	28646	29188	28441	+335	+892
68	12 32 47	69 57 45		28958	27679	28886	27469	+ 36	—133
69	12 36 41	70 02 60		28985	28106	28908	27891	+ 73	+215
70	12 34 32	70 01 21		28998	28342	28933	28133	+ 91	+497
71	12 31 36	70 02 40		29066	28438	28979	28237	+133	+659
72	12 26 34	69 52 40	3 42.3						
73	12 27 11	69 56 41	3 59.8						
74	12 30 14	69 57 41	5 0.5						
75	12 31 39	70 00 14	3 49.0						
76	12 35 16	70 02 08	4 12.8						
77	12 34 31	70 02 29	3 15.8						
78	12 34 25	70 01 25	4 22.1						
79	12 33 34	70 01 01	5 36.5						
80	12 34 27	70 00 16	4 38.6						

[1]) stations 1–25 are located on Bonaire
stations 26–56 are located on Curaçao
stations 57–80 are located on Aruba

[2]) Inclination measurements:
station 32 (Curaçao) I=44°11.8′
station 8 (Bonaire) I=43°55.1′

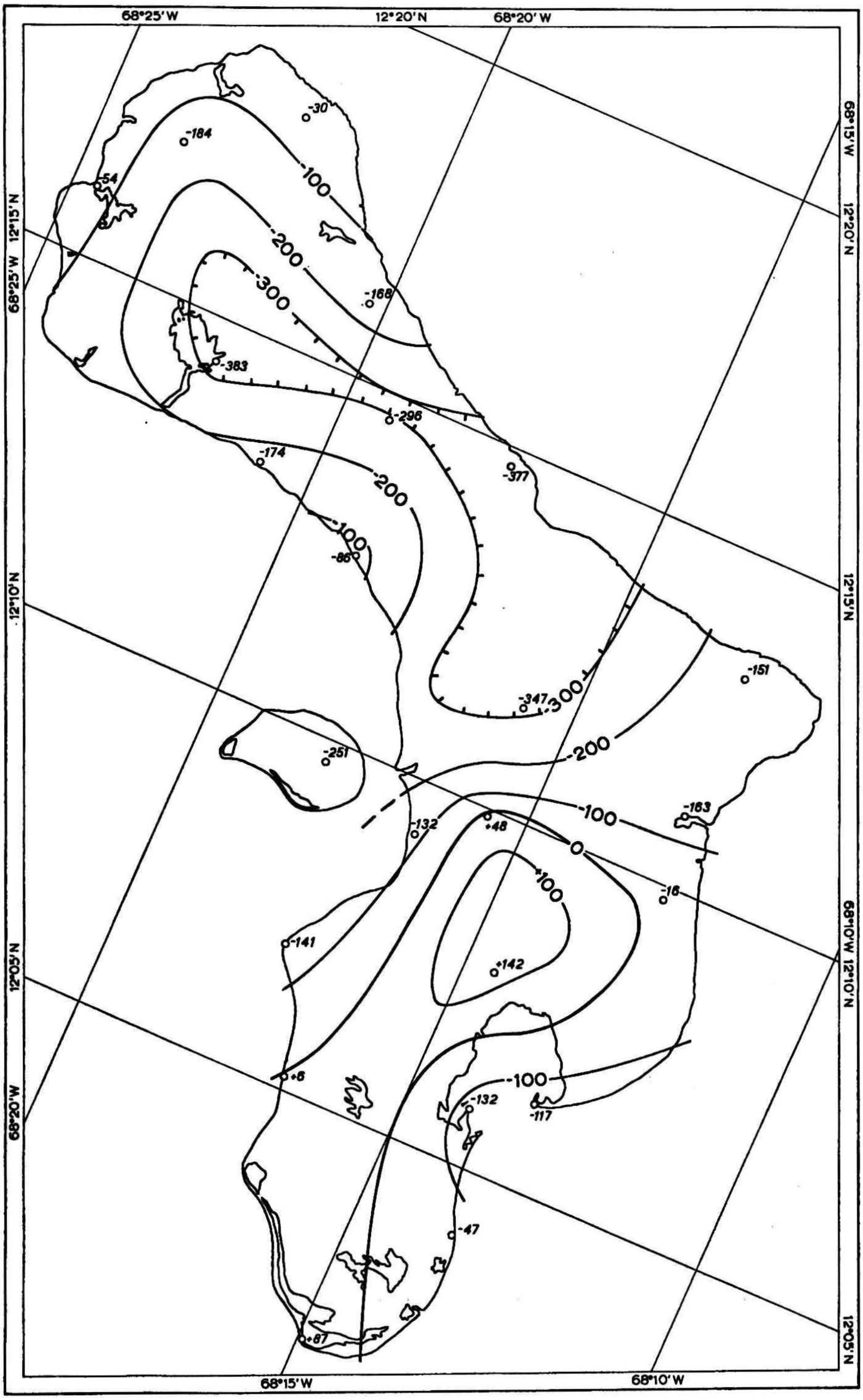

Fig. 6. Magnetic anomaly map of Bonaire for ΔH.

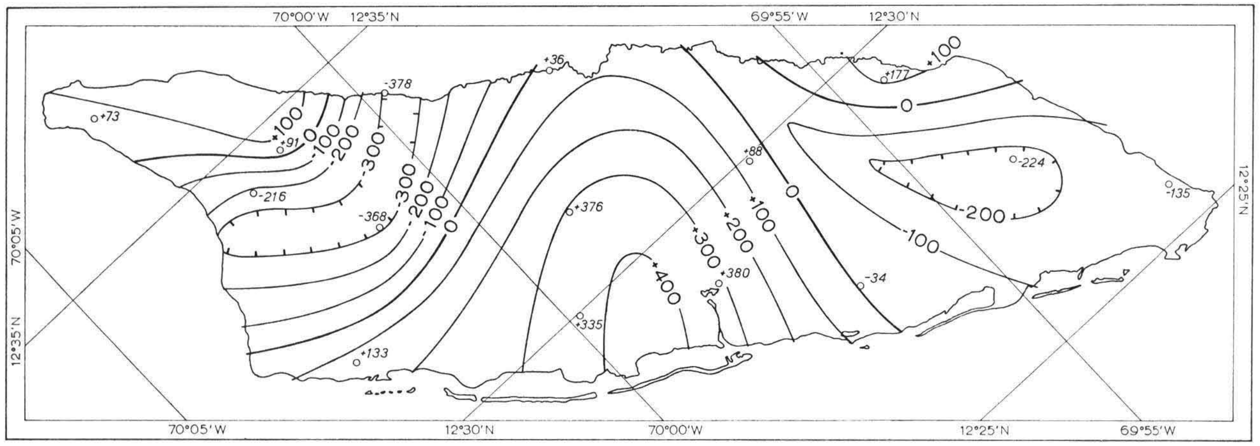

Fig. 4. Magnetic anomaly map of Aruba for ΔH.

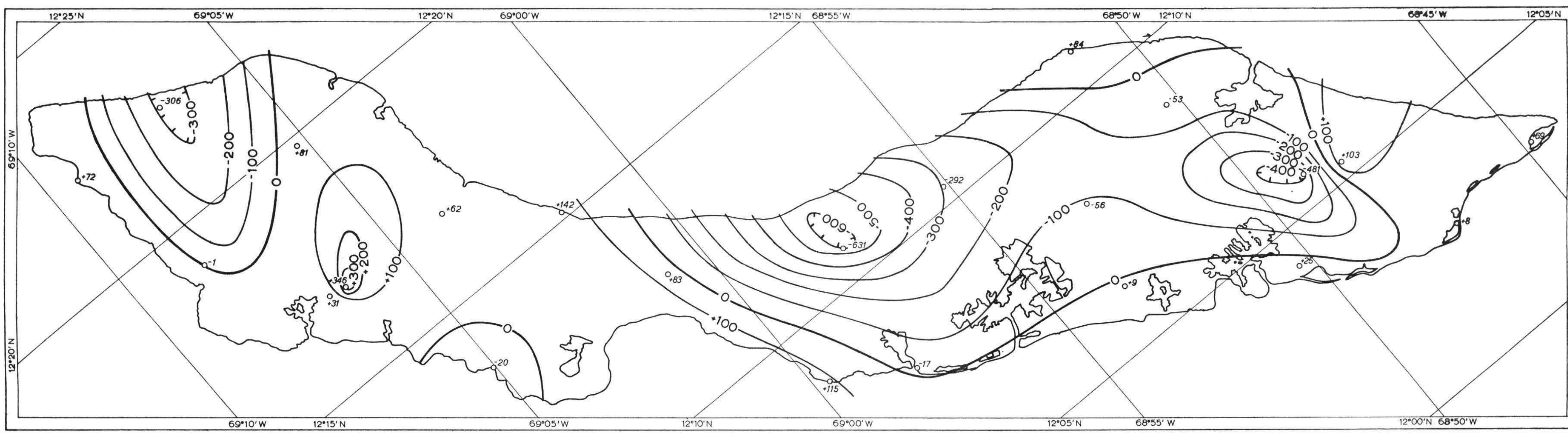

Fig. 5. Magnetic anomaly map of Curaçao for ΔH.

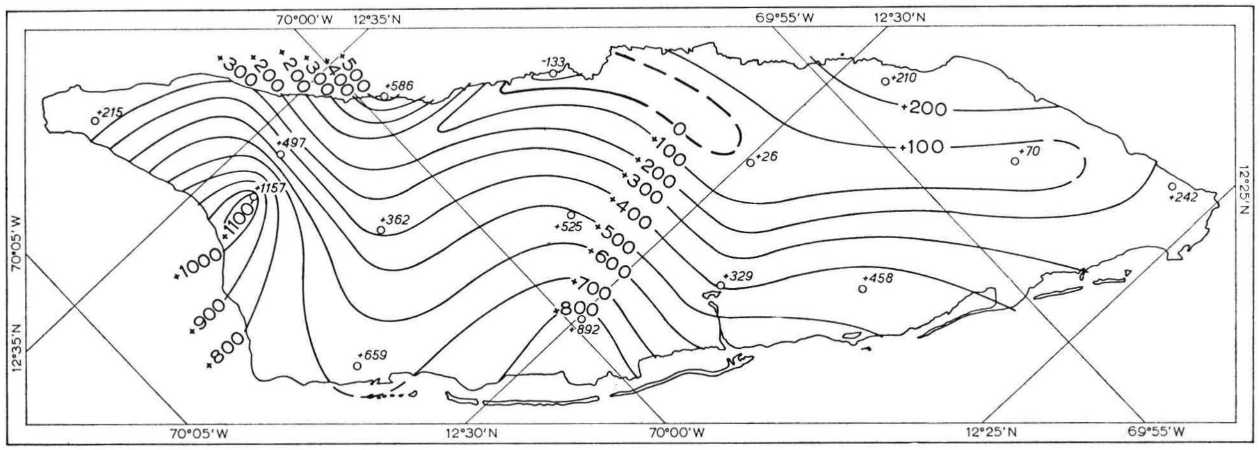

Fig. 7. Magnetic anomaly map of Aruba for ΔZ.

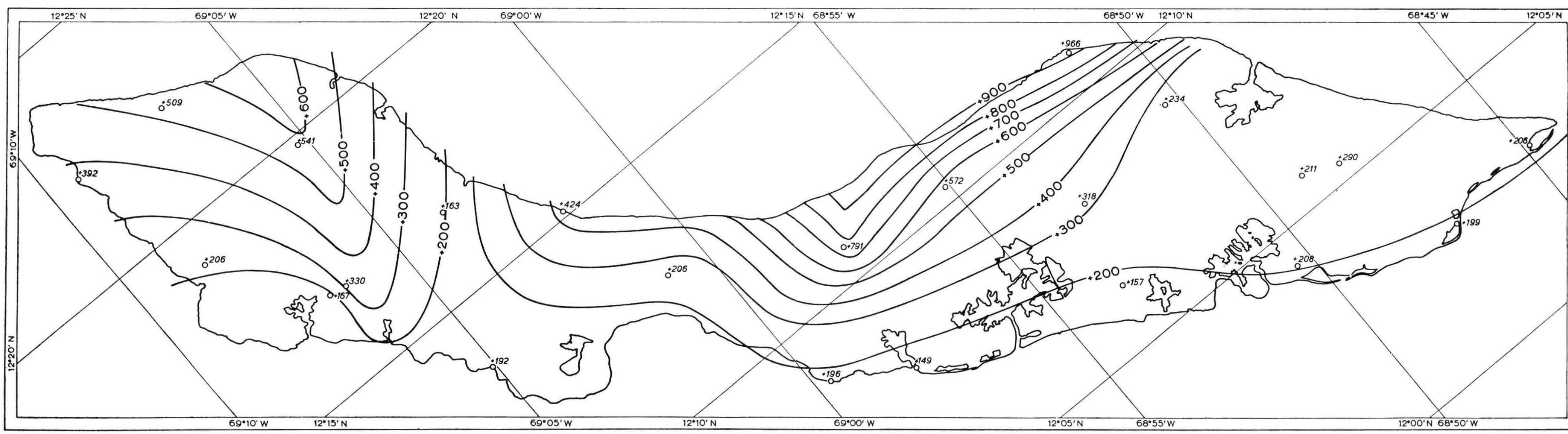

Fig. 8. Magnetic anomaly map of Curaçao for ΔZ.

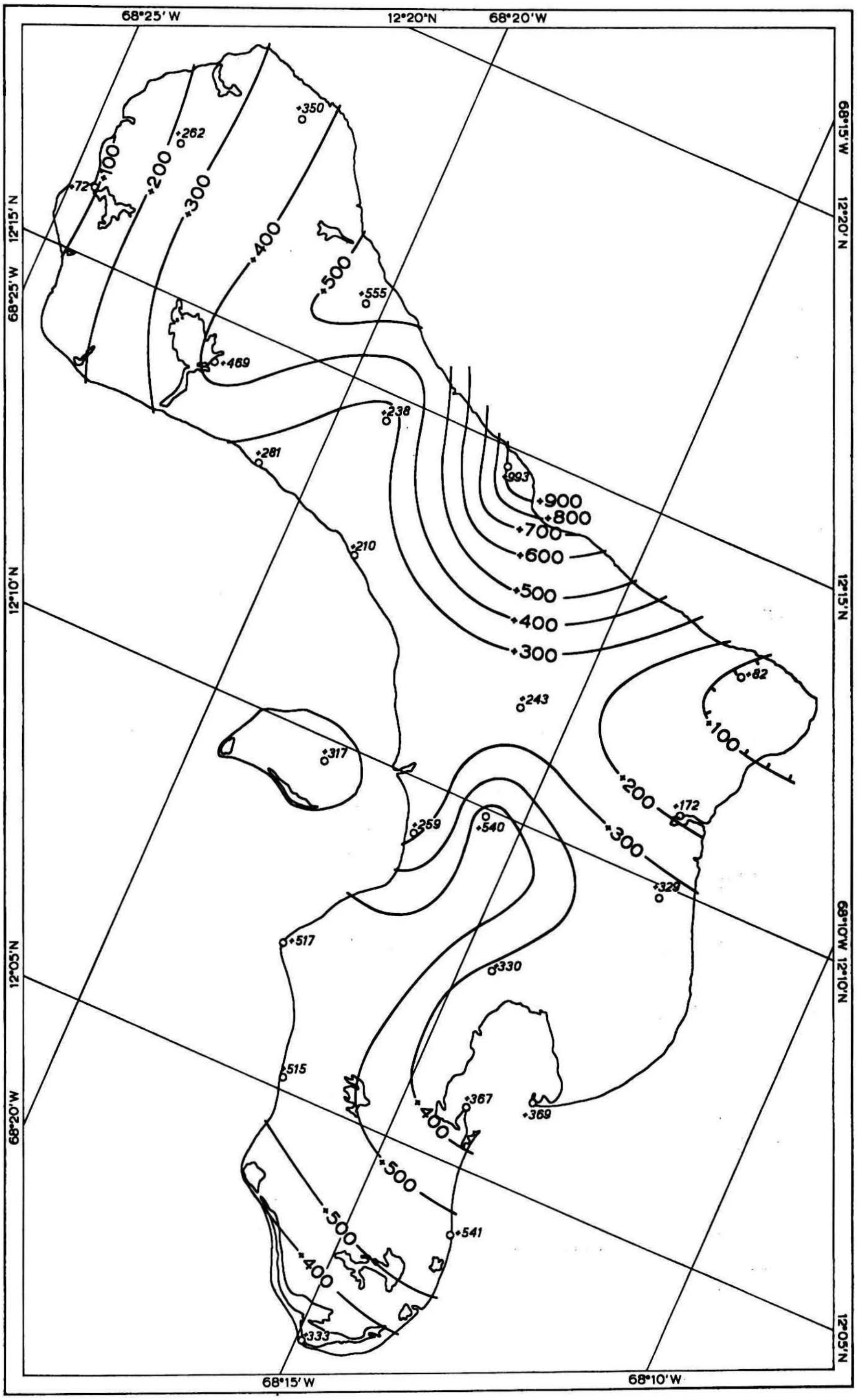

Fig. 9. Magnetic anomaly map of Bonaire for ΔZ.

With these relations we obtained the anomalies for the magnetic components, ΔH and ΔZ, measured on the islands as well as the anomaly curves for the total intensity, ΔF, measured at sea.

Table 5 presents the geographic position of the land stations, the values of D, H and Z determined in 1962, the values of H and Z reduced to the year 1965 and the anomalies ΔH and ΔZ. In profiles 15 and 16 the curve for ΔF is given.

Charts and profiles

Charts were constructed for the islands of Aruba, Curaçao and Bonaire (fig. 4 to 9) with the anomalies of the horizontal component ΔH, and of the vertical component ΔZ. The isogams for ΔH and ΔZ were drawn for every 100γ. ΔH varies between -600γ and $+400\gamma$, ΔZ between -100γ and 1100γ. The anomalies of Z have a predominantly positive character.

From the charts of figures 4 to 9 it appears that the individual anomalies have large amplitudes. For instance the variation in ΔH in central Bonaire (fig. 6) amounts to about 500γ. The anomalies generally have a short

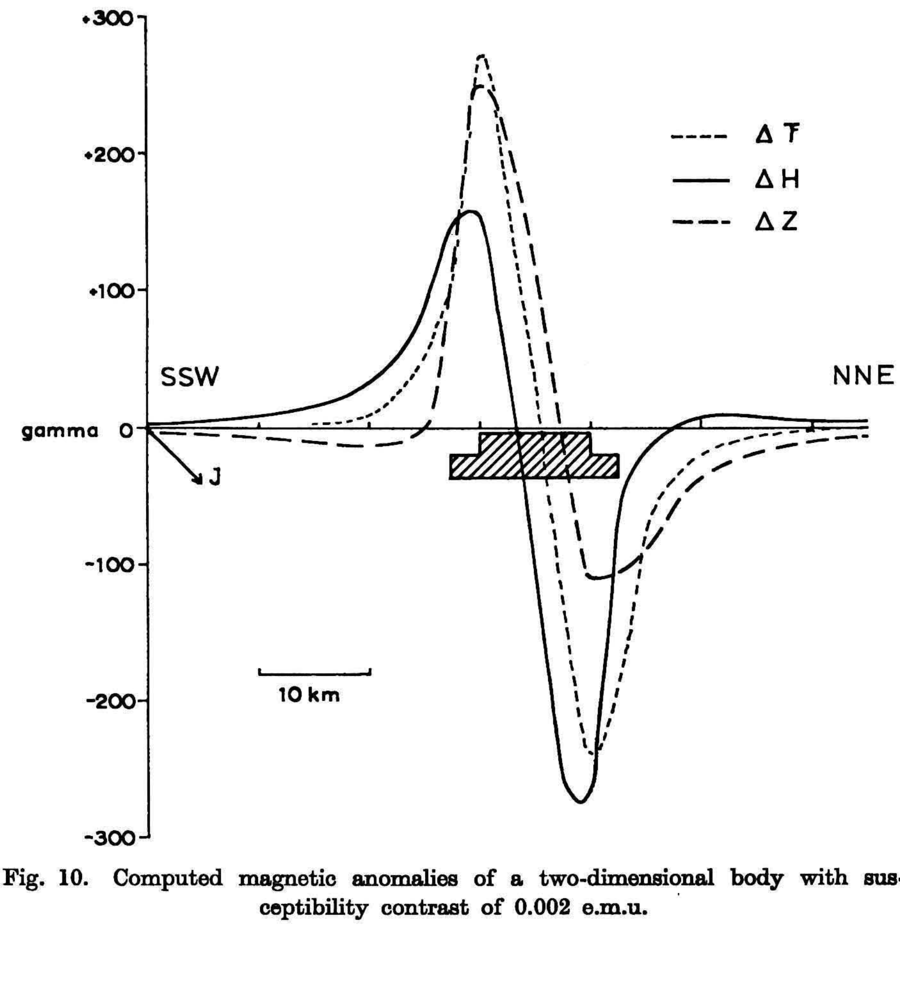

Fig. 10. Computed magnetic anomalies of a two-dimensional body with susceptibility contrast of 0.002 e.m.u.

wave-length character, the wave lengths, as far as can be observed, being around 20 km. This is in accordance with the character of the disturbances in other parts of the Caribbean island arc (EWING, ANTOINE and EWING, 1960). Such a character indicates a shallow seat of the source of the anomalies. The most probable inference is that the large anomalies are caused by the presence of volcanic rock types near the surface. In fact such rocks occur in large outcrops on the islands (see 'Geology'). The anomalies are, in general, not confined to the islands, which means that some of the anomalous magnetic bodies must continue under sea.

In order to give an impression of the parameters of the anomalous bodies we calculated (cf. p. 53) the anomalies in H and Z, assuming induced magnetization for a two-dimensional structure with a direction of 120° (the general direction of the islands) and a susceptibility contrast of 0.002 e.m.u. (fig. 10). It appears that in order to explain the observed amplitudes and the wave lengths, the anomalous body should have dimensions of the same order of magnitude as the islands. It is then not too far-fetched to relate the disturbing body to the diabase cores of the islands. This rock type may well have the mentioned susceptibility.

The anomaly curves of the total magnetic intensity ΔF at sea are given in figures 15 and 16. The curves differ somewhat from those presented in the Navado III report (1967), because of the application of a different expression for the regional field.

3. GEOLOGY

The Leeward Antilles form a chain of islands in the southern part of the Caribbean Sea (fig. 11) off the north coast of Venezuela. This chain of islands can be divided in two rows, one consisting from west to east of the islands of Los Monjes, Aruba, Curaçao, Bonaire, Las Aves, Los Roques, La Orchila, La Blanquilla and Los Hermanos. Southeast of La Orchilla there is another row starting with the island of La Tortuga. It continues eastward as far as the island of Tobago. The western islands may be taken as one group according to their position and their geology. Our study concerns the greater part of this island group and the surrounding sea.

THE WESTERN LEEWARD ANTILLES

The east-west running row of small islands north of Venezuela seem to form a geological unit. According to L. M. R. RUTTEN (1939, 1940) this unit extends at least from the Los Monjes islands in the west to La Blanquilla and Los Hermanos in the east, the geologic interconnection being shown by exposures of quartz-diorites and related rocks.

The following discussion refers mainly to the three isles of the Netherlands Antilles: Aruba, Curaçao and Bonaire. They are the greater in areal extent among the western group. Curaçao is the larger of the three; it comprises about 425 square kilometers. The geology of the Netherlands Antilles is relatively well known in comparison to that of the other isles (BEETS, 1966; BEETS and LODDER, 1967; DE BUISONJÉ, 1964; MACGILLAVRY, 1932; MARTIN, 1888; MOLENGRAAFF, 1929; PIJPERS, 1933; L. M. RUTTEN, 1932, 1935a and b, 1939; VERMUNT and M. G. RUTTEN, 1931a, b and c; and WESTERMANN, 1932, 1949, 1951). The following remarks are based on these studies, in particular on the recent work of Beets and De Buisonjé.

In main lines the three isles show the same geological framework; the core is formed by a Laramide folded complex that is largely of Cretaceous age, with, on some of the isles, intrusions of rocks of intermediate composition. This basal complex is unconformably overlain by younger deposits, mainly limestones of Neogene and Quaternary age (fig. 11, geologic sketch maps).

On Aruba the basal complex consists of an intensely folded series of submarine basic lavas and tuffs, the diabase-schist-tuff formation, which has been intruded by rocks forming a composite batholith, mainly consisting of quartz-diorite and subordinately of intrusive rocks ranging in composition from gabbros to granites. The age of the diabase-schist-tuff formation is unknown. According to WESTERMANN (1932) the intrusion of the quartz-diorite and associated rocks probably took place during folding of the complex. Isotopic age determinations according to the

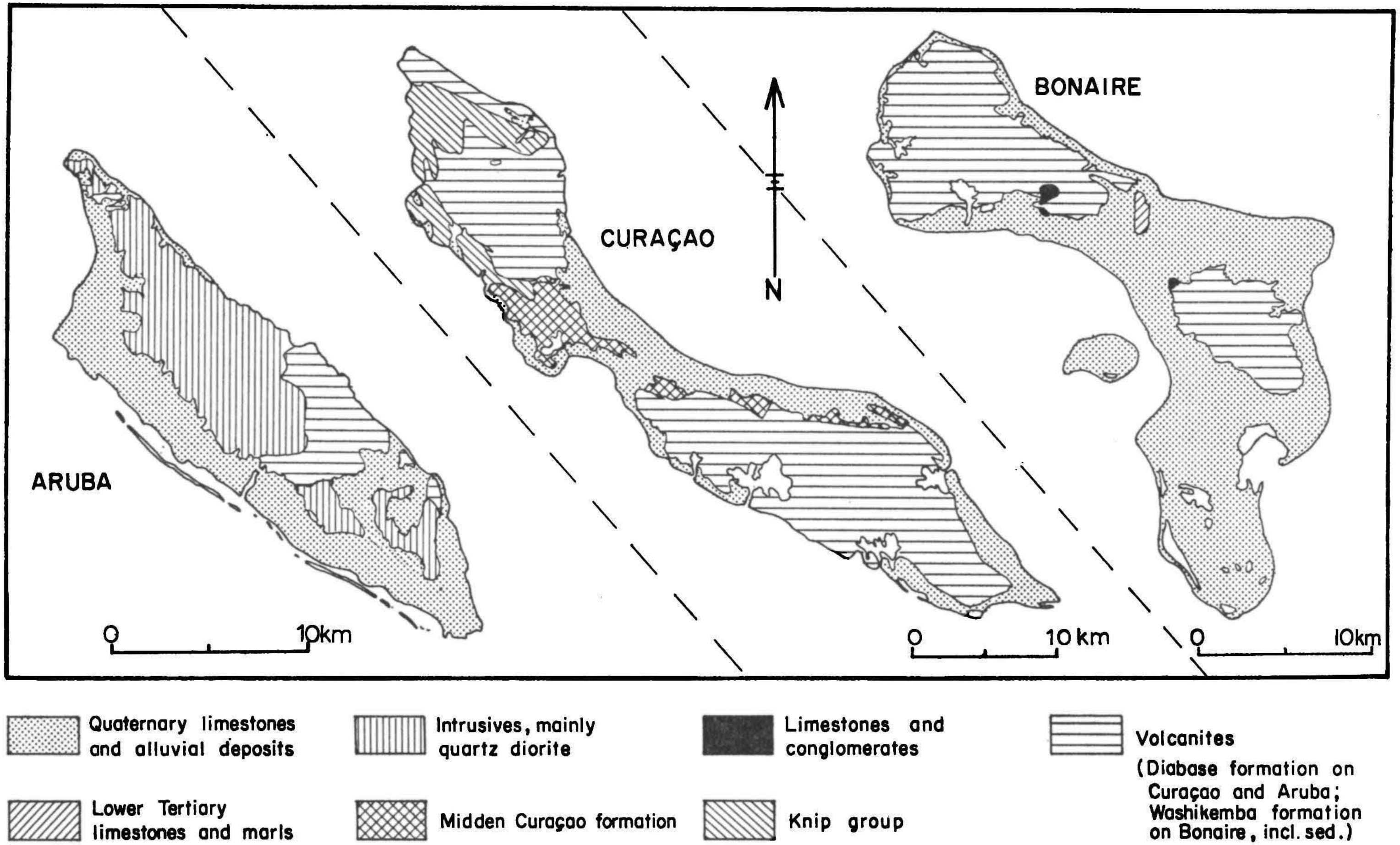

Fig. 11. Geologic sketch maps of Aruba, Curaçao and Bonaire (ref. WESTERMANN, 1932; BEETS, 1966; PIJPERS, 1933).

Rb–Sr and K–Ar method were made on concentrates of biotite from the quartz-diorite, indicating that the biotite crystallized 73 ± 3 m.y. ago (PRIEM, BOELRIJK, VERSCHURE, HEBEDA, LAGAAIJ, 1966). Following the 'Geological Society Phanerozoic time-scale' (1964) this age puts the emplacement of the batholith (and the folding of the diabase-schist-tuff formation) in Upper Cretaceous, probably Campanian time.

On Curaçao the basal complex similarly starts with a thick succession of submarine extruded basic lavas, the Curaçao lava formation or 'diabase formation'. This formation is overlain by the Knip group, a complex unit of Campanian–Maastrichtian age, in which chert-rich sediments prevail. According to BEETS (1966) there are indications that the Curaçao lava formation and the Knip group are separated by a hiatus. Rapid changes in facies and thickness in the Knip group and the presence of a thick sequence of turbidites and slump conglomerates in its basal part point to tectonic unrest during the deposition of this sequence. Tectonic movements reach their climax with the deposition of the Midden-Curaçao formation, a flysch type sequence of Danian age, and the subsequent folding and thrusting of the whole basal complex.

Small dikes, sills and necks of intermediate composition occur at various levels in the basal complex. The oldest are a group of small necks of quartz-dioritic composition which have intruded into the rocks of the Curaçao lava formation in the northwestern part of the island. Whole-rock K–Ar isotopic age determinations of a sample of these intrusions yielded an age of 72 ± 7 m.y., which may be considered as equal to that of the quartz-diorite batholith of Aruba (PRIEM, 1967). Younger, post Danian intrusions are furthermore found as sills in the Knip and Midden-Curaçao strata (Beets, personal communication).

The basal complex of Bonaire is the least well known of the three. The main part of this complex is formed by the Washikemba formation (PIJPERS, 1933), a unit of more than 5000 m thickness, consisting of volcanics of various nature with, subordinate, intercalations of non-volcanic sediment, mainly cherts and radiolarites. Pijpers roughly distinguished a lower part in which basic lavas and tuffs prevail (compare the diabase-schist-tuff formation of Aruba and the Curaçao lava formation), a middle part in which volcanics of intermediate and acid composition predominate, and an upper part in which again basic volcanics appear. Cherts and radiolarites, although occurring throughout the entire formation, are most frequent in the upper part. As this formation includes rock types comparable with rocks of the Curaçao lava formation as well as rocks found in the Knip group, it seems likely that the Washikemba formation can roughly be correlated with these two units of the basal complex of Curaçao. Although Pijpers assumes the formation to be a continuous marine deposit, BEETS and LODDER (1967) point out that some of the so-called 'porphyritic tuffs' from the middle part of the formation show characteristics of ignimbrites, suggesting a period in which land conditions prevailed. Whether this period coincides with the break in sedimentation between the Curaçao lava formation and the Knip group is dubious, and as long as the exact stratigraphic succession in the Washikemba formation is not known a detailed correlation with the other islands remains speculative.

The Washikemba formation has been folded into a broad anticline, of which the present exposures form the northwestern flank. The formation is unconformably overlain by shallow water deposits of Upper Campanian or Lower Maastrichtian age, the Rincon formation, and consequently folding is of Campanian or older age. The youngest deposit belonging to the basal complex is a thin sequence of coarse-grained conglomerates, the Soebi Blanco formation, which, considering the composition of the detritus, may be correlated with the Midden-Curaçao formation. The Rincon formation as well as the Soebi Blanco formation are weakly folded. No intrusions occur in the basal complex of Bonaire, with the possible exception of a number of porphyrites belonging to the Washikemba formation. Mentioned porphyrites, mainly of quartz andesitic composition, are thought to be of the same age as the other volcanites of the Washikemba formation, i.e. Campanian or older.

In some of the islands the basal complex has been altered and metamorphosed to various degree. The diabase-schist-tuff formation surrounding the quartz-diorite experienced contact metamorphism (uralite lavas and hornblende schists). The rocks of the basal complex of Curaçao have been metamorphosed under low temperature and pressure conditions of the zeolite facies and possibly of the pumpellyite-prehnite-metagraywacke facies (personal communication Beets) (cf. COOMBS, 1961). As this metamorphism affects the Midden-Curaçao formation it is of post Danian age.

After deformation and metamorphism of post Danian time, uplift and denudation of the basal complex took place. Only in few places do Tertiary rocks overlie the denuded basal complex. They are slightly warped.

On Curaçao and Bonaire limestones and calcareous marls of Upper Eocene age occur. Deposition was at shallow water depth. It has been suggested that deeper sea basins around the isles were beginning to develop at that time, since foreign material derived from an outside area – found to be present in part of the basal complex – is absent in part of the Eocene sediments. A borehole near Oranjestad, Aruba, struck marine Miocene rocks deposited at shallow depth, indicating slight vertical movements.

Coral limestones and limestone deposits formed by wind action of Neogene and Quaternary age form a rim around the older cores of the islands. Part of the limestones are terraced. These terraces provide evidence for eustatic changes in sea level during the Quaternary (DE BUISONJÉ, 1964). A gradual rising of the Netherlands Leeward Antilles, superimposed on the eustatic changes may be inferred from the circumstance that an older terrace is always in a higher position than its successor. The highest terrace of Curaçao now occurs at a height of about 200 m above sea level. The rising movements started in the Lower Miocene (DE BUISONJÉ, pers. comm.). In contrast, the Aves islands, east of Bonaire being true atolls, have been subject to subsidence during the Quaternary (DE BUISONJÉ, VAN DER WERF, ZANEVELD, ZONNEVELD, 1957).

The geologic history of the Netherlands Antilles may be summarized as follows. During Cretaceous and lowermost Tertiray times a sedimentation trough existed at the site of the present isles in which a thick sequence mainly of submarine character and largely consisting of volcanics was deposited. Important intrusions of diorite rocks occurred in Campanian (Upper Cretaceous) time, but younger intrusions of similar composition are also known. The area was highly mobile during the Upper Cretaceous and lower Tertiary. On Curaçao the main period of folding is of post-Danian age, as is the burial metamorphism.

Uplift and denudation of the basal complex occurred prior to the deposition of Eocene and younger sediments. Possibly the development of deep sea basins started in upper Eocene time. There are no indications of tectonic activity in Mid-Tertiary as found in other areas of the Caribbean; only some warping occurred.

During the Neogene and Quaternary a gradual rising of the Netherlands Antilles and a subsidence of the Aves islands took place.

BATHYMETRY

The bathymetry of the sea surrounding the western Leeward Antilles is given in fig. 12. Depths are contoured every 1000 m. The 200 m contour off Venezuela is also given, being the boundary of the continent. The bathymetric chart was compiled from depth sounding data provided by the Hydrographic Department of the Royal Netherlands Navy. The contours west of 70° western longitude were taken from the Bathymetric Chart of the Caribbean Sea, H.O. 5487. The chart of fig. 12 should be examined together with the two continuous depth profiles given in figures 15 and 16.

Los Monjes islands and Aruba lie inside the 200 m contour and thus belong to the South American continental shelf. Around the other Leeward Antilles the sea has oceanic depth varying between 1200 to 1600 m; these islands lie between the continental shelf of Venezuela and the oceanic Venezuelan basin, which comprises the western part of the Caribbean Sea.

The continental shelf off the north coast of Venezuela has a width of about 15 km. The continental edge has a slope of 1 : 32 toward the Bonaire trench which reaches a maximum depth of a little over 2000 m. The trench bottom is flat, suggesting sediment deposition by turbidity current action.

The Los Roques trench is about 500 km long and 40 km wide running roughly parallel to the western Leeward Antilles, from north of Curaçao to west of La Blanquilla and Los Hermanos. The average depth is about 3000 m, being less than the average depth (appr. 4000 m) of the Venezuelan basin. Depths of more than 4900 m have been found at the foot of the steep northern slope of the islands of Los Roques, suggesting that the sea bottom is depressed towards the islands.

The northern slope of the Leeward Antilles toward the Los Roques trench, north of the isles, is very steep compared with the southern slope toward the Bonaire trench. Slopes of 1 : 3 are present north of the Aves islands and Low Roques isles. This steepness is suggestive of a fault or faults forming the scarp north of the islands.

The Curaçao submarine ridge is an elongated approximately E–W running elevation east of 70° W, superimposed on the general NNE slope. In eastward direction the ridge becomes gradually deeper and it becomes also less clear in the contour lines. It practically dies out north of the Los Roques islands. On the surface of the ridge several narrow secundary ridges appear, running approximately parallel with the main trend of the ridge. One of these secondary ridges is apparent from the elongated loop in the 2000 m contour line north of Curaçao. Others appear north of Bonaire. As far as can be inferred from the available depth data these secondary ridges seem to be discontinuous. The Venezuelan basin is generally flat-bottomed. North of Aruba its bottom becomes deeper toward the island.

Regional structural elements

Some remarks can be made on the regional physiography and structure around the investigated area. In figure 23 the main physiographic and structural elements of northeastern South America and the southeastern part of the Caribbean Sea are presented. The physiography was taken from Bucher (1952). Several elements can be distinguished. In the south the pre-Cambrian Guyana shield is indicated, bordered by the Llanos (= plains), which are sedimentary basins of dominantly Tertiary age. The Caribbean Mountains, along the central and eastern part of the north coast of Venezuela consist of an E–W trending belt of low-grade metamorphics composed of upper Mesozoic sedimentary and volcanic rocks. Metamorphism occurred before the Eocene; it did not take place in a single period affecting all regions at the same time (Hess, 1960, 1966). The Gulf of Venezuela basin and Falcón basin (both east of Goajira) are dominantly Mio-Pliocene structures (Coronel, 1967).

The structure of the Maracaibo basin, the Venezuelan Andes and the Tertiary basin to the southeast of the latter range (the Barinas-Apure basin) results, according to Hospers and Van Wijnen (1959), from reverse faulting, the Venezuelan Andes thrusting over the depression of the Maracaibo basin. This structure of mainly Mio-Pliocene age is expressed by negative anomalies in the depressed basins and positive gravity anomalies in the upthrusted Andes.

A number of important faults, which have, according to ROD (1956) and ALBERDING (1957), a strike-slip character, are indicated.

It should be remarked that it is not well known what geological relation exists between the Netherlands Antilles and nearby continental areas with a similar geology such as the Caribbean Mountains and the Goajira peninsula.

Elongated gravity anomalies are characteristic in the area of fig. 23 (at sea Airy-Heiskanen anomalies of U.S. and Netherlands pendulum stations, on land taken from DE BRUYN's map, 1951). The continuity of the axes of gravity anomalies from sea into land is conspicuous. This is apparent in the southern part of the zone of negative and positive gravity anomalies east of the Lesser Antilles, which turns via Trinidad westward and continues on land in the Tertiary East-Venezuelan basin. It then becomes patchy and cannot be followed with confidence. The Caribbean Mountains are slightly negative, but may be said to be generally in isostatic equilibrium.

West of Grenada, one of the southernmost Lesser Antilles islands another negative zone starts. This South Caribbean anomaly zone runs over the Los Roques trench north of Curaçao, where values as low as −148 mgal are found, then continues west of Goajira and hence seems to turn land inward via the delta of Colombia's Magdalena river. At sea this zone is about 1600 km long; on land it becomes patchy and separates into two zones, following the valleys and plains of the Magdalena river and the Cauca river, while the adjacent Central and Eastern Cordilleras are positive areas. The positive zone that is roughly parallel to the negative zone runs over the Netherlands Antilles where large anomalies are found, up to +100 mgal. To the east of these islands it turns into the Bonaire trench; to the west it probably continues landinward on Goajira.

4. GEOMETRICAL INTERPRETATION

Gravity anomalies

General; gravity and topography

Isostasy, the floating equilibrium of the crust on its substratum, is the normal situation for the crust. This notion forms the starting point of our gravity interpretation. From a compilation of more than 4000 gravity pendulum measurements at sea Worzel (1965b) arrives at the conclusion that generally speaking isostasy holds for the greater part of the water-covered crust, confirming Vening Meinesz' earlier conclusion (1934). Isostatic anomalies are caused by deviations in mass distribution with regard to the isostatic model. With regard to the seat of the anomalous masses one has generally to choose from:

1. a topographic feature that is not compensated isostatically e.g. recent volcanic activity
2. an anomalous mass in the crust itself, e.g. a sedimentary basin
3. an anomalous mass at the lower boundary of the crust, e.g. crustal down warping where crustal material projects in the denser substratum and causes a mass deficiency. If the crust consists of more layers than one, the mass deviations should be placed at the lower boundary of all these layers.
4. density changes in the substratum. Only direct seismic evidence would justify the assumption of upper mantle inhomogeneities in a certain area. Since no such evidence is found in the Netherlands Antilles, and since, moreover, there is no need to assume these inhomogeneities in order to explain the gravity anomalies in this area, the substratum is considered to have a homogeneous density.

The gravity map of local isostatic anomalies (Heiskanen-Airy isostatic reduction) of fig. 13 and the bathymetric chart of fig. 12 are utilized for the gravity interpretation. The construction of these maps is described in chapter 2.

A comparison of both maps indicates a general parallelism of topographic trends and gravity anomalies, which form oblong zones. As a first example of this general parallelism the Los Roques trench coinciding with part of the over 150 km broad negative anomaly zone north of Curaçao is mentioned. One cannot, however, speak of a strict association of this negative zone with an oceanic trench. Such association is true for several other negative zones e.g. the Puerto Rico trench, and the Mindanao trench (Talwani *et al.*, 1959; Vening Meinesz, 1948). In the studied region, however, the trench is not only less deep than the nearby Venezuelan basin, but also decreases gradually in depth in westward direction, with the result that north of Aruba the trench even is completely absent

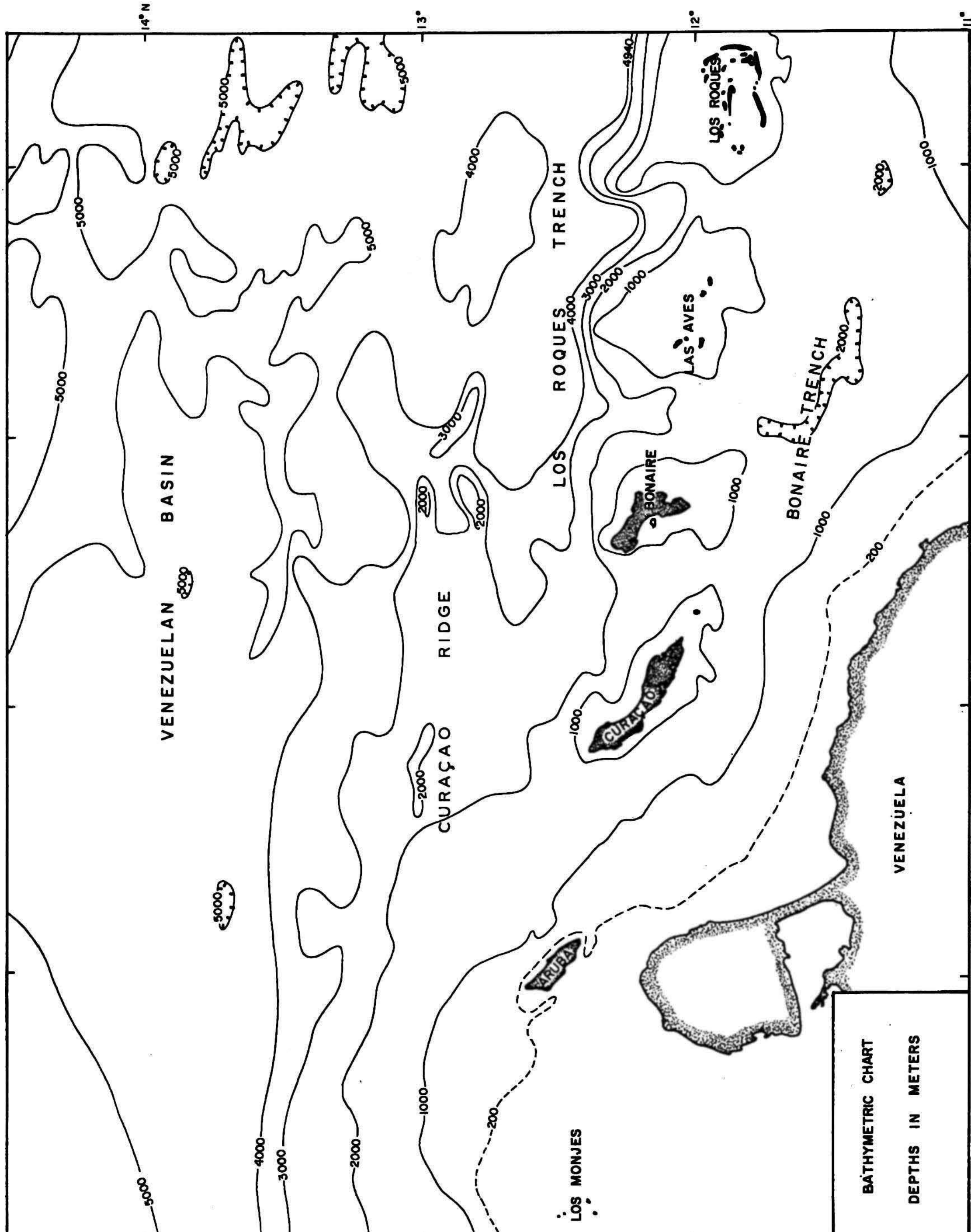

Fig. 12. Bathymetric chart of the sea surrounding the Netherlands Leeward Antilles.

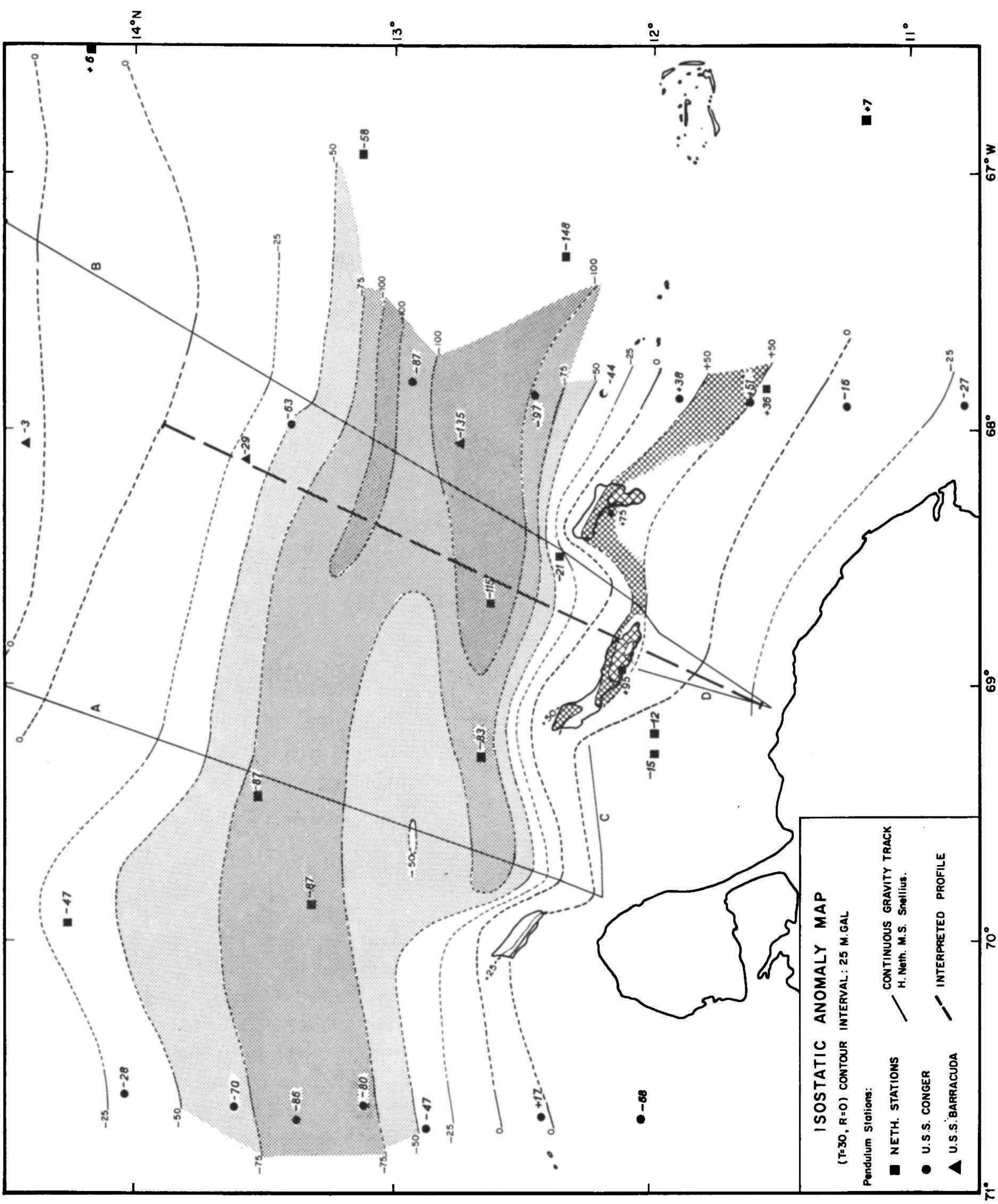

Fig. 13. Isostatic anomaly map of the area surrounding the Netherlands Leeward Antilles. The traverses of H. Neth. M.S. *Snellius* are designated with A, B, C and D.

in the bathymetry (see also the bathymetry in fig. 16). The negative anomaly zone is thus present above (from east to west) the Los Roques trench, the Curaçao submarine ridge and the generally smooth slope from the continental area around Aruba towards the oceanic depths of the Venezuelan basin.

A secondary bulge appears in the negative anomaly zone east of Aruba's meridian; see gravity map fig. 13. This bulge, which has a maximum value of -50 mgal, coincides with the Curaçao ridge. Both extend to the eastern part of the studied region. The gravity minimum south of the bulge, with values as low as -148 mgal, coincides with the Los Roques trench and its westward extension. The northern minimum, with values as low as -120 mgal, lies above the beginning of the nearly flat Venezuelan basin. It may well be possible that these two minima join further to the east with the complete disappearance of the Curaçao ridge, but data are inconclusive. Further north in the Venezuelan basin small positive anomalies appear.

Adjacent to the southern flank of the negative belt we find a long positive zone. This positive zone coincides with the Netherlands Antilles in the western part of the map, where maximum values are $+100$ mgal. East of Bonaire it turns southeastward and runs into the Bonaire trench, where the anomaly values are smaller. The Venezuelan Antilles (Las Aves, Los Roques and La Orchila) are thus locating in the southern flank of the negative zone. The occurrence of several conspicuous indentations in the contour lines of the anomaly map in the region of the Netherlands Antilles should be noted. They follow the *en echelon* arrangement of these islands. Presumably this pattern is due to deep faulting or flexuring. The probable nature of this faulting will be discussed later on.

Concluding, it can be remarked that, although topography and gravity anomalies exhibit the same general trend, no strict relation between topography and gravity anomalies can be found. In fact, the anomaly zones are continuous over entirely different morphological elements. Later we will come back to this observation.

On the basis of the anomaly map and the bathymetric map a geometrical interpretation of the disturbing masses is given. The interpretation will be compared with the result of a gravity profile and seismic investigations in an area more to the east (WORZEL, 1965). We then proceed with a discussion of the possible causes of the deviating mass distribution. In a separate section we will discuss to what extent the gravity interpretation is supported by the magnetic anomalies.

Interpretation

General

A profile was constructed from the anomaly map, which can be used as a representative section for the interpretation. The thick broken line in the gravity map indicates the position of this profile (fig. 13). It runs from the coast of Venezuela across the maximum positive anomaly of Curaçao and across the negative anomaly zone into the Venezuelan basin.

Since the curve of isostatic anomalies was taken from the anomaly map, features of local importance do not appear in the curve; e.g. the small anomaly at 160 km in profile B (fig. 13) does not occur in the isogam chart nor in the curve of anomalies in fig. 14. A schematic picture of the corresponding section through the earth's crust is shown in fig. 14. The topography in the profile has been simplified after the bathymetric map. The lower surface of the crust, which would satisfy the condition of isostatic equilibrium has been drawn with a broken line (short dashes) in the profile. A crustal thickness of 30 km, a homogeneous crustal density of 2.67 g/cm^3 and a density of the substratum of 3.27 g/cm^3 have been used for this isostatic model.

In order to calculate which deviations in mass distribution must be assumed to explain the isostatic anomalies, the isostatic anomaly curve has first graphically been divided into separate anomalies. This graphical procedure is somewhat arbitrary. In this case a separation into roughly symmetrical anomalies was carried out. From north to south the curve has been divided into a broad negative anomaly with a secondary positive anomaly, a sharp positive anomaly and a weak negative anomaly (cf. fig. 14 anomalies a, b, c and d respectively). Since we deal with approximately symmetrical and elongate anomalies an approximate figure for limiting the depth of the disturbing masses can be calculated with the formulas given by NETTLETON (1942) for the gravimetric effect of infinite horizontal cylindrical bodies, the halfwidth of the anomaly being equal to the depth of the axis of the cylinder. For completeness we remark that the effect of a deep body can always be put equal to the effect of a shallower body with the same mass but extended over a broader area or to the effect of combinations of deep and shallow bodies.

When the maximum depth calculation pointed to a deep seated source, it was placed at the lower boundary of the crust. Use was made of geologic and seismic information – the latter from WORZEL (1965) – in selecting the position of shallow masses, their density and in some cases their maximum thickness. Models of simple outline were employed, whose gravity effect was close enough to that observed to give sufficient information on the general structure of the crust.

For the computing of the gravimetric effect of models of disturbing masses the graphical profile method was applied (HUBBERT, 1948)[1].

---

[1]) The vertical component of the gravitational attraction of an elementary, two-dimensional, homogeneous, horizontal prism is

$$dg_z = 2k\varrho \, d\theta \, dz$$

where $d\theta$ is the dihedral angle subtended by the element, dz is the thickness, ϱ the density and k the gravitational constant. This equation allows the computation of the gravimetric effect of a two-dimensional mass by areal integration, which is approximated by

$$g_z = 2k\varrho \, \Sigma\Delta\theta \, \Delta z$$

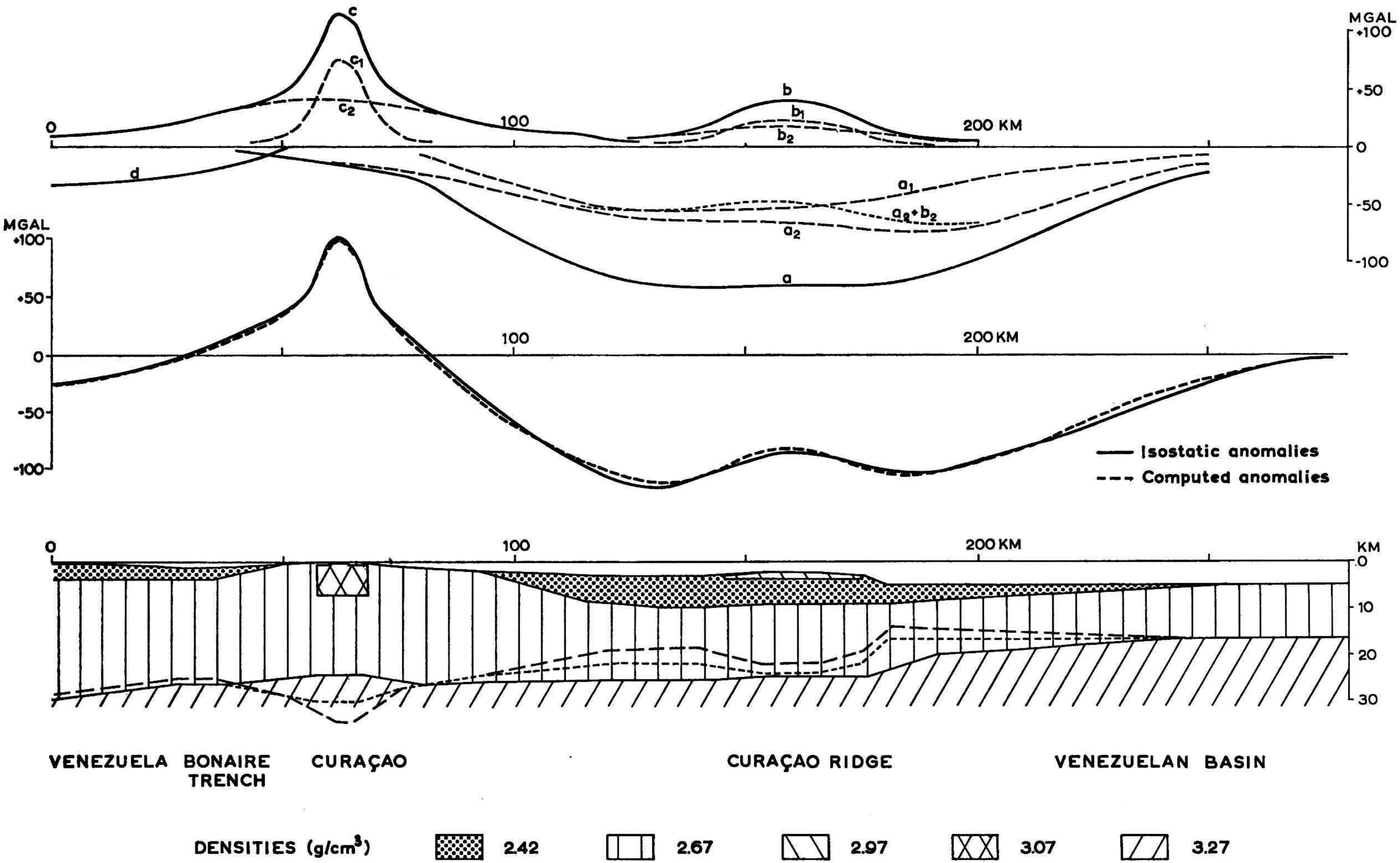

Fig. 14. Interpretation of the isostatic gravity anomalies in the Netherlands Leeward Antilles area.

The anomalies (fig. 14).

Anomaly a

A great part of the mass deficiency beneath the large, elongate negative anomaly is placed at a high level of the crust, since the existence of a thick pile of light sediments was demonstrated seismically (EDGAR, EWING and HENNION, 1967) in a section at 68°W. We assume that the sedimentary body has a homogeneous density of 2.42 g/cm³. The greatest thickness is taken to be 7 km. These assumptions will be explained in the comparison with the section at 68°W.

Since the gravity effect (a_1, −55 mgal) of this disturbing mass in the crust is not sufficient to explain the negative anomaly, part of the mass deficiency (a_2) must be placed in the mantle beneath the crust. We come back to this in our discussion of anomaly b.

Anomaly b

A secondary positive anomaly (b), located above the Curaçao ridge appears in the isostatic as well as in the Bouguer anomaly curve (cf. fig. 15 and 16). This means that the anomaly cannot be the result of an uncompensated or regional compensated topographic feature, since in the Bouguer curve the effect of the topography has been accounted for, while no allowance is made for isostatic compensation of the topography.

The source of anomaly b therefore has to be found in a mass excess in the crust and/or at the lower boundary of the crust. As a first approach we can suppose that the submarine ridge above which the anomaly occurs, has a higher density, e.g. 2.97 g/cm³, the ridge consisting of volcanic rock. Taking for such a body a thickness of 1450 m (see fig. 14), this gives a gravity effect of 20 mgal (b_1). This is not sufficient to explain the whole anomaly. Only if we give the body a thickness of about 2.5 km would the anomaly be fully explained. However, we consider this situation unlikely since large magnetic anomalies might be expected (see 'Interpretation of magnetic anomalies'). Because of this consideration we must place the source of the remaining anomaly (b_2, 25 mgal) at a deeper level. We therefore combined the solution for anomaly a_2 (80 mgal) with the one for b_2 (25 mgal), the mass comprised between the short dashed line and the solid line in fig. 14 accounting for the sum of anomaly (a_2) and (b_2).

We also might have supposed that anomaly b is due to an upward bulge of the main crustal layer only, which would than be of the order of 5 km. Such a supposition finds no confirmation in the seismic measurements at 68° W (see 'Comparison with a section at 68° W'). Admittedly, the solution presented for anomaly b is subject to modification, since we do not dispose of sufficient information on the crustal layering. Important is that anomaly b cannot be explained by supposing the topographic mass of the Curaçao ridge to be noncompensated or regionally compensated.

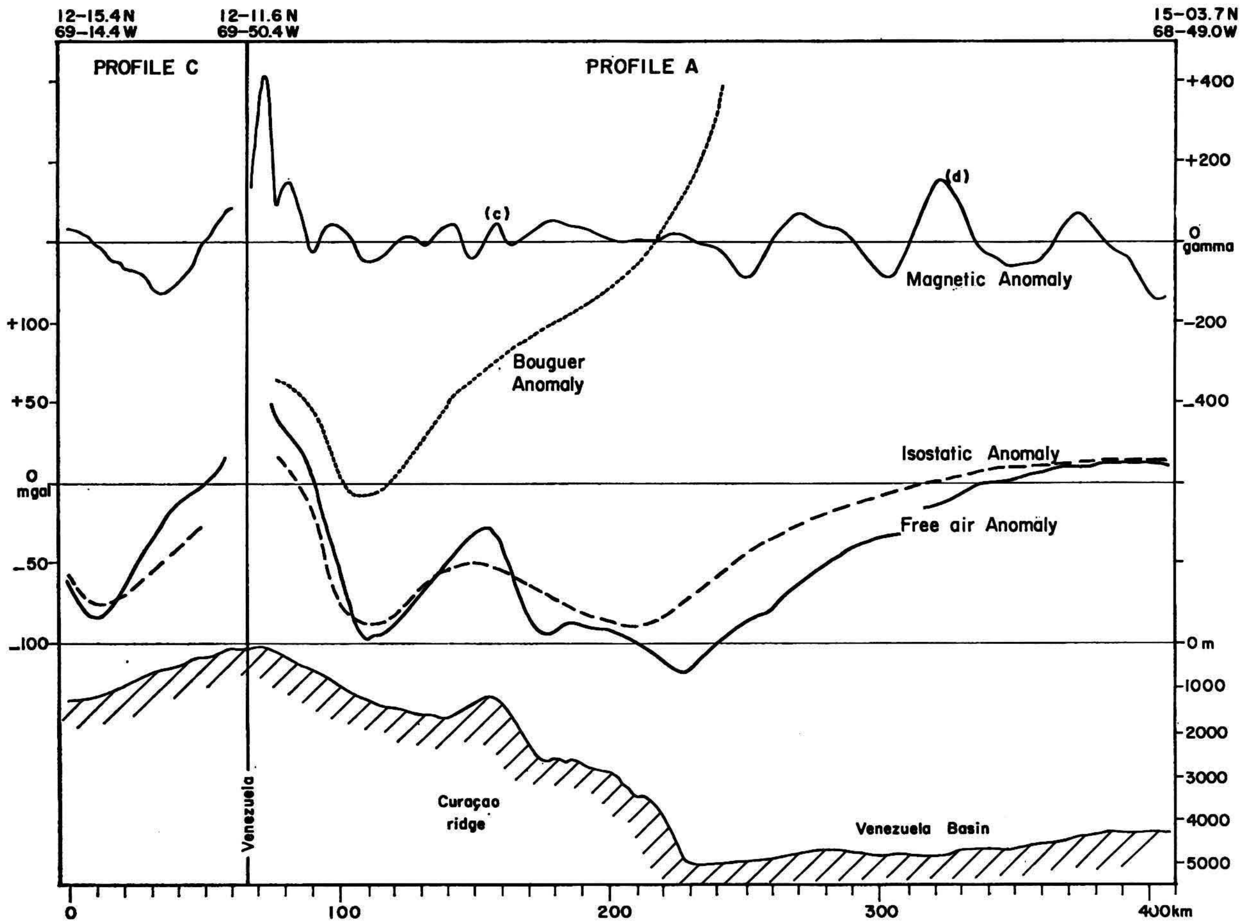

Fig. 15. Geomagnetic-, gravity- and bathymetric profiles A and C, running west of Curaçao and observed on board H. Neth. M.S. *Snellius*.

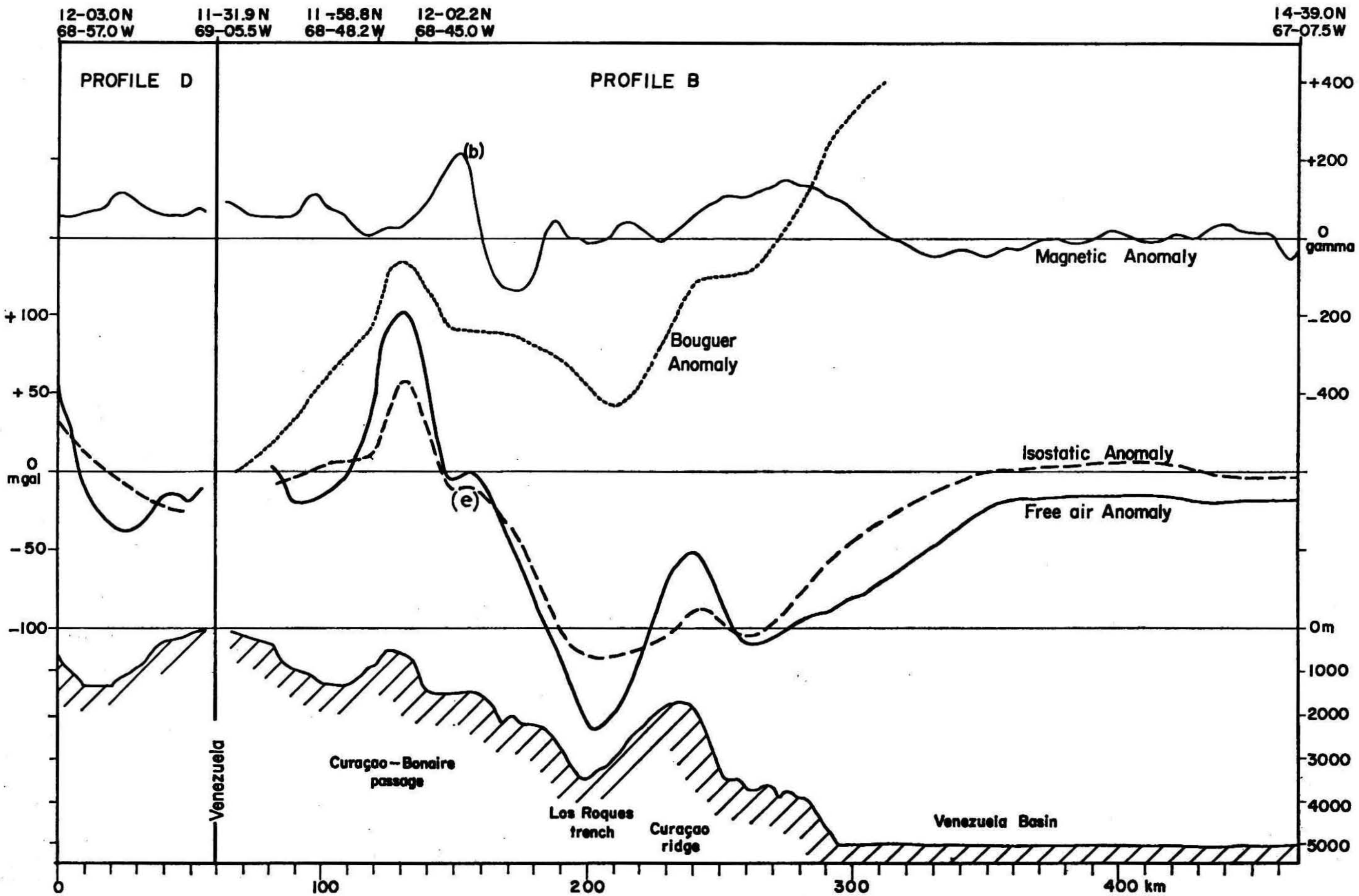

Fig. 16. Geomagnetic-, gravity- and bathymetric profiles B and D, running east of Curaçao and observed on board H. Neth. M.S. *Snellius*.

Anomaly c

Above the island Curaçao a large positive anomaly occurs which, as described already, is situated above an outcrop of volcanic rock. On account of the halfwidth of the anomaly, 9 km, it is reasonable to suppose that the volcanic material is, at least partly, responsible for the anomaly. A density of 3.07 g/cm^3 is acceptable for lava-type rocks. The thickness of the volcanic core of Curaçao is not known, but it has been mentioned already that the estimated stratigraphic thickness of the mainly basaltic Washikemba formation on Bonaire is at least 5 km. We therefore infer that a limit of 6 km may be put to the thickness of the shallow disturbing mass. With a width of 11 km and a density of 3.07 g/cm^3 such a body would account for 75 mgal of the anomaly. Its effect is shown in curve c_1. Not too much importance should be given to the configuration of this body, it may for instance as well be trapezoid.

The remaining 40 mgal can be explained by an upwarp of the crust-mantle interface as given for fig. 14. The effect of this upwarp is drawn as curve c_2. The upwarp is so large that we can no longer speak of an isostatic compensation of the island. The sum of curves c_1 and c_2 gives the total anomaly c.

Anomaly d

The negative anomaly (d) in the area south of Curaçao is explained by a sedimentary body with density 2.42 g/cm^3, that is 3.5 km thick and 80 km wide. In the model only the northern half of the body is drawn. Since the profile does not cover the whole basin, this depth of 3.5 km for the basin should be considered as a rough estimate. The explanation given for the anomaly is suggested by the presence of a considerable pile of low velocity material in the Bonaire trench (Worzel, 1965 in the section at 68° W computed by Hambleton), and by the presence of a thick layer of young sediments in the Falcón and Gulf of Venezuela basin. These areas all belong to the region of negative anomalies south of the Leeward Antilles.

In the foregoing we have obtained configurations explaining the gravity anomalies in the interpretational profile. The total computed anomaly curve is drawn in the middle part of figure 14 together with the observed anomaly curve. The difference between the calculated and observed curves is less than 10 mgal, which is regarded as a sufficient fit. In the lower part of figure 14 the resulting crustal section is drawn by full lines, giving

1. an explanation for that part of the anomaly curve which is due to shallow sources, and,
2. an acceptable depth and general shape of deep masses deviating from the assumed isostatic mass distribution.

With regard to the latter point it should be remarked that, if one wishes to compare the crustal configuration inferred from the gravity anomalies with a compensated model, the compensation of inhomogeneities in the crust should also be taken into account. Therefore a modification of the underside of the crust in isostatic equilibrium, computed for a homogeneous crust – the line with short dashes in figure 14 – is necessary. This can be done by correcting for the mass deficiencies and mass excesses caused by the crustal inhomogeneities. The result is drawn in figure 14 as a line with long dashes. The relative position of this line with regard to the underside of the crust, as computed from the anomalies (solid line), is a measure for the deviation from isostatic equilibrium.

The total magnetic-intensity anomalies

General

With regard to the total magnetic-intensity anomalies we have, besides our own two sea-borne magnetic profiles (fig. 15 and 16) three approximately N–S running aeromagnetic profiles of Ewing, Antoine and Ewing (1960) (fig. 17). The broken lines between the profiles in the upper and lower part of fig. 17 indicate a provisional correlation between the anomalies. Comparing the sea-borne magnetic and gravity profiles it becomes clear that the magnetic anomalies are less regular than the gravity anomalies. In fact, more data would be needed for a thorough interpretation of the magnetic anomalies. We nevertheless want to discuss the magnetic anomalies, especially in context with the gravity anomalies.

The first that can be said is that the anomalies have a general trend of about 120° as indicated by the broken lines in the map of fig. 17. Regions of prevailing wavelength in the anomaly curves can be discerned. In the negative zone north of Curaçao wavelengths of about 30 km occur. Outside this zone where the Venezuelan basin begins, longer wavelengths of approximately 50 km are present. This is also apparent in profile A and B (fig. 15 and 16). This contrast is moreover characteristic of the whole Caribbean area: the Venezuelan basin has appreciably smoother anomalies than the surrounding island arc zones (see the map of Ewing, Antoine and Ewing, 1960, p. 4092).

Interpretation

A few rock samples from the islands were investigated on their magnetic properties at the Paleomagnetic Laboratory of the University of Utrecht. The Königsberger ratio (Q factor) of remanent to induced magnetization, and the susceptibility were measured. The average Q factor of 23 samples appeared to be about 0.4. This applies to both sampled rock types: volcanics and sediments of the Upper Cretaceous. The minimum value for the Q factor was 0.04 and the maximum value 1.5. Mention should be made of two samples taken from the diabase of Aruba which fall beyond this range having Q factors of 18 and 21. However, since the average Q factor is smaller than unity, we may assume that the anomalies are caused by induced magnetization only.

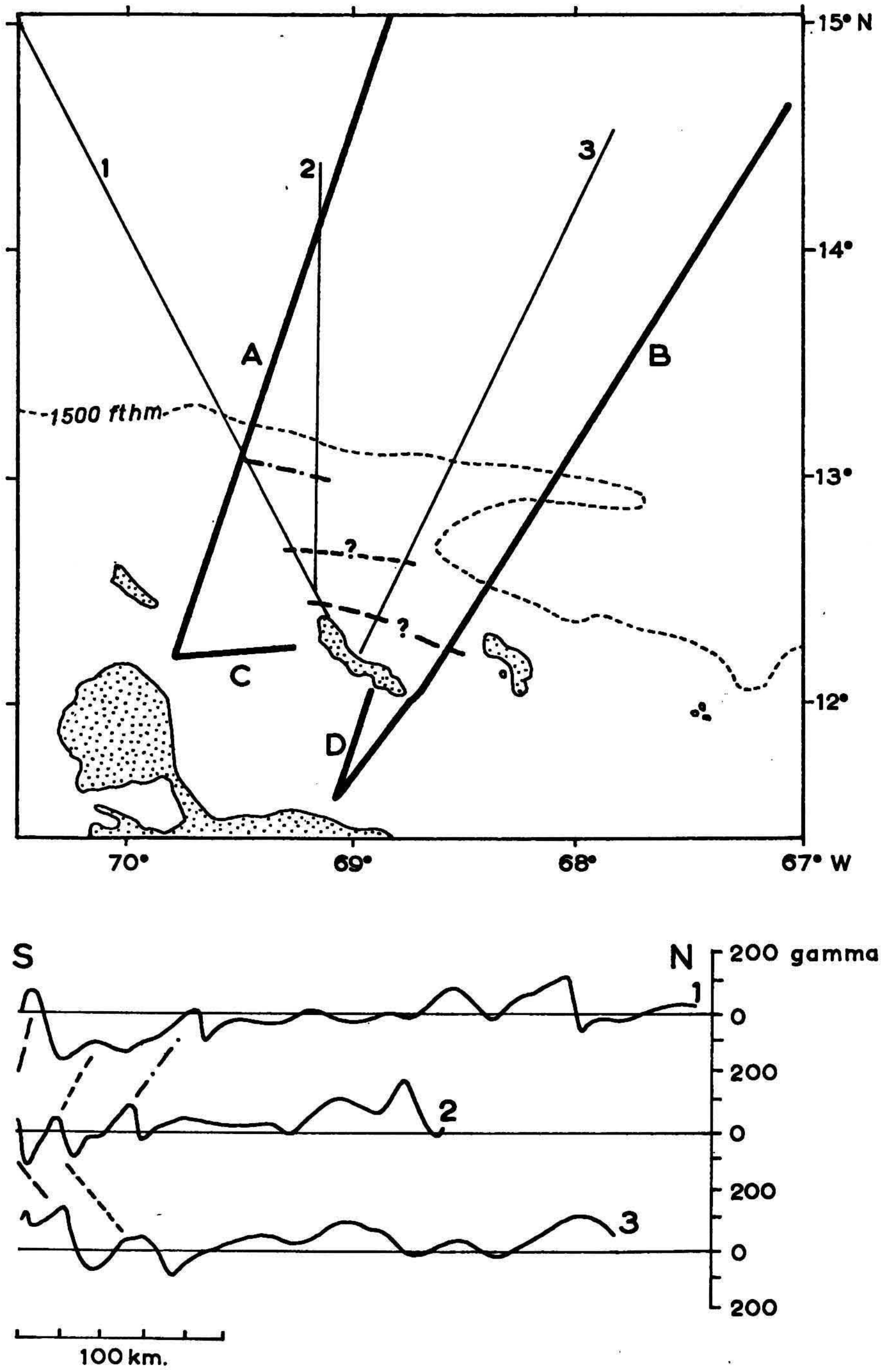

Fig. 17. Traverses of magnetic observations in the area of the Netherlands Antilles. The anomaly curves of total magnetic intensity, 1, 2 and 3 are taken from EWING, ANTOINE and EWING, 1960. The magnetic anomaly trends are indicated with dashed lines.

The susceptibility of the sedimentary rocks (radiolarites, greywackes) varies between 2×10^{-6} and 30×10^{-6} e.m.u. The susceptibility of the volcanic rocks ranges from 3×10^{-6} to 2000×10^{-6} e.m.u. The latter value is characteristic for oceanic basalts. Both extreme values of the susceptibility of volcanics were measured in rocks from the Washikemba formation of Bonaire, which comprises a variety of rock types (e.g. alternating tuffs and submarine lavas).

The maximum depth to magnetic bodies can be estimated, taking it to be equal to the horizontal extent of the steepest slope of the anomaly (cf. PETERS, 1949). Maximum depths vary around 5 km below sea level in the island arc area and around 10 km in the Venezuelan basin. We tried, assuming two-dimensionality, homogeneous susceptibility and induced magnetization, to fit the calculated anomalies of simple models (computing program [1]) of TALWANI and HEIRTZLER, 1964) to the observed anomalies. Only those anomalies of which some indication of their outline exists are considered. Also the magnetic effect of the shallow bodies presented in the gravity interpretation was calculated, using resaonable susceptibility contrasts.

We start with that part of the profile B east of Curaçao (fig. 16), that lies directly east of the island. The diabase body of the island proper would produce an anomaly with a peak to peak amplitude of 500 gamma (cf. p. 33) when utilizing a susceptibility contrast of 0.002 e.m.u. This is a reasonable susceptibility for oceanic basalts (ADE-HALL, 1964) and also was measured in some of the island samples. On profile B (130 km) no such prominent anomaly has been detected. We conclude that the gravity anomaly at that position which is thought to be due to an eastward extention of the diabasic core of Curaçao, finds no appreciable counterpart in the magnetic anomaly curve.

Next the anomaly in fig. 16 at 150–170 km, (b), is considered. A shallow lense-like body with a susceptibility contrast of 0.004 e.m.u. produces an anomaly which fits the observed anomaly (fig. 18). A deeper, slightly dipping, tabular body with greater dimensions (fig. 19) and the same susceptibility contrast, however, could produce the anomaly as well, since we have only a single profile across the anomaly. It should be noted that the observed magnetic profiles are not perpendicular to the general trend of the anomalies, whereas the anomalies of the models were computed for that direction. The magnetic anomaly (b) coincides with a small positive gravity anomaly (e) (fig. 16). The gravity anomaly may be due to a shallow body of density contrast $+0.5$ with approximately the same

---

[1]) This program was rewritten in ALGOL for the El–X8 computor of the Electronic Computing Centre of the University at Utrecht. The program is based on formulas given by HEILAND (1940, p. 397). These are used to obtain the vertical and horizontal components of the magnetic anomalies caused by a two-dimensional, homogeneously magnetized body with a polygonal cross section. Total-intensity anomalies are also obtained.

dimensions as the shallow body assumed for the magnetic anomaly (our first solution). A basaltic body, forming a platform in the bottom topography and embedded in light sediments, could be responsible for the gravity and the magnetic anomaly. Since we find anomalies with the same characteristics in the aeromagnetic profile it may be that this body is

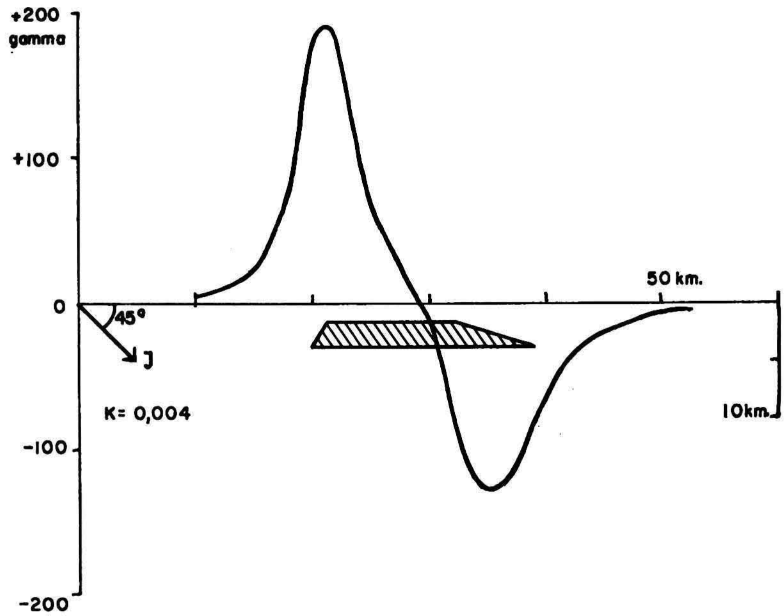

Fig. 18. Computed anomaly of total magnetic intensity (b).

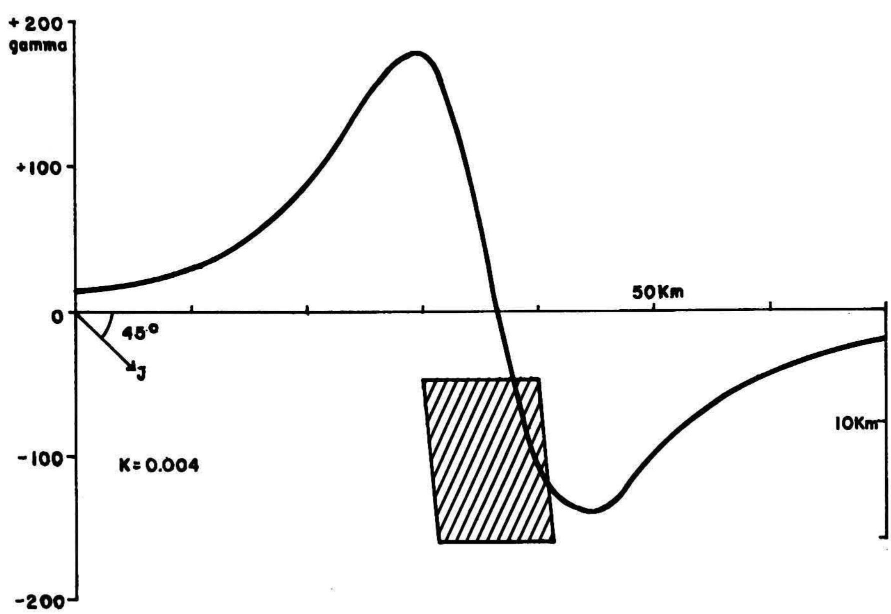

Fig. 19. Computed anomaly of total magnetic intensity (b).

present along the whole northern coast of Curaçao (the most southern anomalies in profiles 1 and 3 in fig. 17).

The configuration of the lense-like body in the Curaçao Ridge (at 235 km), which was found from gravity data, was used as a model for the magnetic interpretation. It produces an anomaly with a peak to peak amplitude of 70 gamma (susceptibility contrast 0.002 e.m.u.) (fig. 20). In profile B, east of Curaçao (fig. 16), this small anomaly may be hidden by the presence of the broad anomaly between 230 and 300 km. The other sea-borne profile (fig. 15) shows an anomaly (c), which may be produced by the assumed body. In the aeromagnetic profiles anomalies are present which seem to be associated with the Curaçao Ridge. In profiles 1 and 2 these are much more prominent, probably indicating a local increase in the susceptibility contrast.

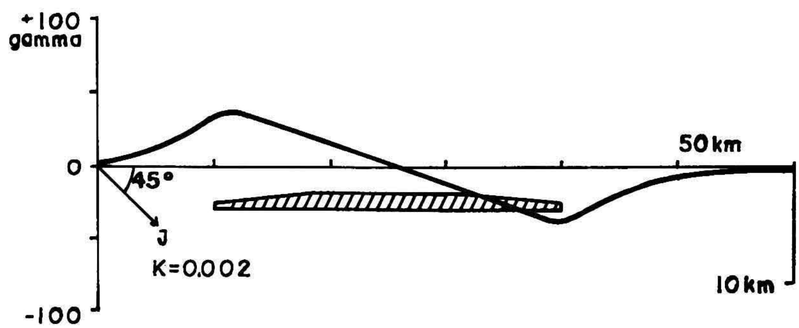

Fig. 20. Computed anomaly of total magnetic intensity (c).

The foregoing demonstrates that the gravity anomalies of shallow bodies in the area have their greatly varying counterparts in magnetics. The susceptibility values used for the model studies lie within the known range of susceptibilities for submarine lavas (Ade-Hall, 1964; Bullard and Mason, 1963). In view of this and the density contrast used in the gravity interpretation it is not unreasonable to think of a basaltic composition of the superficial disturbing bodies.

Some remarks can be made on the anomalies in the Venezuelan basin. The broader anomalies in the Venezuelan basin area ((d) in fig. 15) are possibly produced by bodies of about 20 km width having a susceptibility contrast of about 0.002 e.m.u. These bodies must be situated in the layer beneath the sedimentary veneer. Seismic velocities of this layer range from 3 to about 5.5 km/sec (Officer *et al.*, 1959). Such velocities are characteristic of many sedimentary, metamorphic and igneous rocks. It is therefore difficult to identify the layer to a specific rock type on account of the seismic velocities. However, because of the susceptibility value mentioned, a basaltic composition is suggested. The question arises whether the anomalies are due to susceptibility contrasts in the layer itself or are produced by buried seamounts, extending upward from this layer, as were found since by reflection profiling elsewhere in the Caribbean.

Finally, the sharp anomaly of more than 400 gamma in the profile west of Curaçao (at 75 km, fig. 15) needs consideration. The profile here crosses an oval shoal lying on the continental shelf of Venezuela. The minimum observed depth was 30 m. The Admiralty chart of the north coast of South America gives 13 m. The anomaly may be due to a submerged volcanic intrusion, whose outline appears in the shoal. No quantitative data on the anomaly source can be gained from this one crossing.

Comparison with a section at 68° W

Worzel (1965a, p. 345; 1965b, p. 259) gives a geometrical interpretation computed by Hambleton on the basis of free air anomalies and seismic refraction data, of a N–S profile running from the northern coast of Venezuela at 68° W and at a distance of about 50 km east of our profile.

The free air method of interpretation was described by Worzel and Shurbet (1955) and Talwani (1964). It starts from isostatic equilibrium, using so-called standard sections. The free air anomalies are explained by computing the effect of mass distributions deviating from the standard section. The configuration of these masses is given by seismic information; densities are found by converting seismic velocities on the basis of an experimentally derived relation (Nafe and Drake, 1957). In general two-dimensionality of the structures is assumed. We investigated the error resulting from this assumption in the correction for topography and isostatic compensation for the section at 68° W. It appeared to be less than 15 mgal. The method is direct and rapid, use being made of digital computors. It is equivalent to the isostatic interpretation method, if a curve of mass excess or deficiency per unit area is given with the geometrical interpretation.

The 68° west section (fig. 21) and our section (fig. 14) agree in that no crustal thickening is needed to account for the negative anomaly zone, and that both show a deformed transitional zone from continent to ocean. We will later come back to this, but will now discuss the difference between both interpretations.

The 68° W section differs with our model in that:

1. Beneath the positive zone, which runs over the Bonaire–Las Aves passage and which is equivalent to the Curaçao positive, the crust has a continental thickness, while about 13 km of high density material occupies the upper part of the crust.
2. The 68° W section shows an extremely large accumulation of sediments (up to 12 km according to Edgar, Ewing and Hennion, 1967) beneath the negative zone north of the islands, leaving about 3 km for the crustal rocks having a density of 3.0 g/cm^3.

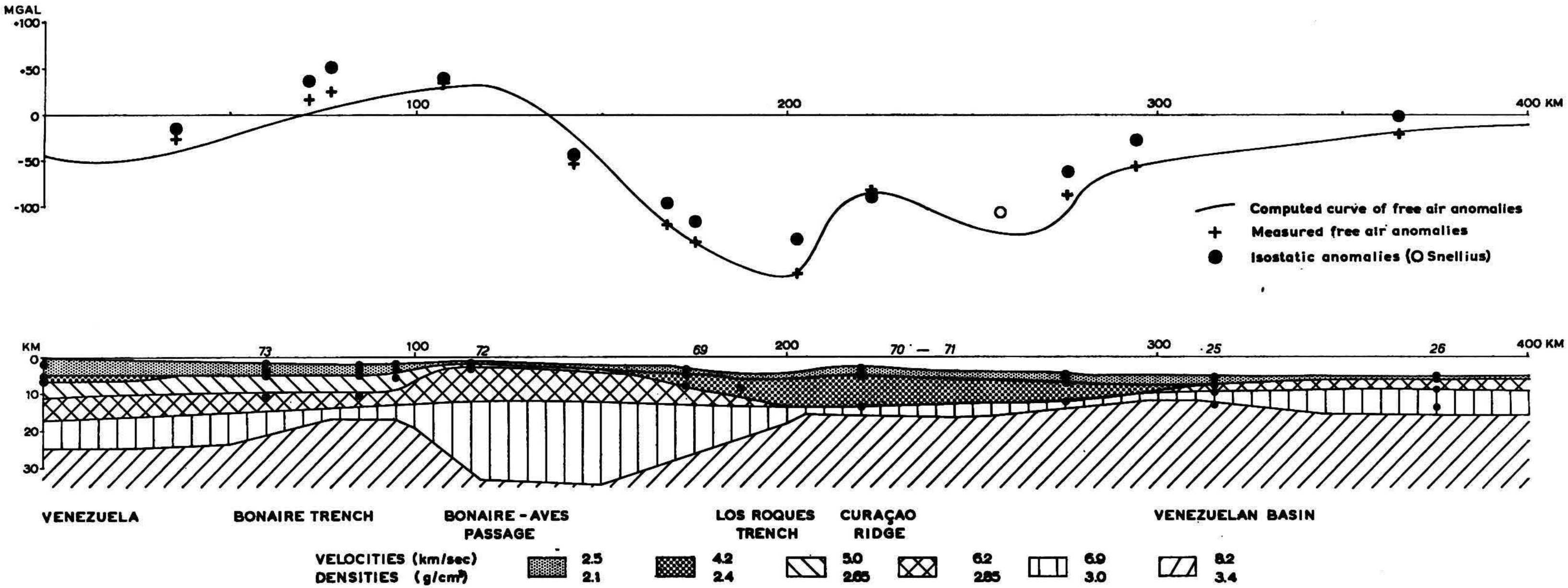

Fig. 21. Section at 68°W, constructed by Hambleton (WORZEL, 1965) from free air anomalies and seismic information. The black dots indicate the position of the observed seismic discontinuities.

ad 1: Seismic refraction indicates that material with a velocity of 6.2 km/sec lies at a shallow depth beneath the positive anomaly. On the basis of the density-velocity curve of NAFE and DRAKE (1959) a density of 2.85 g/cm³ is attributed to this material. Hambleton assumes that this material extends to a depth of about 13 km. This makes a surplus positive. The necessity of assuming a root of light crustal material reaching to a depth of nearly 35 km beneath the positive zone is thereby induced. In order to make a good fit with the observed anomaly two positives produced by upward extensions of denser mantle material on both sides of the root are needed additionally.

The question arises, whether this configuration of an (approximately 100 km wide) continental block in the transitional region from continent to sea is the only solution or whether it can be replaced by a simpler one. The gravity anomaly requires high density material in a shallow position in the crust (see section on gravity interpretation). This material, having a higher velocity, may mask arrivals of lower velocity layers lying beneath it. Assuming that such a lower velocity layer is indeed present one could arrive at a configuration of a crust that lies above its equilibrium position, analogous to what has been found in our section. The high velocity (6.2 km/sec) found seismically at shallow depth then probably represents an extension of the volcanic rocks exposed on Curaçao.

ad 2: Beneath the negative zone a light mass mainly consisting of material with a velocity of 4.2 km/sec and a density of 2.4 g/cm³ is shown on the 68° W section to have a thickness of 12 km. In the upper part a few kilometers of lighter material (velocity 2.5 km/sec, density 2.1 g/cm³) occurs. It is justified to question the assumption of a constant velocity and density to depths of 12 km; an increase in velocity and density with depth is more likely to occur. Intermediate velocities, hidden since they come in as second arrivals – or a continuous increase in velocity with depth – may be present. If so, this also holds good for the density-depth distribution. The density-depth relation for post-Eocene strata in the nearby Maracaibo basin for instance exhibits an exponential increase in density from 2.1 g/cm³ at the surface to about 2.6 g/cm³ at a depth of 3 km (J. CARR in HOSPERS and VAN WIJNEN, 1959).

The order of magnitude of the effect resulting from hidden velocity discontinuities may be estimated, using the seismic data in stations 70 and 71 of Hambleton's section. A time-distance diagram was constructed from this section. Elsewhere in the section, layers with velocities of 5 km/sec (density 2.65 g/cm³) and 6.2 km/sec (density 2.85 g/cm³) were found between the 4.2 km/sec layer and the 6.9 km/sec layer. Assuming the former horizons to be also present beneath stations 70 and 71, their depth beneath sea level would become 10 km and 13 km respectively, water depth being 3 km. In this way the thickness of lighter density material with velocities of 4.2 km/sec or less would be reduced to about

7 km [1]). Beneath these sediments the three crustal layers with velocities of 5 km/sec, 6.2 km/sec and 6.9 km/sec would have thicknesses of 3 km, 3 km and 6 km respectively. The latter thickness was estimated, considering that the negative gravity effect of this modified section must be the same as the one presented by Hambleton.

The above solution of the 68° W section saves the necessity of explaining the existence of an extremely thin crust beneath the light sediments in the negative zone. As long as seismic data do not yield compelling evidence for the existence of such a thin crust, a solution in which the crust retains thicknesses and densities not deviating considerably from those of areas adjacent to the negative zone north of Curaçao is preferred.

It should be mentioned that the question of the seismic velocity distribution with depth in this region is by no means settled by the foregoing discussion. To find the vertical distribution of velocity in a sedimentary section the use of reflection seismics will be needed. For the time being it appears that the differences between Hambleton's and our interpretation are not essential. We prefer our interpretation since it gives a simpler picture of the crustal structure, taking into account an acceptable density distribution within the crust.

Discussion of results

The result of our interpretation in figure 14 shows the configuration of the crust and the mass deviations with respect to isostatic equilibrium i.e. the masses between the underside of the crust as computed from the anomalies and the underside of the crust as computed for isostatic equilibrium (the broken line with long dashes).

The most important feature is the too low position of the underside of the crust beneath the broad zone of negative anomalies north of Curaçao, whereas in the centre of this zone the lower boundary of the crust is somewhat higher, but still too low. South of the negative zone, beneath the positive anomaly and Curaçao, the lower boundary of the crust is too high with respect to its normal position, suggesting that the crust has been raised above its equilibrium position. This is corroborated by the fact that upper Cretaceous rocks, now exposed at the surface, underwent a low grade metamorphism, indicating that a cover of at least a few kilometers thickness has been present above these rocks, which since has been eroded. In the southern part of the profile the underside of the crust is too low with respect to its normal position.

With respect to the geometry of the section, it can best be described as a wave-like deformation of the crust. Beneath the negative anomaly north of Curaçao a crustal downwarp is present, where a sedimentary body of appreciable size is deposited. Beneath Curaçao itself the crust is

---

[1]) This value was used in our interpretation for the thickness of the sedimentary body (density 2.42 g/cm³) beneath the Curaçao ridge (fig. 14).

raised above its normal position, while a body of large density occurs near the surface. South of Curaçao the crust is downwarped slightly and a layer of sediments is deposited.

The thickness of the crust, disregarding the light sedimentary layers, increases gradually from the oceanic thickness in the Venezuelan basin toward continental thickness in Venezuela. The deformation thus affects the transitional region between oceanic type of crust and continental crust. Beneath the negative zone north of Curaçao the crust has an intermediate thickness (16 km). The downwarp of the crust at that place only partly appears in the bathymetry, because of the thick fill of sediments. More to the south – beneath Curaçao and the Bonaire trench – the thickness of the crust approaches that of the continental type viz. about 20 km.

There is no need to call for crustal thickening to explain the gravity anomaly zones in the Netherlands Leeward Antilles area. The structure is best described as a wave-like deformation of the crust in the transitional region between ocean and continent.

5. MECHANISM OF DEFORMATION

DISCUSSION OF HYPOTHESES

Before discussing the deformation mechanisms that may account for the structure of the Netherlands Leeward Antilles we recall some general conclusions following from the mere presence of isostatic anomalies. Positive anomalies indicate a mass excess which exerts a downward force. Negative anomalies indicate a mass deficiency which exerts an upward force. In the first instance one would expect therefore subsidence of the crust beneath a positive anomaly and a rising of the crust beneath a negative anomaly. In the Curaçao area this is not observed. The geology of the Quaternary on the islands even suggests opposite movements as has been discussed in the section on the geologic setting. The islands in the positive zone, Aruba, Curaçao and Bonaire, have been subject to rising; the islands which are lying in the southern flank of the negative zone (Venezuelan Antilles) have been subject to subsidence. Other forces are thus acting on the crust, which at least sustain the anomalous mass distribution. This conclusion is independent of the mechanism of deformation.

The vertical component of these forces in the Curaçao area may be computed from our model (fig. 14): Comparison of the normal column of 30 km thickness with the column under the negative zone north of Curaçao shows a difference in pressure at equal depth of the order of 400 kg/cm^2 or 5 % of the total pressure.

The most important hypotheses for mechanisms causing negative gravity anomaly zones are:

1. tension fractures causing the downfaulting of a crustal block in the negative anomaly zone (WORZEL, 1965a and b).
2. plastic buckling of the crust under the negative anomaly zone due to horizontal compression (VENING MEINESZ, 1934, 1955).
3. shear fracturing in which the continental side of the crust overrides the oceanic crust (VENING MEINESZ, 1934; GUNN, 1949).

The tension hypothesis

We will first discuss the mechanism proposed by WORZEL (1965a and b). Worzel's ideas are based on an extensive comparative study of coastal margins and oceanic trenches. Quoting WORZEL 1965b (p. 335): '. . . coastal margins, as represented in generalized and somewhat simplified form, are used to show that a small downwarp or graben fault in the transitional region (*between continent and ocean, R.A.L.*) produces a structure and gravity anomaly similar to those found for oceanic trenches'. Tensional forces are then thought to act in a trench area. However, Worzel continues by saying that a simple graben structure would not provide anomalies of sufficient magnitude.

The structure of the Curaçao area – where the negative anomalies are the embodiment of a depressed zone in the transitional region from continent to ocean without crustal thickening – is entirely consistent with Worzel's results. We want to consider into more detail whether a graben structure in the negative anomaly area north of Curaçao resulting from tension in the crust indeed cannot yield anomalies of sufficient magnitude. Vening Meinesz described the mechanism of a graben formation as a consequence of stress release in the crust (HEISKANEN and VENING MEINESZ, 1958). From the theory of faulting of ANDERSON (1951), HUBBERT (1951) and HAFNER (1951), it follows that when a gradually increasing tension occurs in the crust, normal faulting along a tilted fault plane will take place. A reasonable angle of dip of this fault is about 60°. We will not enter further into the details of this faulting process (for a further discussion we refer to HEISKANEN and VENING MEINESZ, 1958), but start from the results of Vening Meinesz who predicts the formation of two fault planes at a certain distance, which dip towards each other. A trapezium-shaped crustal block is formed (fig. 22). This block will tend to isostatic equilibrium, i.e. it will sink because of the extra weight of uncompensated upper parts at the sides of the trapezium (the shaded triangles of fig. 22). This sinking gives rise to a negative gravity anomaly since subcrustal material moves sideways from under the sinking block. The adjoining crustal parts are subject to upward directed forces at the broken ends. We will later revert to the rising occurring there.

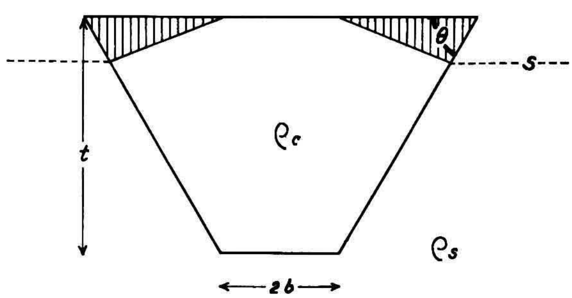

Fig. 22.

The negative gravity anomaly resulting from a complete readjustment to isostatic equilibrium of a graben block can be computed as follows. In fig. 22 the surface of the substratum if no crust were present has been drawn by a broken line (S). The underside of a rectangular block would be at a depth $h = t(\varrho_c/\varrho_s)$ under this surface S, t being the thickness of the block, ϱ_c the crustal density and ϱ_s the density of the substratum. The depth of the lower boundary of the trapezium-shaped block under the surface S of the substratum when in isostatic equilibrium, is denoted by x.

The amount of sinking needed to attain isostatic equilibrium is then $x-h$. The value of x can be calculated from the equation:

$$(bx + \tfrac{1}{2} x^2 \cot \theta)\varrho_s = (bt + \tfrac{1}{2} t^2 \cot \theta)\varrho_c$$

b = halfwidth of the underside of the block

θ = dip of the faultplane

which says that the weight of the displaced substratum is equal to the weight of the block when in floating equilibrium.

We computed the sinking and negative gravity anomalies resulting from adjustment to equilibrium for several models of graben blocks. In the first three graben block models, faults with angles of dip of 60° were assumed, this angle being acceptable for tensile faulting; in the last model this angle was taken at 35° from the configuration under the negative zone shown in Hambleton's interpretational section. The value of b was estimated from our model of the crust under the negative zone and from that of Hambleton.

Model 1. A homogeneous crust is assumed with $\varrho_c = 2.67$ g/cm^3, $\varrho_s =$ 3.27 g/cm^3. Values of t = 26 km and b = 50 km are taken. The thickness t corresponds to that which would explain the negative anomaly north of Curaçao for a homogeneous crust. The angle of dip θ is taken to be 60°. The sinking caused by the uncompensated mass in this graben block would be about 500 m. The gravity effect of a Bouguer plate of this thickness, with density contrast 3.27, is 68.3 mgal, being the maximum negative anomaly that can be expected after isostatic readjustment of the supposed graben block.

Model 2. In the upper part of the crust under the negative anomaly zone a layer with a thickness of 7 km and density 2.42 g/cm^3 is assumed, as discussed for fig. 14. Beneath this layer material of density 2.67 g/cm^3 and a thickness of 16 km lies on the substratum with a density of 3.27 g/cm^3. Values for b and θ as in model 1. Sinking to equilibrium would be about 330 m. The negative gravity anomaly would be about 50 mgal. These values are smaller than in the preceding model, owing to the fact that a smaller density for the upper layer is used.

Model 3. In this model the layering in the assumed graben block is as indicated in Hambleton's interpretation of the 68°W section: 12 km with a density of 2.4 g/cm^3 on top of 3 km with a density of 3.0 g/cm^3, and a substratum with a density of 3.4 g/cm^3. This block would sink 200 m when the value of b, as taken from Hambleton's model is 40 km and $\theta = 60°$. The negative gravity anomaly resulting from this sinking would be about 30 mgal.

Model 4. Thicknesses and densities as in model 3. The angle of dip of the faults is taken to be 35°. This value is taken from the dip of the sides of the block consisting of material with a density of 2.4 g/cm^3 as presented in Hambleton's section. The sinking would be 450 m. The negative gravity anomaly resulting from a complete readjustment to isostatic equilibrium would be about 60 mgal.

In these computations the presence of a water layer has been neglected. To calculate the sinking in this case, the density of sea water ϱ_w has to be subtracted from the densities in the relation given above. This means that the downward movement and the negative gravity effect resulting from readjustment to equilibrium will be smaller.

The depth of the sea above a crust in equilibrium and with a layering as given in models 1–4, is between 1 and 1.5 km. Sea depth above the graben blocks in equilibrium (models 1–4) is less than 2 km, with a negative anomaly of about 70 mgal for model 1 and no more than 50 mgal for models 2–4. Compared with the observed situation a sea depth of about 3 km and an isostatic anomaly of about -120 mgal in the area north of Curaçao, the values found from the graben models appear to be insufficient.

Let us next consider the effect of a tensional graben structure in the area north of Curaçao on the island itself, which then would lie on the broken end of the crustal part adjoining the graben. Since the crust adjoining the graben would bend upward tending to isostatic equilibrium, Curaçao would undergo an upward movement .The amount of this upward bending may be computed with formulas for the deformation of a crust broken and loaded vertically at its broken end (Heiskanen and Vening Meinesz, 1958, p. 323). With the dimensions and density values used in our first computation of the negatvie effect of a graben subsidence (one layer model) the broken end of the crust adjoining a hypothetical graben north of Curaçao would rise about 200 m. In the section on gravity interpretation it has been argued that at least 1 km must have been eroded from Curaçao island, i.e. at least the same amount of rising must have occurred. This is much more than the rising that would be due to a tensional structure.

We thus can infer that a simple graben structure with acceptable dimensions and densities indeed fails to explain the structure in the negative zone north of Curaçao and of the island itself.

It should be noted that the previous discussion starts from the normal assumption of a mantle viscosity of 10^{22} poises which allows the graben block to reach isostatic equilibrium within a reasonable time. It is possible to surmise that a local high mantle viscosity permits the formation of a deep reaching fissure, tensional stress acting. The surface expression of this fissure would then be the oceanic trench with associated negative anomalies. This hypothesis was advocated by Van Bemmelen in 1958.

For the moment, however, there is no reason for supposing a much higher viscosity of the mantle to be present locally. In later papers, VAN BEMMELEN (1964, 1966) relates the structures in the southern Caribbean to the westward drift of the American continent, involving shear movements at the sides of the drifting crustal segments. The dextral shear fault system of the southern Caribbean, bounding the right side of the South American continent, will be discussed in Chapter 6.

An additional argument against tension is found in the following. Worzel's tension hypothesis is primarily based on a comparison of oceanic trench areas with continental margin areas. Negative anomaly zones are, however, not exclusively associated with deep sea trenches, but also occur over submarine ridges, islands and continental areas. The continuity of negative anomalies in Indonesia over entirely different morphological structures has already been emphasized by VENING MEINESZ (1948, p. 34).

In the Caribbean area, a continuous negative belt stretches from the Puerto Rico trench, over the Barbados Ridge – on which the island of Barbados is situated – into the northwestern part of the South American continent (Eastern Llanos basin) (see DE BRUYN's isogam map, 1951 and fig. 23). While the morphology of the Puerto Rico trench at first sight may suggest a tensional structure, it is difficult to account for the Barbados Ridge in the same manner, where the island of Barbados was raised in the shape of a dome up to a height of 300 m above sea level during the Quaternary (BUTTERLIN, 1956). Moreover, the same can be said of the southward thrusting of the Caribbean ranges over the thickly sediment-filled Eastern Llanos basin in Venezuela, occurring at the north flank of the negative zone (HEDBERG, 1956).

As has already been remarked, the negative zone of the Leeward Antilles – though interrupted by the Oca fault – continues at its western end landinward in the valleys of the Magdalena and Cauca rivers. These sediment-filled valleys are, according to WATERS and HEDBERG (1939), downthrusted basins comparable in age and structure with the Maracaibo basin and the Venezuelan Llanos basins. Again, a tensional origin for these features seems difficult to account for.

Concluding, it can be said that a tension hypothesis for the crustal structure beneath the negative anomaly zone of the Leeward Antilles does not well account for the existent large departures from isostatic equilibrium. Neither the negative anomalies nor the positive anomalies in this area can be due to a simple graben structure of acceptable dimensions. A graben structure involving a higher mantle viscosity has to be rejected for the time being. Apart from this, it is argued that tension does not well account for the different morphological features found in the zone of negative gravity anomalies.

Plastic buckling

The mechanism of plastic buckling by which Vening Meinesz explained the crustal deformation of certain areas in island arcs, may be put in the following general terms. Under lateral uniaxial compression the crust deforms plastically in a narrow strip. Initially the crust thickens symmetrically with respect to the median plane of the crust. This configuration is not in isostatic equilibrium. As a result a downward displacement of the plastic strip occurs. This downbending accelerates under continuing stress leading to a downbuckle of the crust. The root of crustal material thus formed represents the seat of negative gravity anomalies observed in long continuous belts. Owing to the buoyancy of the root, upward bulges of the crust are formed at both sides of the plastic zone. Positive anomaly belts are thus to be expected parallel to the negative anomaly belt.

Theoretical treatments of the phenomenon have been given by BIJLAARD (1936) and VENING MEINESZ (1955). VENING MEINESZ (1948, 1954) demonstrated that this type of deformation may account for the gravity anomalies and structure of the Java trench.

We do not consider it likely that plastic downbuckling constitutes the principal mechanism responsible for the deformation of the crust in the Netherlands Antilles area. First, no crustal thickening is observed in the area. Although it is possible that only part of an oceanic buckle finds its expression in gravity anomalies (VENING MEINESZ, 1954), one should still have to find indications of some crustal thickening in case of plastic buckling in oceanic environment. That only part of an oceanic buckle will be apparent in gravity anomalies is clear from the circumstance that the lower boundary of the mechanical crust in oceanic areas is deeper than the crust – mantle boundary as defined by a definite density contrast.

Symmetry of the negative gravity anomaly curve across a deformed belt has been called in as an indication of plastic buckling (VENING MEINESZ, 1964). This holds however only for deformation in an area where the crust is symmetrical with regard to the axis of the deformed belt. In the Netherlands Antilles area we are dealing with a transitional region between continental and oceanic crust. Since the density of the continental crust is smaller than the oceanic crust it may be expected that the continental side in such a transitional region will lag behind in sinking with respect to the oceanic side. This leads to an asymmetric downbulge of the crust and gravity anomaly curve.

The asymmetry of the gravity anomaly curve across the Netherlands Antilles and the Los Roques trench, therefore, does not exclude the possibility of plastic downbuckling. It is mainly because of the absence of crustal thickening in the area that we prefer another mechanism than that of plastic buckling.

Shearing

Another reaction of the crust to compressive stress, as suggested by VENING MEINESZ (1948) and later in different form by GUNN (1949), would chiefly consist of shear fracturing.

1. According to the Coulomb theory a strike-slip shear plane (wrench fault or transcurrent fault) may be formed under the influence of a stress field where the intermediate principal stress axis is vertical. On account of experimental and observational studies (ANDERSON, 1951; HUBBERT, 1951) an angle of about 30° between the shearing plane and the axis of largest principal stress may be expected. If one assumes that the direction of the relative movements of crustal blocks on both sides of the shearing interface approximately coincides with the axis of compression, the component of movement normal to the shearing plane will cause an asymmetric downbulging of the crust, which will be expressed in an asymmetric gravity anomaly curve.

VENING MEINESZ (1948) meant this mechanism to explain the anomaly belt west of Sumatra, where the northern continental crustal block overrides the southern oceanic crustal block.

2. The crust may react with dip-slip shearing (reverse faulting) instead of strike-slip shearing, when the largest and intermediate principal stress axes lie in the horizontal plane. The resulting fault plane is parallel to the intermediate principal stress axis. Reverse faults at the continental margin will result in an overriding of the continental side over the oceanic side since a couple is produced by the fact that the continent stands higher than the adjacent ocean. A trench is thus formed at the depressed oceanic side, a mountain range at the upthrusted continental side. Negative gravity anomalies, brought about by the underthrusted part of the deformed crust, are asymmetric with largest values at the continental side and decreasing values seaward as the downward displacement decreases in that direction. Positive anomalies having the same distribution landward as the negative anomalies seaward are produced if no erosion of the overthrusted block occurs. In general, however, erosion products of the overthrusted block will fill the adjacent depression, shifting load from the overthrusted to the underthrusted segment. In the overriding continental block secondary failure would occur as a result of the bending of the upthrusted crust (GUNN, 1949).

HOSPERS and VAN WIJNEN (1959) demonstrated in a gravity study of the Venezuelan Andes and adjacent basins, that the thrust fault mechanism accounts well for the structure of that area, the Venezuelan Andes having been thrust to the northwest over the Maracaibo basin. In the following it will be seen to what extent a shearing mechanism fits in with the structure and other geophysical data of the Netherlands Leeward Antilles and the surrounding region.

DEFORMATION OF THE NETHERLANDS LEEWARD ANTILLES AREA

With regard to the mechanism of deformation in the Netherlands Antilles area we recapitulate the following points of interest.

1. The anomaly curve across the negative belt is asymmetric, with

steepest slope on the island side and a gradual decrease toward the Venezuelan basin (see profiles A and B of fig. 15 and 16 and the gravity anomaly map fig. 13).

2. The asymmetry is also reflected in the bathymetry of the Los Roques trench, being best developed in the area of Los Roques. A steep southern slope is present there; it is at the foot of this slope that greatest depths are found. The trench tapers gradually off in northeasterly direction i.e. toward the Venezuelan basin (fig. 12). In the region north of Curaçao sediments and possibly volcanics obscure the trench, while there is no trench at all north of Aruba. A deepening of the Venezuelan basin toward the axis of the negative zone, comparable with the northward tapering of the trench in the Los Roques area is, however, still apparent north of Aruba (fig. 15, profile A).

3. The crust is several kilometers depressed in the negative zone, the depression largely filled with sediments. In the positive zone the crust is above its normal position. The general structure is thus one of a wavelike deformation.

4. No crustal thickening is necessary to account for the anomalies.

Concerning the deformation types dominated by shear faulting it can be said that the deepening of the sea from the flat Venezuelan basin to the southern edge of the Los Roques trench, where the largest depths occur, may well reflect the downbending of the crust as a result of downthrusting of the northern crustal segment. The asymmetry in the anomaly curve supports this idea.

It is difficult to decide whether the shear faulting is predominantly strike-slip or dip-slip. From the gravity data in the area no information can be gained on the position of a fault plane or planes. The presence of faults (along the north coast of Venezuela) of great extension with mainly strike-slip components leads to the suggestion that, if shear faults are present in the Leeward Antilles zone, they will have an important strike-slip component. In a following section this question will be investigated into some more detail. For the monent it seems justified to assume that the deformation in the Netherlands Antilles area mainly consists of shearing with some overriding of the southern block in a direction normal to the anomaly belt.

In this connection it is interesting to note that the bathymetry and the gravity anomalies in the Leeward Antilles area greatly resemble those of the section of Sumatra across Benkulen towards the Indian Ocean (VENING MEINESZ, 1948; COLLETTE, 1954). As has been remarked before the structure of this region is, according to Vening Meinesz, also due to a shearing mechanism. The trench west of Sumatra is asymmetric, as is the anomaly curve. Both show the steepest slope at the side of the continent. The cross section of the negative local isostatic anomalies shows two minima, the upward bulge in the anomaly curve coinciding with a submarine ridge, on which elsewhere islands are located. A difference is that the negative anomalies west of Sumatra are somewhat smaller than in the Leeward Antilles area.

Here we may give some additional comment on (1) the position of the islands with respect to the positive anomaly zone, (2) the submarine Curaçao ridge and the bulge in the negative anomaly zone north of Curaçao and (3) the negative anomalies that roughly coincide with the Bonaire trench.

ad 1. The deeper structure beneath the positive zone is characterized by a high position of the lower boundary of the crust; the crust is upwarped. This upwarp is not clearly expressed in the topography (the islands in the positive zone are not located on a marked ridge). The positive zone even occurs in deep water southeast of Bonaire, where anomalies become smaller. In this connection it should be borne in mind that the high positive anomalies on the islands partly result from the presence of shallow bodies of dense material. These bodies are formed by Cretaceous volcanic rocks locating in the core of the islands. However, the Cretaceous volcanism has no direct relation to the positive anomaly zone, such as is the case with the volcanic Lesser Antilles, since indications are that the anomalies are post-Cretaceous (see Chapter 6). The Leeward Antilles therefore should not be designated as the volcanic arc of an island arc system. In fact no Tertiary or recent volcanism occurs on the Leeward Antilles.

The question remains why further east the islands do not coincide with the positive zone, but are situated in the negative anomaly strip. An explanation may be found by assuming that the upwarp took place in a direction crossing the older Cretaceous structure.

Alternatively, the position of the eastern islands in the negative zone can be explained by assuming that in that area the southern crustal block infringes over the downthrusted block of the Caribbean Sea. The subsiding movements of the Aves islands, evidenced by the geology, may then be the result of a secondary downward sliding of these islands into the Los Roques trench.

ad 2. The relative maximum in the negative anomaly north of Curaçao coinciding with the Curaçao ridge, is partly due to anomalous masses in the crust, but a slight upward bulge of the main crustal layer ($\varrho = 2.67$ g/cm^3) also contributes to it (see fig. 14). This situation could incidate that the compression on the negative zone decreased in a recent period so that parts of the belt could adjust to isostatic equilibrium. A subsequent period of increasing compression led to a wave formation of wavelength shorter than that of the depressed crust elsewhere in the anomaly belt. The Curaçao ridge was thus pressed upward and the adjoining negative belts further downward. Since nothing is known of the actual movements of the Curaçao ridge, while further no indications of such events are present on the nearby islands, this solution is conjectural.

Another possibility is that the up-arching of the crust beneath the Curaçao ridge represents a secondary reaction of the crust to the continued downbending under increasing compression. It is then brought about by secondary buckling in that region.

ad 3. It is well possible that the negative anomalies of the Bonaire trench continue westward via the Falcón area into the Gulf of Venezuela (East of Goajira) where also weak negative gravity anomalies have been found. These anomalies possibly constitute a second negative belt which is, however, rather weak and patchy (see DE BRUYN's map, 1951). The anomaly of the Bonaire trench is interpreted as being due to a downwarp of the crust which is filled with sediments; the same situation occurring in the Gulf of Venezuela (CORONEL, 1967). This downwarp is thought to be related to secondary failure which may be expected when the upthrusted segment of the crust undergoes continued deformation. This situation is comparable to what is found on Java and Sumatra (COLLETTE, 1954).

6. THE REGIONAL STRUCTURAL PATTERN

Seismicity in the Caribbean

Conclusions from focal mechanism studies in island arcs have been related to geotectonic hypotheses (Ritsema and Veldkamp, 1960; Ritsema, 1964; Orowan, 1965). In general the horizontal component of the largest principal stress direction is about normal to the tectonic trend of island arcs.

Sykes and Ewing (1965) relocated a large number of hypocentres of Caribbean earthquakes occurring between 1950 and 1964. Most Caribbean earthquakes are confined to a belt that can be traced from Central America to the Greater and Lesser Antilles and thence into northeastern Venezuela. There is a general parallelism of seismic belts and gravity anomaly zones in the Caribbean. Mendiguren (1966) published a statistical study on the direction of greatest principal stress in South American earthquakes. He concludes to an azimuth of 150° for the horizontal component of this stress direction for the shallow earthquakes in the eastern Caribbean Mountains, which are related to the El Pilar fault zone.

Remarkably enough the region of gravity anomaly zones of the Leeward Antilles is nearly aseismic (L. M. R. Rutten and Van Raadshoven, 1940; Sykes and Ewing, 1965). In this area only 4 epicentres are shown on Sykes and Ewing's map [1]). This atypical behaviour deprives us from determining directly the direction of the present stress field in the Leeward Antilles.

Structural pattern of northern South America

Vening Meinesz (1964) studied the stress direction in the Caribbean area and South America. He thought the Andes Mountain system and the Caribbean islands arcs to be the result of a movement of the South American continent in a direction of about 30°, the movement having been brought about by a convection current in the same direction. Assuming that the direction of movement and the direction of largest horizontal stress approximately coincide, the angle between the negative belt of the Leeward Antilles that strikes in a direction of about 100° (fig. 23) and the direction of largest horizontal stress would be about 70°. Vening Meinesz attributes the negative zone of the Leeward Antilles to plastic buckling. The angle just mentioned is not too different from the angle of 55° which, according to the theory of Bijlaard (1936), a strip of plastic

---

[1]) These are all shallow earthquakes, located at 12°04N – 72°66W, 13°23N – 71°01W, 12°05N – 65°40W and 11°20N – 65°82W. The epicentres are spreaded through the area and have no clear relationship to tectonic features.

buckling should make with the direction of greatest horizontal stress. We have, however, discussed already that the deformation of the Leeward Antilles area is probably not controlled by plastic buckling. Moreover, the mentioned stress direction does not account very well for the structural pattern of Venezuela and Colombia, as will be seen in this section, where HOSPERS and VAN WIJNEN's (1959) ideas will mainly be followed.

Several long linear faults occur in the northeastern part of the South American continent (fig. 23). According to ROD (1956) and ALBERDING (1957) these faults are predominantly strike-slip faults. From the pattern they form one can derive the direction of largest horizontal stress according to ANDERSON (1951), HUBBERT (1951) and MOODY and HILL (1956).

In a direction of 90°, along the northern coast of Venezuela runs the El Pilar fault which is a right lateral strike-slip fault. We note here that METZ (1964) found in a study of this fault zone near Caracas, that its strike-slip is not as great as suggested by Rod. Westwards this fault apparently continues into Colombia, where it changes direction to 100° and where it is called the Oca fault. Also in Colombia we find the Great fault, a left lateral strike-slip fault with an azimuth of 330° to 350°. The fault separates the Colombian Cordillera Central from the Sierra Nevada de Santa Martha.

Two other strike-slip faults which terminate against one of the just mentioned strike-slip faults, are: the Tigre fault, a left lateral strike-slip with direction 30°, located south of the Goajira peninsula, and the Bocono fault, a left lateral strike-slip with direction 60°, cropping out in the Venezuelan Andes. The Bocono fault, seems to have a considerable dip-slip component (HOSPERS and VAN WIJNEN, 1959). It is not certain what the ratio of horizontal to vertical displacement in this fault is. However, on account of Hospers and Van Wijnen's interpretation (their fig. IX–2) it seems that the dip-slip component is predominant. Little is also known of the dip-slip components of the other mentioned faults; the extreme linearity of their outcrops, however, points toward a predominance of strike-slip in the faults.

In determining the direction of the stresses that caused the fault system, distinction should be made between 1st order faults and 2nd and higher order faults. The direction of the latter depends on the change of the primary compressive stress after 1st order faults have been formed (see MOODY and HILL, 1956). According to Moody and Hill, 2nd order faults should terminate against first order faults. With this in mind it appears that the El Pilar-Oca faults and the Great fault belong to the first order category and that the Tigre and Bocono faults are second order faults.

The direction bisecting the compressed segment between the 1st order strike-slip faults indicates the direction of the horizontal compressive stress (ANDERSON, 1951). This direction is approximately 125°. The angle of about 25° that this direction makes with the Great fault and the El Pilar-Oca fault zone, compares well with the angle of about 30° to be ex-

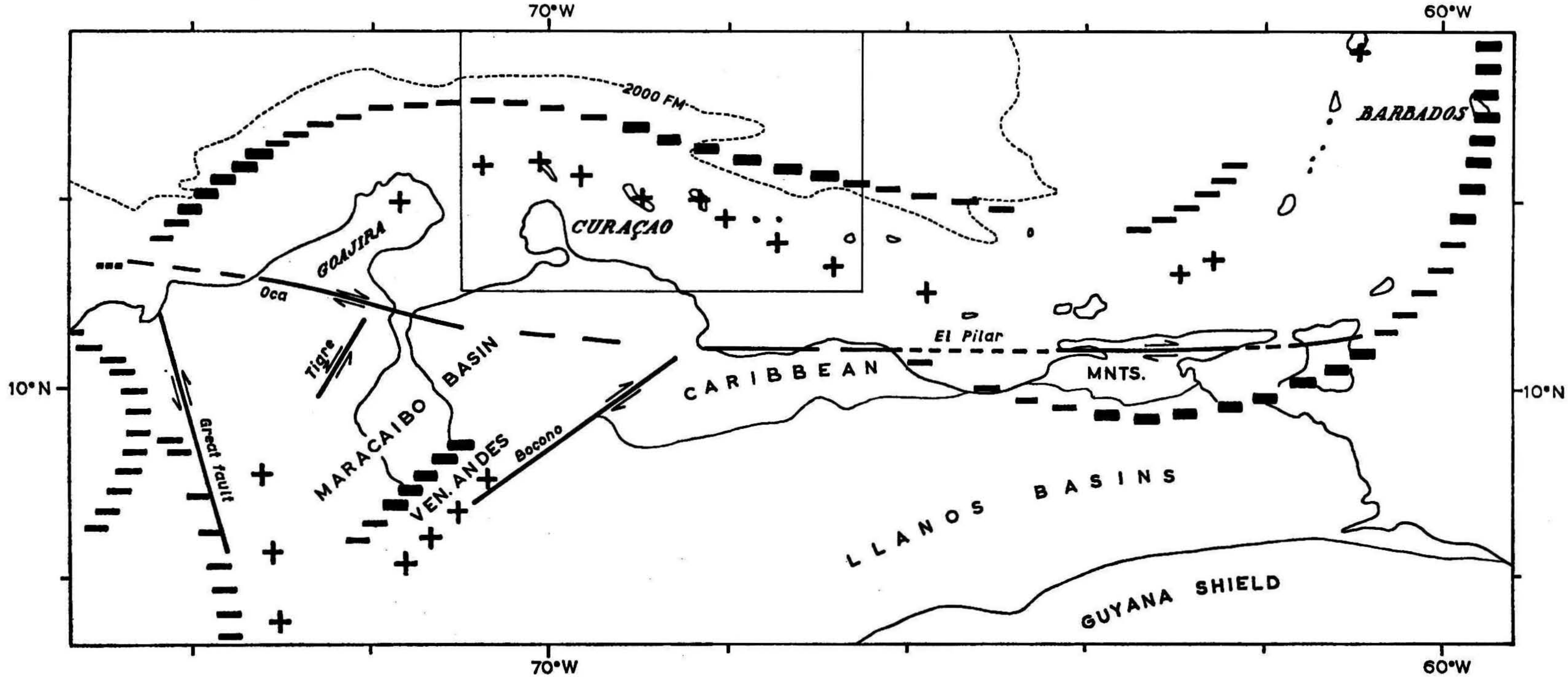

Fig. 23. Regional structural elements and gravity axes in the southern Caribbean area. The rectangular area in the upper part of the figure marks the region for which a detailed gravity map was constructed (fig. 13).

pected in shear faulting (HUBBERT, 1951). The stress direction also accounts for the reverse faulting that took place in the Venezuelan Andes.

We recall MENDIGUREN's (1966) figure of 150° for the direction of the present greatest horizontal stress in the Eastern Caribbean Mountains. It compares reasonably with the result of Hospers and Van Wijnen from geological observations. According to RITSEMA (1964) a difference of 10°–20° in the direction of the principal axes is acceptable for structural interpretation. Besides, local variations in the stress field may obscure the regional tectonic picture.

Before comparing the above results with the situation in the southern Caribbean, it should be remarked that it is not well known in what period or periods the faulting originated. They seem to have been active from Mid or Upper Cretaceous time, movements having gone on during the Tertiary (cf. ALVAREZ, 1967 on the faults in Goajira). Some faults show fairly recent activity; for instance the Bocono fault, which has displaced the local drainage pattern (ROD, 1956). In the foregoing it has been assumed that the primary faults have been active simultaneously.

COMPARISON WITH THE SOUTHERN CARIBBEAN

How does the generally NW-SE directed compressive stress of northern South America fit into the pattern of gravity anomaly zones in the southern Caribbean, which in our opinion are due to shearing and compression. Over a distance of at least 500 km the negative zone has a direction of 100°. Isostatic anomalies over the Los Roques trench have values of up to −150 mgal. Towards the west the negative zone turns around the Goajira peninsula and then continues in a direction of 55° over a distance of about 300 km. Isostatic anomalies there amount to −125 mgal. An angle of 135° is thus enclosed by these two parts of the southern Caribbean negative anomalies strip.

The general parallelism of this zone with the principal directions of the faults in northern Venezuela is striking: There is only a small difference in direction between the zone of the Leeward Antilles and the Oca-El Pilar fault zone. In Colombia the negative anomalies of the Magdalena river valley trend approximately in the same direction as the Great fault.

If it is correct that shear faulting is an important factor in the structure of the Leeward Antilles-Los Roques trench area, it is justified to assume that the faulting results from a stress field with the same general orientation as that responsible for the shear fault pattern in northern Venezuela and Colombia. The Leeward Antilles-Los Roques trench structure is then dominated by right lateral strike-slip faulting in the direction of the anomaly zones, combined with compression in a direction normal to the fault plane(s). The negative zone west of Goajira can be interpreted as being due to a dip-slip fault in which the eastern crustal block overrides the western crustal block (as the Maracaibo-Venezuelan Andes structure).

The negative zone of the Magdalena river valley is interpreted as due to left lateral strike-slip faulting with compression in a direction normal to the fault zone. Because of insufficient data the structure of the latter two areas will not be discussed here further[1]).

It is, however, of interest to make the following observation: the negative belt west of the Goajira peninsula apparently dies out abruptly against the western extension of the Oca fault. Pendulum station no. 1029 (BRUINS, DORRESTEIN, VESSEUR, BAKKER and OTTO, 1960) located just north of the extended Oca fault direction gives a local isostatic anomaly of −82 mgal. Some 30 miles to the southwest station no. 1028, which lies south of the extended Oca fault direction, gives an isostatic anomaly of −2 mgal. In fig. 23 this station is indicated with dashes. Other pendulum sea-stations south of the extended Oca fault also give only weak negative anomalies. The dying out of the anomaly zone west of Goajira suggests that the seaward extension of the Oca fault separates the crustal block south of that fault from the northern block, the latter block being compressed in the area of negative anomalies in the southern Caribbean Sea.

In connection with the above described mechanism controlling the Leeward Antilles-Los Roques trench structure some tentative remarks may be made on the indentations in the positive zone over the Netherlands Antilles (fig. 13). The pattern of the positive zone is suggestive of strike-slip faults or flexures of the Tigre fault type (south of the Goajira peninsula). Left lateral strike-slip movements of the 2nd order, associated with the primary right lateral strike-slip at the northern edge of the positive belt may thus cause the pattern of the positive zone and the position of the Netherlands Leewards Antilles.

In the foregoing, the hypothesis has been put forward that the younger (= Tertiary) structure of northern South America is related to that beneath the gravity anomaly zones of the southern Caribbean. It is worthwhile to consider whether the age of the structures beneath the anomaly zones of the southern Caribbean supports this assumption.

The crustal upwarp associated with the positive anomaly zone of the Netherlands Antilles must be younger than Cretaceous. Thick submarine volcanic and sedimentary layers were deposited during the Upper Cretaceous in that area. In post-Danian time emergence and erosion took place; it is after that time that the deformation associated with the anomaly zone should be placed. WESTERMANN (1949) suggests that the formation of ridges and troughs was incipient in the Upper Eocene. Possibly the islands stayed at approximately the same level (shallow water depth or higher) during a great part of the Tertiary. In that period some shallow warping occurred. From Lower Miocene the islands were subject to gradual rising movements.

---

[1]) A deformation by plastic buckling seems also possible for the area of negative anomalies west of Goajira.

Additional information on the Tertiary is available from the nearby continent. The Falcón basin and the basin of the Gulf of Venezuela lie approximately in the line with the negative anomalies of the Bonaire trench. In the former two areas basin-formation culminated in Mio-Pliocene times. All three areas are characterized by thick sedimentary fills and weak negative anomalies.

The preceding remarks indicate that the deformation in the Netherlands Antilles area should be placed in the Tertiary, beginning in the (Upper?) Eocene with possibly culmination of movements in the Mio-Pliocene. Movements persist through the Quaternary. This is in general agreement with observations elsewhere in the Caribbean: the Maracaibo-Venezuelan Andes deformation being predominantly Mio-Pliocene (HOSPERS and VAN WIJNEN, 1959), the East Venezuelan basin (eastern Llanos) being mainly Tertiary with culmination of basin formation in the Oligo-Miocene (HEDBERG, 1956) and the deformation associated with the negative strip of the Greater and Lesser Antilles initiating in the Eocene, later deformations taking place in the Mio-Pliocene (BUNCE, 1965; BUTTERLIN, 1956; FISHER and HESS, 1963; see also EWING, TALWANI, EWING and EDGAR, 1967).

Summarizing we may conclude that the deformation of the crust in the southern Caribbean, which is expressed in long gravity anomaly zones, can be explained as being the result of a compressive stress in a general NW-SE direction. Movement of the South American continent in a northwesterly direction may have been the reason for that stress field. The movement was accompanied by predominantly strike-slip faulting, combined with compression and possibly some overriding of the crustal block at the continental side over the crustal block at the side of the Caribbean Sea in a direction normal to the faults. The deformation of the southern Caribbean fits reasonably well into the general deformation pattern of northeastern South America.

Finally, the relation of the structural directions in the southern Caribbean to those in the eastern and northern parts of the region poses some problems that cannot easily be solved. We think it hazardous to extrapolate our conclusion to the Greater and Lesser Antilles. It cannot be precluded that we are not dealing with an uniform stress field, but that large deviations occur in the direction of maximum stress that are effected by the geometry of the distribution of continental and oceanic crust.

7. ISLAND ARCS, ISOSTATIC EQUILIBRIUM AND GEOSYNCLINES

Without entering into every aspect whether the structures beneath negative anomaly zones represent an early stage in the development of a geosyncline we want to consider the present data on the crustal structure in the zone of negative gravity anomalies in the Netherlands Antilles area as well as published data on the negative zones elsewhere in the Caribbean in the light of this problem. We use the term geosyncline: denoting an elongate area, initially subject to long-continued, considerable subsidence and sedimentation, which in a later stage is folded and elevated, forming a mountain system (HOLMES, 1965). The origin of geosynclines has been formulated by VENING MEINESZ (1955) as being due to plastic buckling of the earth's crust. Subsidence and plastic thickening of the crust occurs during the process taking place under continuing compressive stress. Relaxation of the stress allows the deformed crust to readjust isostatic equilibrium and a high mountain range comes into being. In this concept the zones of strong negative gravity anomalies would represent the recent areas of plastic buckling.

We restrict our discussion to the question whether the subsidence and sediment-filling beneath the Caribbean negative zones is comparable to that in fossil geosynclines and whether high mountain systems will be formed if the crust would be allowed to come to isostatic equilibrium. For a discussion of the nature of sedimentation in fossil geosynclines and recent equivalents we refer to KUENEN (1966).

We first consider the Netherlands Antilles area. The pile of sediments, present in the elongated crustal depression beneath the zone of negative anomalies north of the islands is in thickness comparable to that of fossil geosynclines. One might, looking at the section in fig. 14, even go further and suggest that the structure beneath the negative zone north of the islands can be taken as the modern equivalent of a eugeosyncline; and the structure beneath the negative anomalies south of the islands (the Bonaire trench, the Falcón- and the Gulf of Venezuela basin) as the equivalent of a miogeosyncline. Should this be the case then the equivalent is yet limited: consider the position of the crust when it would be allowed to reach isostatic equilibrium. Figure 24 gives the section across the Netherlands Antilles area when in equilibrium. The whole area is then below sea level. In general, sea depth increases from the south beginning with the South American continent toward the oceanic depth of the Venezuelan basin in the north. At the site of the present negative zone a shallow submarine ridge appears (depth about 1 km). Where now the island of Curaçao is located the sea will be deepest namely about 2.5 km. Even if the sediment body beneath the negative zone north of the isles were not present and the total mass deficiency was placed beneath the crust, no mountain would come into being. Illustratively, we note that in the actual situation a crustal thickening at a factor 2.5 would be needed to elevate the Curaçao ridge to a height of about 4 km by isostatic readjustment.

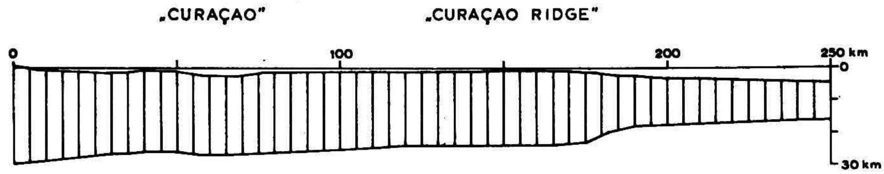

Fig. 24. The section of fig. 14 in isostatic equilibrium.

In order to see whether the foregoing is also valid for the negative zones in the Caribbean area in general, we first make a distinction between them as regards their physiography. We can distinguish 4 types:

1. deep sea trenches with thin or moderate sedimentary fill – Puerto Rico trench
2. submarine ridges with thick sediments – Barbados ridge and Curaçao ridge
3. basins near the continental edge with thick sedimentary fill – East Venezuelan basin
4. basins in the continent with thick sedimentary fill – Maracaibo basin

The thickness of the light sedimentary layers in the mentioned areas is presented in table 6.

TABLE 6

Sediment thicknesses beneath zones of negative gravity anomalies in the Caribbean

Type	Area	Sediment thickness km	Reference
1	Puerto Rico trench	2	OFFICER et al., 1957
2	Barbados ridge	10	OFFICER et al., 1957
2	Curaçao ridge	min. 7	12 km acc. to EDGAR et al., 1967
3	East Venezuelan basin	15	DE BRUYN, 1951
4	Maracaibo basin	8	HOSPERS and VAN WIJNEN, 1959

With the exception of the Puerto Rico trench sediment thicknesses are sufficient to compare with the contents of a fossil geosyncline.

The equilibrium situation of these areas is as follows.

1. *The Puerto Rico trench* (OFFICER, EWING, EDWARDS and JOHNSON, 1957; TALWANI, SUTTON and WORZEL, 1959). A few kilometer of light sediments is deposited in a crustal downwarp beneath the trench. The mass deficiency in the trench reaches a largest value of -10×10^5 g/cm^2.

With a mantle density of 3.4 g/cm³, as assumed by Talwani et al., the trench would rise at the most 4.2 km to reach its equilibrium position. The present sea depth being approximately 7 km, the trench area would still remain deep sea when in isostatic equilibrium.

2. *Barbados ridge* (OFFICER, EWING, EDWARDS and JOHNSON, 1957); WORZEL, 1965b, p. 272). A great accumulation of sediments exists in a crustal downwarp beneath the ridge. The crust there is two times thicker than beneath the adjacent ocean. In the equilibrium situation a submarine ridge of some 700 m depth below sea level would exist. It is estimated that the island of Barbados itself would not rise appreciably, and would become an island in height comparable to the present Greater Antilles.

3. *East Venezuelan basin* (DE BRUYN, 1951). De Bruyn's best solution to fit the computed gravity curve to the observed curve across the basin, is a 15 km deep basin-shaped depression, filled with sediments (see also HEDBERG, 1950), the crust retaining its original thickness. Densities used for the computation were 2.5 g/cm³ for the sediment, 2.7 g/cm³ for the granitic crust of 25 km thickness and 3.0 g/cm³ for subcrustal material. Equilibrium would be reached if the basin rises to form a topographic height of 2.7 km, above sea level, at its maximum height.

4. *Maracaibo basin* (HOSPERS and VAN WIJNEN, 1959). The structure of the Maracaibo basin results from shear fracturing, the Venezuelan Andes thrusting over the adjacent Maracaibo basin where light sediments reach a thickness of about 8 km. If the basin would be allowed to reach isostatic equilibrium, a topographical height of about 2 km would come into being.

We come to the conclusion that none of the present structures beneath the negative anomaly zones in the Caribbean area, whether oceanic or continental will develop into a high mountain system upon readjustment of the isostatic equilibrium, although several of them resemble fossil geosynclines as regards size and thickness. There are several points of interest in this respect.

First, seismic work of RAITT (1967) shows that some 4 km of sediments occur in the Java trench, the area from which Vening Meinesz elaborated the hypothesis on the development of geosynclines. The seismic information of Raitt demonstrates that although the crust in the Java trench is thick, a large part of the negative isostatic anomaly can be explained by the occurrence of light sediments, so that only a low submarine ridge is formed upon readjustment of equilibrium. Also the Java trench is not a mountain system *in statu nascendi*.

The other point to make refers to the observations of DRAKE, EWING and SUTTON (1959) and of HEEZEN and DRAKE (1964) on the eastern continental margin of North America. These authors demonstrated that the sedimentary cross section through the continental margin east of North America strikingly corresponds to the restored section through the Appalachian geosyncline in eastern North America. The sedimentary pile beneath the continental shelf is compared with the miogeosyncline and the thick sediment pile beneath the base of the continental slope with the eugeosyncline and therefore answers the requirements of a geosyncline in a young stage following Holmes' definition. The continental margin off the eastcoast of North America is, however, virtually in isostatic equilibrium, which evidently excludes the possibility of appreciable elevation by readjustment of equilibrium.

Thus, apart from the fact that KUENEN (1966) objects on sedimentological grounds to the comparison drawn by Drake et al., one still needs another mechanism to produce a mountain system from the continental margin area. We will not enlarge on this problem, but stick to the foregoing conclusion concerning the development of the structures in the Caribbean negative anomaly zones, which, without a mechanism other than isostatic readjustment, do not represent areas of mountain building in a young stage.

In mentioning the structure of the continental margin off the east coast of North America, we also wanted to draw attention to the fact that the area around the Netherlands Leeward Antilles resembles the continental margin east of North America in sedimentary build and in crustal type, both having a transitional crust. The Leeward Antilles area differs in that the crust is deformed considerably as is evinced by the isostatic anomalies. We think this deformation to be due to a northwesterly movement of the South American continent. The Leeward Antilles area seems to be a deformed continental margin finding its undeformed counterpart in the continental margin as observed off the east coast of America. Such an interpretation of the structure of the southern Caribbean would not hold for the other Antilles, since these do not border a continental mass. The Lesser Antilles [1]) also show considerable seismicity and volcanic activity, which both are absent in the Leeward Antilles. The suggestion arises that these phenomena are related to the process of formation of the Atlantic Ocean. In this respect it may be of significance that both for the Lesser Antilles area and the Mid Atlantic ridge, which lies at a relatively short distance from the islands (approximately 1500 km), the Mio-Pliocene has been an important period of activity in their formation. If the structure of the Mid Atlantic ridge is related to the formation of oceanic crust during a process of ocean spreading, the island arc of the volcanic Lesser Antilles may be the place where oceanic crust is lost by underthrusting to compensate for the formation of new crust at the Ridge crest. The zone of negative anomalies, the volcanicity and the seismicity are then expressive of this process (see also OLIVER and ISACKS 1967 on the Tonga trench area). In a study of continuous reflection profiles in the North Atlantic Ocean between 10° and 19° N, COLLETTE, EWING, LAGAAY and TRUCHAN (in preparation) go further into the relation

---

[1]) See note on pag. 5.

between the ridge and the Lesser Antilles island arc. It should also be noted here that OROWAN (1965) suggested a similar origin for the island arcs in the Pacific Ocean.

Summing up, it can be said that the origin of the structure of the Leeward Antilles, and that of the Lesser Antilles is different but closely related. The Leeward Antilles area is interpreted as a continental margin area which is deformed by a movement of the South American continent, considerable piles of sediments being deposited in the resulting crustal downwarps. The Lesser Antilles area represents a region where oceanic crust is carried downward, which is accompanied by considerable volcanic and seismic activity and the formation of crustal upwarps and downwarps. The structures are both governed by the process of continental drift/ocean floor spreading.

ACKNOWLEDGEMENTS

I wish to express my gratitude to all those who with their generous help and advice contributed to the preparation of this work; to the Head of the Cadastral Survey of the Netherlands Antilles who provided indispensable facilities during the measurements on the islands; to the Hydrographer of the Royal Netherlands Navy, who permitted H. Neth. M.S. *Snellius* to sail during the NAVADO expedition in courses suggested by us; to Prof. G. J. Bruins for his cooperation in the measuring of gravity at sea; to D. J. Beets, Prof. M. G. Rutten and Dr J. H. Westermann for their help in the composition of our chapter 3; to E. M. J. Bertin and G. J. A. Jansen for their assistance in programming the computor for reducing the gravity observations; to Prof. W. Nieuwenkamp and Prof. G. H. R. von Koenigswald who kindly showed their interest by reading through the MS; to Dr B. J. Collette to whom I am particularly indebted for many constructive suggestions and discussions; and above all, to my Promotor, Prof. J. Veldkamp, who guided my first measurements on the islands and whose criticism has greatly improved this study.

The financial support of the Netherlands Foundation for the Advancement of Research in Surinam and the Netherlands Antilles (WOSUNA) and the Netherlands Organization for the Advancement of Pure Research (ZWO) is gratefully acknowledged.

REFERENCES

ADE-HALL, J. M., The magnetic properties of some submarine oceanic lavas. Geophys. J. Roy. Astron. Soc., 9, 85–92 (1964).

ALBERDING, H., Application of principles of wrench-fault tectonics of Moody and and Hill to northern South America. Bull. Geol. Soc. Am., 68, 785–790 (1957).

ALVAREZ, W., Geology of the Simarua and Carpintero areas, Guajira Peninsula, Colombia. Thesis Princeton University (1967).

ANDERSON, E. M., The dynamics of faulting. Oliver and Boyd, Edinburgh (1951).

BEETS, D. J., Stratigraphic position and age of a Cretaceous Ammonite from Curaçao, Netherlands Antilles. Mem. Fac. Sci., Kyushu Univ., Ser. D, 17, 287–294.

——— and W. LODDER, Indications for the presence of ignimbrites in the Cretaceous Washikemba formation of the isle of Bonaire, Netherlands Antilles. Proc. Kon. Ned. Akad. Wetensch., Amsterdam, B, 70, 63–67 (1967).

BOTT, M. H. P., The use of electronic digital computers for the evaluation of gravimetric terrain corrections. Geophys. Prosp., 7, 45–54 (1959).

BRUINS, G. J., R. DORRESTEIN, H. J. A. VESSEUR, G. BAKKER, and L. OTTO, Atlantic, Caribbean and Pacific cruises. In: Gravity Expeditions 1948–1958, 5. Publ. Neth. Geod. Comm., Delft (1960).

BRUYN, J. W. DE, Isogam maps of the Caribbean Sea and surroundings and of Southeast Asia. Proc. 3rd world Petrol. Congr., 1, 598–612 (1951).

BUISONJÉ, P. H. DE, Marine terraces and sub-aeric sediments on the Netherlands Leeward islands, Curaçao, Aruba and Bonaire, as indications of Quaternary changes in sea level and climate. Proc. Kon. Ned. Aked. Wetensch., Amsterdam, B, 67, 60–79 (1964).

———, P. A. VAN DER WERF, J. S. ZANEVELD and J. I. S. ZONNEVELD, Informe acerca de un reconocimiento biologico y geologico de las Islas Venezolanas Las Aves. Bol. Soc. Venez. Cienc. Natur. 17, 86, 184–210 (1957).

BULLARD, E. O., and R. G. MASON, The magnetic field of the oceans. In: The Sea, ed. M. N. Hill, 3, Interscience, New York, 175–210 (1963).

BUNCE, E. T., The Puerto Rico trench. In: Continental margins and Island arcs. Geol. Survey Canada, 66-15, 165–176 (1965).

BUTTERLIN, J., La constitution géologique et la structure des Antilles. Centre Nat. Recherche Scient., Paris (1956).

BIJLAARD, P. P., Théorie des déformations plastiques et locales par rapport aux anomalies négatives, aux fosses océaniennes, aux géosynclinaux, etc. Congr. d'Edinbourg. Intern. Union. Geod. Geoph., Rept. 6th Gen. Assembly, Assoc. Geod. (1936).

CHAPMAN, S., and J. BARTELS, Geomagnetism. Clarendon Press, Oxford (1940).

COLLETTE, B. J., On the gravity field of the Sunda region (West-Indonesia). Geol. en Mijnb., 16, 271–300 (1954).

———, J. EWING, R. A. LAGAAY and M. TRUCHAN, Sediment distribution in the Ocean: The Atlantic between 10° and 19°N. (in preparation).

COOMBS, D. S., Some recent work on the lower grades of metamorphism. Australian J. Sci., 24, 203–215 (1961).

CORONEL, G., Geology of the Gulf of Venezuela. 7th World Petrol. Congr., Mexico (1967).

DRAKE, C. L., M. EWING, and G. H. SUTTON, Continental margins and geosynclines. Physics and chemistry of the earth, 3, 110–198 (1959).

EDGAR, T., J. I. EWING, and J. HENNION, Seismic refraction and reflection in the Caribbean Sea (abstract). Trans. Am. Geophys. Union, 48, 128 (1967).

EWING, J., I. ANTOINE, and M. EWING, Geophysical measurements in the Western Caribbean Sea and in the Gulf of Mexico. J. Geophys. Res., 65, 4087–4126 (1960).

———, M. TALWANI, M. EWING and T. EDGAR, Sediments of the Caribbean. Proc. Int. Conf. Trop. Oceanography, 1965. Studies in tropical oceanography, 5, 88–102, Univ. of Miami (1967).

EWING, M., Gravity measurements on the U.S.S. Barracuda. Trans. Am. Geophys. Union, 18, 66–69 (1937).

———, J. L. WORZEL, and G. L. SHURBET, Gravity observations at sea in U.S. submarines Barracuda, Tusk, Conger, Argonaut and Medregal. In: 'Gedenkboek F. A. Vening Meinesz'. Verh. Kon. Ned. Geol. Mijnbouwk. Genootschap, Geol. Ser., 18, 49–116 (1957).

——— and I. ANTOINE, New seismic data concerning sediments and diapiric structures in Sigsbee deep and upper continental slope, Gulf of Mexico. Bull. Am. Ass. Petr. Geol., 50, 479–504 (1966).

Geological Society, Phanerozoic time-scale. Quart. J. Geol. Soc. London, 120 s, 260–262 (1964).

FISHER, R. L., and H. H. HESS, Trenches. In: The Sea., ed. M. N. Hill, 3, Interscience, New York, 411–436 (1963).

GUNN, R., Quantitative aspects of juxtaposed ocean depths, mountain chains and volcanic ranges. Geophysics, 12, 238–255 (1947).

HAFNER, W., Stress distribution and faulting. Bull. Geol. Soc. Am., 62, 373–398 (1951).

HEDBERG, H. D., Geology of the eastern Venezuelan basin (Anzoategui-Monagas-Sucre-eastern Guarico portion). Bull. Geol. Soc. Am., 61, 1173–1216 (1950).

———, Northeastern Venezuela. In: Handbook of South American Geology. Geol. Soc. Am., mem. 65, 337–340 (1956).

HEEZEN, B. C. and C. L. DRAKE, Gravity tectonics, turbidity currents and geosynclinal accumulations in the continental margin of eastern North America. University of Tasmania Symposion, D, 1–10 (1964).

HEILAND, C. A., Geophysical exploration. Prentice-Hall, New York (1940).

HEISKANEN, W. A., and F. A. VENING MEINESZ, The earth and its gravity field. McGraw-Hill, New York (1958).

HESS, H. H., Geological interpretation of data collected on cruise of U.S.S. Barracuda in the West Indies. Preliminary report. Trans. Am. Geophys. Union, 18, 69–77 (1937).

———, Gravity anomalies and island arc structures with particular reference to the West Indies. Proc. Am. Phil. Cos., 79, 71–96 (1938).

———, Caribbean research project: progress report. Bull. Geol. Soc. Am., 71, 235–240 (1960).

———, Caribbean research project, 1965, and bathymetric chart. Geol. Soc. Am., mem. 98, 1–10 (1966).

HOLMES, A., Principles of Physical Geology. Nelson, London (1965).

HOSPERS, J., and J. C. VAN WIJNEN, The gravity field of the Venezuelan Andes and adjacent basins. Verh. Kon. Ned. Akad. Wetensch., Amsterdam, 23, 1–95 (1959).

HUBBERT, M. K., A line-integral method of computing the gravimetric effects of two-dimensional masses. Geophysics, 13, 215–225 (1948).

———, Mechanical basis for certain familiar geologic structures. Bull. Geol. Soc. Am., 62, 355–372 (1951).

KÄRKI, P., L. KIVIOJA and W. A. HEISKANEN, Topographic-isostatic reduction maps for the world for the Hayford zones 18–1, Airy-Heiskanen system, T=30 km. Publ. Isost. Inst. of the Int. Assoc. Geodesy, 35, (1961).

——— and P. PAANANEN, Isostatically reduced anomaly fields on the sea in the vicinity of South and Central America. Publ. Isost. Inst. of the Int. Assoc. Geodesy, 36, (1961).

KUENEN, PH. H., Geosynclinal sedimentation. Geol. Rundschau, 56, 1–19 (1966).

LEJAY, P., Développements modernes de la gravimetrie. Gauthier-Villars, Paris (1947).

MAC GILLAVRY, H. J., The rudist fauna of Seroe Teintje limestone (Northern Curaçao). Proc. Kon. Ned. Akad. Wetensch., Amsterdam, 35, 381–392 (1932).

MARTIN, K., Geologische Studien ueber Niederlaendisch West-Indien auf Grund eigener Untersuchungsreisen. Brill, Leiden (1888).

MATTHEWS, D. J., Tables of the velocity of sound in pure water and sea water for use in echo sounding and sound ranging. Admiralty, London (1939).

MENDIGUREN, J. A., Focal mechanism and pressure axis direction in Central America and South America. Bull. Int. Inst. Seismology and Earthquake Eng., 3, 1–20 (1966).

METZ, H. L., Geology of the El Pilar fault zone State of Sucre, Venezuela. Thesis Princeton University (1964).

MOLENGRAAFF, G. J. H., Geologie en geohydrologie van het eiland Curaçao. Thesis Delft (1929).

MOODY, J. D., and M. J. HILL, Wrench-fault tectonics. Bull. Geol. Soc. Am., 67, 1207–1246 (1956).

NAFE, J. E., and C. L. DRAKE, Variation with depth in shallow and deep water marine sediments of porosity, density, and the velocities of compressional and shear waves. Geophysics, 22, 523–552 (1957).

NAVADO III, Bathymetric, magnetic and gravity investigations H. Neth. M.S. Snellius, 1964–1965. Hydrographic Newsletter, Spec. Publ., 3, (1967).

NETTLETON, L. L., Gravity and magnetic calculations. Geophysics, 7, 293–310 (1942).

OFFICER, C. B., J. I. EWING, R. S. EDWARDS, and H. R. JOHNSON, Geophysical investigations in the eastern Caribbean: Venezuelan basin, Antilles island arc, and Puerto Rico trench. Bull. Geol. Soc. Am., 68, 359–378 (1957).

———, ———, J. F. HENNION, D. G. HARKRIDER, and D. E. MILLER, Geophysical investigations in the eastern Caribbean: summary of 1955 and 1956 cruises. In: Physics and Chemistry of the Earth, 3, Pergamon, London, 17–109 (1959).

OLIVER, J., and B. ISACKS, Deep earthquake zones, anomalous structures in the upper mantle and the lithosphere J. Geophys. Res., 72, 4259–4275 (1967).

OROWAN, E., Convection in a non-Newtonian mantle, continental drift, and mountain building. In: A symposion on continental drift. Phil. Trasn. Roy. Soc. London, A, 258, 284–313 (1965).

———, Island arcs and convection. Geophys. J. Roy. Astron. Soc., 14, 385–393 (1967).

PETERS, L. J., The direct approach to magnetic interpretation and its practical application. Geophysics, 14, 290–320 (1949).

PRIEM, H. N. A., N. A. I. M. BOELRIJK, R. H. VERSCHURE, E. H. HEBEDA, and R. A. LAGAAIJ, Isotopic age of the quartz-diorite batholith on the island of Aruba, Netherlands Antilles. Geol. en Mijnb., 45, 188–190 (1966).

———, Beknopt verslag over de werkzaamheden in het jaar van september 1966 tot september 1967. Z.W.O. Laboratorium voor isotopengeologie, Amsterdam (1967).

PIJPERS, P. J., Geology and paleontology of Bonaire (D.W.I.). Geogr. en Geol. Med., 8, Utrecht (1933).

RAITT, R. W., Marine seismic studies of the Indonesian Island Arc. Trans. Am. Geophys. Union, 48, 217 (abstract) (1967).

RITSEMA, A. R., and J. VELDKAMP, Fault plane mechanisms of Southeast Asian earthquakes. Med. en Verh., Kon. Ned. Meteor. Inst., De Bilt, 76, (1960).

———, Some reliable fault plane solutions. Pure and Appl. Geophys., 59, 58–74 (1964).

ROD, E., Strike-slip faults of northern Venezuela. Bull. Am. Assoc. Petrol. Geol., 40, 457–476 (1956).

ROMERO, A. C., Notas sobre magnetismo terrestre y su cartografía. Publ. Direccion Cartogr. Nacional, Venezuela (1961).

RUTTEN, L. M. R., De geologische geschiedenis der drie Nederlandsche Benedenwindsche Eilanden. De West-Indische Gids, 13, 401–441 (1932).

———, Ueber den Antillenbogen. Proc. Kon. Ned. Akad. Wetensch., Amsterdam, 38, 1046–1058 (1935a).

———, Alte Land- und Meeresverbindungen in Indien und Zentral Amerika. Geol. Rundschau, 26, 26–94 (1935b).

———, The age of the quartz-dioritic and granodioritic rocks of the West Indies. Geol. en Mijnb., 1, 128–133 (1939).

———, New data on the smaller islands North of Venezuela. Proc. Kon. Ned. Akad. Wetensch., Amsterdam, 43, 828–841 (1940).

———, and B. VAN RAADSHOVEN, On earthquake epicentres and earthquake shocks between 1913 and 1938 in the region between 0° and 30°N and 56° and 120°W. Verh. Kon. Ned. Akad. Wetensch., Amsterdam, 39, 1–44 (1940).

SYKES, L. R., and M. EWING, The seismicity of the Caribbean Region. J. Geophys. Res., 70, 5065–5074 (1965).

TALWANI, M., H. G. SUTTON, and J. L. WORZEL, A crustal section across the Puerto Rico Trench. J. Geophys. Res., 64, 1545–1555 (1959).

———, A review of marine geophysics. Marine Geol., 2, 29–80 (1964).

———, and J. R. HEIRTZLER, Computation of magnetic anomalies caused by two dimensional structures of arbitrary shape. In: Computors in the mineral industries, ed. G. A. Parks, Stanford University, 469–480 (1964).

VAN BEMMELEN, R. W., Stromingstelsels in de silicaatmantel. Geol. en Mijnb., 20, 1–17 (1958).

———, The evolution of the Atlantic mega-undation (causing the American continental drift). Tectonophysics 1, 385–430 (1964).

———, On mega-undations: a new model for the earth's evolution. Tectonophysics, 3, 83–127 (1966).

VELDKAMP, J., The geomagnetic field of the Netherlands reduced to 1945. 0. Publ. Kon. Ned. Meteor. Inst., 134, 1–30 (1951).

VENING MEINESZ, F. A., Gravity expeditions at sea 1923–1932; 2. Publ. Neth. Geod. Comm., Delft (1934).

———, Tables for regional and local isostatic reduction (Airy system) for gravity values. Neth. Geodetic Comm., Delft (1941).

———, Gravity expeditions at sea 1923–1938; 4. Publ. Neth. Geod. Comm., Delft (1948).

———, Indonesian Archipelago: a geophysical study. Bull. Geol. Soc. Am., 65, 143–164 (1954).

———, Plastic buckling of the earth's crust; The origin of geosynclines. Geol. Soc. Am., spec. paper 62, 319–330 (1955).

———, Interpretation of gravity anomalies on the westcoast of South America and in the Caribbean, and the Puerto Rico trench; two types of deep ocean trenches. Neth. Geod. Comm., Delft, Publ. on Geodesy, 2, 5–28 (1964).

VERMUNT, L. W. J., and M. G. RUTTEN, Geology of Central-Curaçao. Proc. Kon. Ned. Akad. Wetensch., Amsterdam, 34, 271–276 (1931a).

———, and ———, Geology of the surroundings of 'St. Martha' and 'St. Kruis' (Curaçao). Proc. Kon. Ned. Akad. Wetensch., Amsterdam, 34, 558–562 (1931b).

———, and ———, Some remarks on the geology of N. Curaçao. Proc. Kon. Ned. Akad. Wetensch., Amsterdam, 34, 1028–1031 (1931c).

WATERS, A. C., and H. D. HEDBERG, The North American Cordillera and the Caribbean region. Reg. Geol. d. Erde, 3, IVa (1939).

WESTERMANN, J. H., The geology of Aruba. Geogr. en Geol. Med., 7, Utrecht (1932).

———, Overzicht van de geologische en mijnbouwkundige kennis der Nederlandse Antillen. Med. Kon. Ned. Ver. Ind. Inst., Amsterdam, 85, Afd. Trop. Prod., 35 (1949).

———, The water bore of Oranjestad 1942–1943, and its implication as to the geology and geohydrology of the island of Aruba. (Netherlands West Indies). I and II. Proc. Kon. Ned. Akad. Wetensch., Amsterdam, B, 65, 140–159 (1951).

WEYL, R., Geologie der Antillen. Borntraeger, Berlin (1966).

WORZEL, J. L., and G. L. SHURBET, Gravity interpretations from standard oceanic and continental crustal sections. Geol. Soc. Am., spec. paper 62, 87–100 (1955).

———, Deep structure of coastal margins and mid-oceanic ridges. Proc. 7th Symp. Colston Res. Soc., Bristol, 335–361 (1965a).

———, Pendulum gravity measurements at sea 1936–1959. John Wiley, New York (1965b).